Cleaner Materials 11 (2024) 100225

Contents lists available at ScienceDirect

Cleaner Materials

journal homepage: www.journals.elsevier.com/cleaner-materials

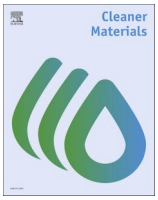

Review on the mechanical properties of rubberized geopolymer concrete

Sunday U. Azunna [a,*], Farah Nora Aznieta Binti Abd Aziz [a,*], Noor Abbas Al-Ghazali [b], Raizal S.M. Rashid [b], Nabilah A. Bakar [b]

[a] Housing Research Centre, Department of Civil Engineering, Faculty of Engineering, University Putra Malaysia (UPM), 43400 Serdang, Selangor, Malaysia
[b] Department of Civil Engineering, Faculty of Engineering, University Putra Malaysia (UPM), 43400 Serdang, Selangor, Malaysia

ARTICLE INFO

Keywords:
Mechanical properties
Geopolymer concrete
Rubberized concrete
Rubberized geopolymer concrete
Impact resistance

ABSTRACT

Rubberized geopolymer concrete (RuGPC) is a new, environmentally safe building material requiring less energy and carbon footmark than normal cement-based systems, which can significantly reduce global warming concerns. Using waste rubber tyres by incorporating them in concrete as a substitute for natural aggregate, helps to reduce pollution and depletion of natural resources. Research shows that incorporating waste crumb rubber in geopolymer concrete (GPC) can reduce carbon dioxide emissions by 90% compared to ordinary Portland cement (OPC) and attain sufficient and mechanical properties and durability. This paper reviews the material properties of RuGPC and the possible structural application. It can be concluded, that RuGPC can substitute normal concrete (NC) particularly due to its impact resistance, and energy absorption performance. However, more research still needs to be conducted to be able to come up with practical design standards and conduct full-scale studies on RuGPC elements structurally to promote its practicability.

Introduction

Every economy relies heavily on the construction industry (Giang and Pheng, 2011) and concrete is the most common building material because of its sturdiness, conductive mechanical qualities, simplicity of handling, versatility, and accessibility of its constituent materials. Water, binders, fine and coarse natural aggregates (FA and CA), and other natural resources are the primary components of concrete (Mačiulaitis et al., 2009). Ordinary Portland Cement (OPC), a common binder used in the manufacturing of concrete, depletes natural resources significantly. To create 1 tonne of OPC, for instance, 1.5 to 2.8 tonnes of raw materials are required (Aly et al., 2019; Park et al., 2016) of which 70 % is limestone. Additionally, the heating required for OPC production results in substantial energy usage at kiln temperatures of around 1500 °C (Aly et al., 2019). According to several studies (Luhar et al., 2018; Charkhtab Moghaddam et al., 2021) the energy needed to produce 1 tonne of OPC is around 4 GJ. In the end, this results in higher CO_2 emissions, with OPC production being in charge of 5–8 % of global anthropogenic CO_2 emissions and 12–15 % of global energy consumption (Akbarnezhad et al., 2015; Qiu et al., 2019; Teh et al., 2017). In addition to the release of CO_2, the formation of OPC also produces the damaging chemicals nitrogen oxide (NO_2) and sulphur trioxide (SO_3), both of which hasten global warming and aid in acid rain (Rajendran and Akasi, 2020). By 2050, the yearly demand for OPC is anticipated to increase to up to 4.38 x 10^9 tonnes due to the urban population growth (United Nations Department of Economic and Social Affairs, 2023; Schneider et al., 2011; Hasanbeigi et al., 2012). Water and air pollution may also be caused by cement production (Amin et al., 2020). The fatal impact that the production of cement is having on the environment have increased as a result of recent urbanization, particularly in developing nations (Alaloul, 2020). To preserve the environment's sustainability, sustainable alternatives be employed in construction applications rather than cement (Ober and Survey, 2018; Hamada et al., 2020). Alkali-activated materials, which produce geopolymer concrete (GPC) (Tayeh et al., 2021; Adesina, 2021), a cutting-edge and environmentally friendly construction material that uses aluminosilicate precursors (de Azevedo et al., 2020; Azevedo, 2021) activated by an alkaline solution as a substitute for cement (Krivenko, 2017; Yeddula and Karthiyaini, 2020; Davidovits, 1988; Davidovits, 1988), are one such favorable surrogate that can stand-in place of cement in concrete. Natural materials

Abbreviations: GPC, Geopolymer concrete; NC, Normal/Nominal concrete; OPC, Odinary Portland cement; RTR, Recycled tyre rubber; RuC, Rubberized concrete; RuAAC, Rubberized alkali activated concrete; RuGPC, Rubberized geopolymer concrete; RuGPM, Rubberized geopolymer mortar; SP, Superplasticizer; CR, Crumb rubber; A-S-P, Aluminosilicate precursor; AAS, Alkaline activator solution; GNP, Graphene nanoplatelets.

* Corresponding authors.
E-mail addresses: gs67063@st.upm.edu.my (S.U. Azunna), farah@upm.edu.my (F.N.A.B.A. Aziz).

https://doi.org/10.1016/j.clema.2024.100225
Received 29 November 2023; Received in revised form 6 February 2024; Accepted 9 February 2024
Available online 11 February 2024

like metakaolin (derived from kaolinite), clay, red mud, and rice husk are frequently utilized as precursors to alumina silicates, as are by-products of industry such as fly ash (FA) and ground granulated blast furnace slag (GGBFS) (Luhar et al., 2019; Zaetang et al., 2019; Amran et al., 2020). Fly ash is a by-product from thermal power plants, and steel plants produce ground-granule blast furnace slag as a by-product. Both fly ash and GGBFS are treated using the proper technology and employed for projects made of geopolymer concrete. Alkaline activators are necessary for the geo-polymerization process; these alkaline activators include sodium hydroxide (NaOH), sodium silicate (Na_2SiO_3), potassium hydroxide (KOH), and potassium silicate (K_2SiO_3) (Yeluri and Yadav, 2020; Azmi et al., 2016).

Alkaline activator solution is made using a catalytic liquid system. In addition to distilled water, it consists of a mixture of alkali silicate and hydroxide solutions. The alkaline activator solution's function is to activate Si and Al-containing geopolymeric source materials such as fly ash and GGBFS. GPC is far more environmentally friendly than NC. For instance, when compared to NC, less than 80 % of carbon dioxide is released by FA-based GPC into the atmosphere and requires less than 60 % energy in production (Duxson et al., 2007; Li et al., 2004). Greater cost reductions are associated with this, which are predicted to be between 10 and 30 % of NC (Rangan et al., 2017). Along with being more affordable and environmentally friendly, GPC can also be more durable than NC (Al et al., 2011), as evidenced by its lower shrinkage and creep (Azmi et al., 2016), enhanced resistance to freeze and thaw (Luhar et al., 2019), better resistance to chloride, acid, and sulphate attacks (Pratiwi, 2020; Deb et al., 2016), improved fire resistance (Hakem Aziz et al. 2023), and superior thermal insulation properties, GPC has good bond characteristics (Dong et al., 2020) and can achieve compressive strengths comparable to those of NC (Živica et al., 2016; Wongpa et al., 2010). Additionally, GPC is perfect for applications with rapid strength development (Rosenberger, 2018) because it may reach 90 % of its ultimate compressive strength in just three days (Tayeh et al., 2020). Depending on the binder and alkaline activator solution employed, using geopolymer concrete as a surrogate to standard Portland cement concrete has been shown to reduce embodied carbon by up to 80 % (Tayeh et al., 2021). A thorough life cycle analysis of geopolymers revealed that GPC outperformed NC in terms of its effect on global warming and potential for eutrophication (Esparham et al., 2023). Other life cycle analyses of geopolymers have shown that they are sustainable alternatives, and a more significant increase in sustainability can be made by using locally accessible precursors and alternative activators (Tayeh et al., 2020).

The disposal of end-of-life tyres (ELTs), which are expected to amount to between 1000 and 1200 million yearly and of which more than half end up in landfills (Thomas and Gupta, 2016; Azevedo et al., 2012; Rashad, 2016), is another serious environmental issue. A tyre that has reached the stage where it cannot be used on vehicles is known as an ELT (even after being re-treated or re-grooved). ELTs are often landfilled, burned to create fuel, or pyrolyzed to recover carbon black (Thomas and Gupta, 2016) and cannot be directly reused in the automotive industry, even with re-grooving. Many affluent nations forbid landfilling because it poses numerous environmental and health risks, including the possibility of fires (Guelmine et al., 2016) and the leaking of chemicals from tyres into subterranean water systems (Park et al., 2016). Tires are a perfect home for rodents and insects that carry disease since they are not biodegradable and can accumulate water for a prolonged period of time (Thomas and Gupta, 2016). Tyres that have reached the end of their useful lives should not be burned because doing so emits hazardous gases, which has prompted some nations to enact laws prohibiting tyre burning (Luhar et al., 2019). Millions of old tyres are produced each year as a result of the rise in the number of automobiles on the highways of developed and industrialized countries. Each year, approximately 1.4 billion tyres are sold worldwide, and a similar number inevitably come under the category of end-of-life tyres. Because they employ a larger number of automobiles, developed nations produce the majority of the world's ELTs. However, wealthy countries have seen a sharp increase in ELT recovery rates over the past 15 years, and recycling costs have dropped dramatically as a result of more effective management systems and recovery pathways. In many developing nations, such as Malaysia, Indonesia, the Philippines, and Thailand, where land-use and disposal restrictions are still lax and recycling infrastructure is still very much in its infancy, high recycling/recovery rates are not reached. Adding to the already troublesome stockpiles of ELTs from local sources, many places even receive imported ELTs, which exacerbates the issue. According to the US Environmental Protection Agency, in 2003 about 290 million trash tyres were collected, (EPA, 2007), of which 45 million were used to create new tyres for cars and trucks and the remaining are in landfills. More than 30 % of potentially recyclable materials, like plastic and old tyres, are nevertheless disposed of in landfills as a result of unseparated garbage (Recycling, 2020). When scrap tyres are not properly disposed of, there may be a risk to human health (fire risk, habitat for rats or other pests like mosquitoes) as well as an increase in environmental risks.

Many nations, both in Asia and around the world, have traditionally disposed of used tyres by placing them in landfills, however due to space constraints and the possibility that they could be reused, several nations have outlawed this method. The current estimate for these historical stocks across the EU is 5.5 million tonnes (1.73 times the annual used tyre production in 2009), and the expected yearly cost for waste tyre handling is estimated to be € 600 million (Vredestein, 2023). Numerous new markets have emerged for scrap tyres due to landfills' decreasing acceptance of complete tyres and the hazards that storing tyres poses to human health and the environment thus increasing the accessibility of recycled tyre rubber (RTR) for other forms of recycling. Given that RTR is highly robust and can be used in other goods, the qualities that make scrap tyres such a concern also make them one of the most recycled waste commodities. In many developed countries, where it still has a significant growth potential, these efforts should, for instance, contribute to the continued development of the use of waste tyres in the manufacturing of rubber concrete (Vredestein, 2023).

The original purpose of rubberized concrete (RuC) was to lessen the massive amounts of waste tyres that are being dumped in landfills annually. In the process of recycling, rubber and steel fibre are the typical materials recovered. After processing, the rubber is divided into chips or crumb rubber (CR), which is then utilised in several applications, one of which is the substitution of nominal aggregates in concrete. Fig. 1(a), 1(b), and 1(c) correspondingly depict waste rubber tyres, tyre chips, and crumb rubber. Rubber has a substantially greater Poisson's ratio of roughly 0.3 compared to natural aggregates, however its elastic modulus and compressive strength are lower (approximately 1 MPa) (Edeskär, 2004). This will cause the concrete matrix to expand excessively perpendicular to the applied load, resulting in microcracking. Moreover, there are gaps at the interfacial transition zone (ITZ) because of the tyre rubber's poor adherence to the concrete matrix resulting from the smooth, soapy water repelling layer caused by the presence of the residual zinc stearate that minimises friction and bonding (Elchalakani et al., 2018). These two reasons significantly reduce the compressive strength of concrete when rubber is introduced. Previous research observed a reduction by 77 % with respect to the control when 30 % rubber was used as natural aggregate replacement (Elchalakani et al., 2018; Raffoul et al., 2016; Dong et al., 2019). Consequently, sodium hydroxide is commonly used as a pre-treatment for rubber aggregates to roughen their surface and remove the layer of zinc stearate (Elchalakani et al., 2018). Despite its significant drawback of low strength, RuC offers better impact resistance (Aly et al., 2019), energy absorption (Elchalakani et al., 2018), ductility (Dong et al., 2019; Dong, 2019), sound absorption (Gandoman and Kokabi, 2015), and fire resistance (Turgut and Yesilata, 2008; Hernández-Olivares and Barluenga, 2004), than concrete made with natural aggregates. Furthermore, because rubber has a low specific gravity ranging from 0.5 to 0.9 (Edeskär, 2004), RuC has a lower density and thus lesser dead load thereby making it more user friendly in

Fig. 1. (a): Waste, Fig. 1(b): chips, Fig. 1(c): Crumb rubber (Ali and Hasan, 2019).

construction sites.

The advantages of geopolymer concrete (GPC) and rubberized concrete (RuC) are combined when crumb rubber (CR) is added to GPC to create Rubberized geopolymer concrete (RuGPC), where some or all of the NA is replaced by CR (Park et al., 2016). Compared to RuC, RuGPC offers a number of benefits. First off, geopolymer has sodium hydroxide available as an activator for pre-treatment. Secondly, geopolymer's reduced elastic modulus makes it more compatible with rubber aggregates. Thirdly, the specific gravity of fly ash, the primary binder, is 2.25, much lower than that of OPC which is 3.15. This may enhance mix homogeneity by lowering the floating propensity. Furthermore, it is reported that the silicate-based geopolymer is stickier when mixed, which strengthens the bond between the geopolymer matrix and rubber aggregates (Luhar et al., 2019). With respect to GPC, the high impact resistance and energy absorption of RuGPC makes it more suitable for application in areas prone to lateral impact and energy absorption e.g., earthquake prone areas, airstrips slab etc. In conclusion, RuGPC combines the advantages of the GPC and RuC and, theoretically, is lighter, more fireproof, and encourages waste material recycling. The key features of RuGPC are summarised in Fig. 2.

This paper provides incitive review of previous literature on rubberized geopolymer concrete, including a relatively significant analysis of important attributes where appropriate. The review features the primary components of RuGPC, beginning with the aluminosilicate precursors (geopolymer binders), alkaline activator solutions, natural and rubber aggregates, and admixtures. The method of preparing RuGPC and different methods of curing RuGPC are also discussed, and then a review of the material's chemical, physical and mechanical properties follow. To promote the adoption of RuGPC in practice, the study then outlines gaps in the literature that need for additional research and improvement.

Rubberized geopolymer concrete components

Generally, prior research on RuGPC showed that it has tremendous potential as a sustainable building material, also gave basic details about the raw materials' constituent parts, both preparing and curing RuGPC, properties of fresh and hardened RuGPC. This chapter provides an overview of a few earlier studies on RuGPC.

Aluminosilicate (A-S) precursors (Binders)

FA, GGBFS, metakaolin, red mud, waste wood ash, rice husk ash, and silica fume are typical aluminosilicate precursors utilised in the creation of GPC. When these substances are combined with an alkaline liquid, geopolymer gels are created that release aluminium and silica (Singh et al., 2015). The chemical and mineralogical makeup of source materials has a significant impact on their reactivity (Yeluri and Yadav, 2020). Based on summary made in Table 2, the majority of research used either FA or GGBFS, and frequently the two in combination, to create rubberized alkali activated concrete (RuAAC).

Fly ash is an unwanted by-product of burning coal to make energy (Arunkumar et al., 2021; Davidovits, 1999; Liu et al., 2016; Amran et al., 2020). The annual output of FA is estimated between 375 and 400 million tonnes worldwide (Luhar et al., 2018). FA contains aggregates that are glassy and spherical in shape and have pozzolanic characteristics, which enable them to react with alkaline liquids (Rangan, 2009). Due to differences in particle form, gradation, and content, FA has a specific gravity of about 2.0 but can range from 1.6 to 3.1 (Bhatt et al., 2019). BS EN 450–1:2012 states (B.S. EN, 2012), for FA used in concrete, the quantity of SiO_2 should be more than 25 % by mass while aluminium oxide (Al_2O_3), iron oxide (Fe_2O_3), and silicon dioxide (SiO_2) are to exceed 70 % by mass. In addition, the FA's loss on ignition (LOI) shouldn't surpass 5 % (B.S. EN, 2012). Table 1 lists the chemical make-up of type I OPC, FA, GGBFS, and MK employed in various research to create RuGPC.

Fly ash is sub-divided into two classes based on the quantities of CaO and of Fe_2O_3, Al_2O_3, and SiO_2 in their chemical make-up, namely: high (Class C) and low (Class F) calcium fly ash (ASTM, 2012). According to Table 1, Class F FA has a CaO percentage of less than 10 % (most often less than 5 %) by mass, while Class C FA has a CaO level that is larger than 10 % by mass. Furthermore, compared to Class F FA, Class C FA contains compositions of Al_2O_3 and Fe_2O_3 that are typically lower. Hence, to obtain high strength at early age and at room temperature, high calcium FA (Class C) is frequently used, whereas to get the best binding qualities, Class F is utilized. When the latter is used, development of strength can also be hastened by heat curing. FA's ability to fill gaps in concrete because of its tiny aggregate size is one of its benefits, which makes concrete more dense, enhanced workability, and reduced permeability. However, Class C FA frequently experience flash setting

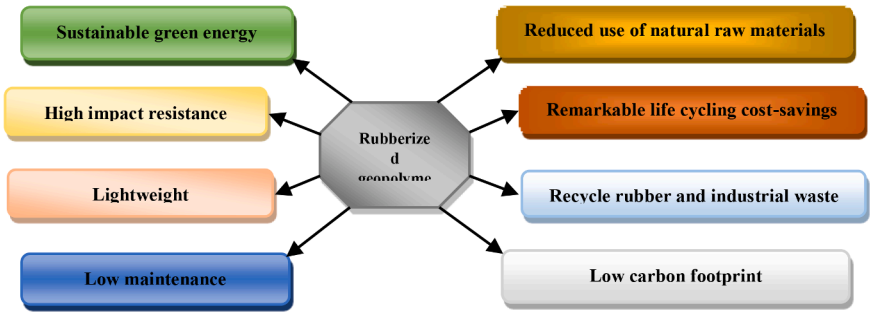

Fig. 2. Characteristics of RuGPC.

Table 1
Chemical composition of aluminosilicate precursors and type I cement.

	Chemical composition (%)													Ref.
	SiO_2	Al_2O_3	Fe_2O_3	MnO	MgO	Na_2O	SO_3	CaO	K_2O	P_2O_5	TiO_2	CL	SrO	LOI	
OPC	20.27	4.80	3.43	/	1.58	/	/	63.71	/	/	/	/	/	2.51	(Kaja et al., 2018)
	22.89	3.67	3.25	/	1.56	/	/	63.22	/	/	/	/	/	2.14	(Qu et al., 2022)
	20.27	6.11	3.43	/	2.79	/	/	61.27	0.12	/	/	/	/	2.56	(Alhozaimy, 2008)
Class F fly ash	54.70	29.00	6.74	/	0.80	1.88	0.10	1.29	/	/	/	/	/	2.72	(Luhar et al., 2018)
	55.90	27.80	7.09	/	/	/	/	3.95	1.55	/	2.25	/	0.37	/	(Yahya et al., 2018)
	50.00	23.40	17.29	0.22	/	/	0.08	5.06	1.41	/	1.60	/	/	/	(Azmi et al., 2016)
	50.40	31.50	10.40	/	1.10	0.30	0.10	3.30	0.50	0.50	1.90	/	<0.1	/	(Aslani et al., 2020)
	50.30	22.90	8.17	0008	2.00	/	0.58	3.38	3.55	/	1.15	/	/	/	(Zhong et al., 2019)
	61.75	24.61	6.47	/	1.53	/	/	3.45	0.55	/	0.91	/	/	/	(Rajendran and Akasi, 2020)
	55.90	23.90	7.90	0.10	1.30	0.40	0.30	7.00	1.00	0.50	1.30	/	/	0.30	(Dong et al., 2021)
	52.47	26.22	7.83	/	1.09	/	/	5.42	1.49	/	/	/	/	2.56	(Klima et al., 2022)
	51.73	28.40	6.57	/	1.47	/	/	4.93	1.95	/	1.15	/	/	/	(Suh et al., 2020)
	51.30	26.92	7.61	/	1.10	/	/	5.20	1.45	/	1.43	/	/	3.62	(Luo et al., 2022)
Class C fly ash	39.40	20.80	11.50	/	2.20	1.40		14.5	2.40	0.20	0.50	/	/	1.50	(Wongsa et al., 2018)
	50.67	18.96	6.35	/	3.12	0.69	0.74	14.14	/	/	/	/	/	0.17	(Park et al., 2016)
	45.85	16.82	12.05	0.18	2.90	0.50	3.76	12.97	1.83	0.28	0.48	/	0.50	/	(Mucsi et al., 2018)
GGBFS	34.10	12.30	0.41	0.25	8.12	/	2.59	44.20	0.56	/	0.96	/	/	/	(Zhong et al., 2019)
	36.95	10.01	1.48	0.52	6.43	1.39	3.52	33.07	0.74	0.10	0.52	0.05	/	/	(Rashad and Sadek, 2020)
	31.40	13.10	0.80	0.20	5.50	0.30	4.00	43.20	0.30	0	0.60	/	/	0.60	(Sajedi and Razak, 2011)
	32.92	13.80	0.58	/	5.76	0.20	3.33	42.13	0.32	0.034	0.57	/	/	/	(Aslani et al., 2020)
	34.95	13.58	0.53	0.15	3.58	0.26	2.52	42.88	0.61	/	0.63	/	/	/	(Lương et al., 2021)
	35.12	14.20	0.62	0.69	8.47	0.98	/	39.08	/	/	0.71	/	/	0.13	(Long et al., 2018)
	36.10	9.30	0.03	/	8.90	0.80	2.20	39.00	0.60	/	/	/	/	1.01	(Ameri et al., 2020)
	36.00	11.80	0.30	/	5.80	/	/	42.60	0.3	/	/	/	/	/	(Qu et al., 2021)
	33.30	12.30	0.39	/	7.84	/	/	40.80	0.67	/	1.29	/	/	/	(Dai et al., 2022)
	36.93	15.55	1.86	/	7.21	/	/	34.69	–	/	/	/	/	2.19	(Qu et al., 2022)
MK	47.9	41.29	4.93	/	0.08	/	/	0.09	0.7	/	1.10	/	/	3.18	(da Cruz et al., 2022)
	54.3	40.26	2.28	/	0.08	/	/	0.39	0.5	/	/	/	/	/	(Bright Singh and Murugan, 2022)
	54.1	42.3	0.51	/	0.37	/	/	0.12	0.7	/	0.41	/	/	1.23	(Al-Sodani et al., 2022)

issues (Tudjono et al., 2014).

The by-product GGBFS, which has pozzolanic properties, comes from the production of pig iron (Luukkonen et al., 2018; Shi and Qian, 2000; Shang et al., 2018). GGBFS has a specific gravity between 2.7 and 2.9 and a glass content of over 85 % by volume (Saraya, 2014). From Table 1, it can be seen that GGBFS has a high CaO concentration (more than 30 %), but the volume of SiO_2 fluctuates from 30 to 40 %. Furthermore, while the Al_2O_3 percentage of GGBFS is between 10 and 15 %, the Fe_2O_3 level is less than 1.5 %. Alkali-activated concrete (AAC), rubidium-activated concrete, and normal concrete can all be formed using the regularly used aluminosilicate precursor GGBFS (Özbay et al., 2016) since it aids in the development of early strength when cured in ambient temperature (Mithun and Narasimhan, 2016; de Vargas et al., 2014).

Flash setting and significant shrinkage, however, are important challenges for this material because of the high CaO component of GGBFS (Rajendran and Akasi, 2020; Zhong et al., 2019). As aluminosilicate precursors, Class F FA and GGBFS were mixed in various ratios in several investigations on RuGPC as shown in Table 2 (Rajendran and Akasi, 2020; Zhong et al., 2019; Aslani et al., 2020; Dong et al., 2021). When used together, they ensure proper workability, setting time, and strength development at room temperature (Fang et al., 2018; Lee and Lee, 2013; Tu et al., 2019).

Given that $SiO_2 + CaO + Al_2O_3 + Fe_2O_3 + MgO$ are present in MK, FA, and GGBFS with concentrations between 91.41 and 97.69 %, or more than 70 % MK, FA, and GGBFS may be employed as pozzolanic components for GPC. GGBFS is a substantially calcium-enriched cement that may react in a relatively less alkaline environment without needing a very high curing temperature because it has a composition of more than 70 % $CaO + SiO_2$ and less than 20 % Al_2O_3. For the preparation of RuGPC, crumb rubber was utilised as a partial replacement for fine and/or coarse aggregate with grain sizes ranging from 73 μm to 16 mm and replacement levels ranging from 5 percent to 100 percent by volume (Luhar et al., 2018; Luhar et al., 2019; Azmi et al., 2016; Youssf et al., 2016; Bhavani, 1132).

Alkaline-activator solution (AAS)

The available AAS in the market Na_2SiO_3 and NaOH are employed in RuGPC, although GPC can also be produced using K_2SiO_3 and KOH (Pavithra et al., 2016). To create geopolymer matrix, the alkaline liquids aids in extracting SiO_2 and Al_2O_3 from the raw aluminosilicate precursor (Yeluri and Yadav, 2020), and are often made a day in advance of mixing (Park et al., 2016; Azmi et al., 2016). NaOH generally comes in the form of pellets, granules, or flakes and is white in color and slowsoluble in water (Aly et al., 2019). The molarity number of NaOH determines how concentrated it is in a solution. A 1 M solution is made by dissolving 40 g of NaOH in 1 L of water, where M is the number of moles of solute per litre of solution (Park et al., 2016). As shown in Table 2, the NaOH solutions employed in RuGPC mixtures ranged in molarity from 6 M to (Kangar, 2011) 20 M (Wongsa et al., 2018). The compressive strength of GPC and RuGPC blends is influenced by the molarity of the NaOH solution (Kangar, 2011; Hardjito and Rangan, 2005). The ideal NaOH molarity is from 12 to 14 M, and greater concentrations adversely influence the mechanical characteristics (Hamidi et al., 2016; Elyamany et al., 2018), but the fineness of the precursor material's alongside its chemical makeup, reactivity must be considered (Mucsi et al., 2018).

Na_2SiO_3 can be created in a highly viscous form or in a solid state (Aly et al., 2019). Sodium oxide (Na_2O) and silicon dioxide (SiO_2) make up the majority of the chemical makeup of Na_2SiO_3, which has a density of 1.35 to 1.5 g/mL. The modulus of silicate (MS), or the ratio of SiO_2/Na_2O in Na_2SiO_3, determines how effective Na_2SiO_3 is as an activating liquid. Sodium silicate with a 1.86–4.50 silicate modulus (Mucsi et al., 2018) (Gandoman and Kokabi, 2015) was used in various studies on rubberized concrete, with optimal values between 2.0 and 2.50 (Luhar et al., 2018; Rajendran and Akasi, 2020; Singh et al., 2015; Dong et al., 2021). The qualities of GPC are determined by the SS/SH ratio (Rajendran and Akasi, 2020). The SS/SH ratio in the rubberized concrete studies shown in Table 3 ranged from 0.33 to 0.44 (Nuaklong et al., 2020) to 2.90 (Gandoman and Kokabi, 2015), even though most of the investigations employed a ratio ranging from 1.50 to 2.50 (Charkhtab

Table 2
Summary of aluminosilicate precursor, admixture, alkaline activator, and curing techniques from previous research.

Precursors	Alkaline activators				Admixture		Curing			Ref.
	Na_2SiO_3 (modulus ofsilicate)	NaOH (molarity)	SS/SH	AA/AP	Type	Dosage (SP/AP)	Type	Duration (hrs)	Temps. (°C)	
Class C FA	2.41	10, 15, 20	0.51 1.5	0.650 0.750 0.85	^	^	Oven	48	25 60 90	(Aslani et al., 2020)
	2.41	10	1	0.75	^	^	Oven	48	60	(Azmi et al., 2016)
	1.85	12	N.P	N.P	^	^	Oven	6	60	(Mucsi et al., 2018)
	2.15	6, 8, 10, 12	0.33	0.6	^	^	Ambi.	UT	25	(Nuaklong et al., 2020)
Class C FA +Class F FA	2.5	8, 14	0.52	N.P	PA	N.P	Steam	7-d	46	(Park et al., 2016)
Class F FA	3.2	12	2.0	0.40	^	^	Ambi.	UT	20–22	(Azmi et al., 2016)
	2.0	14	2.5	0.40	NA	2 %	Oven	48	90	(Luhar et al., 2018)
	N.P	14	2.5	0.40	NA	2 %	Oven	48	90	(Luhar et al., 2019)
	N.P	10	N.P	0.45	NB	2 %	Hot water curing	48	60	(Ali et al., 2020)
	N.P	12	2.5	0.5	^	^	seawater	UT	U.M	(Yahya et al., 2018)
	N.P	10	2	0.4	^	^	Ambi.	UT	20–22	(Azmi et al., 2019)
	N.P	10, 12, 14	1.52 2.5	0.30 0.350 0.4	NA	2 %3%4%	Oven	24, 48, 72	60, 75, 90	(Luhar and Luhar, 2020)
Class F FA +GGBFS	N.P	8	2.5	0.45	NA	2 %	Oven	24	60	(Saloni et al., 2021)
	2.0	10	2.0	0.4	PA	1 %	Ambi.	UT	20±2	(Zhong et al., 2019)
	3.2	14	2.5	0.4	PA+ VMS + setting time retarder	55.5 mL/kg 55.5 mL/kg 11.12 mL/kg	Ambi.	UT	23	(Aslani et al., 2020)
	2.3	12	1.58	0.37	^	^	Ambi.	UT	25±5	(Dong et al., 2021)
	2.0	12	2.5	0.40	^	^	Oven	48	80	(Rajendran and Akasi, 2020)
Class F FA +PC	N.P	12	2.5	0.4	Super lubricant	1.5 %	Oven+ Ambi.	48 until the test	60 N.P	(Charkhtab Moghaddam et al., 2021)
Class F FA + Waste woodash	N.P	10	2.5	0.8	^	^	N.P		N.P	(Arunkumar et al., 2021)
FA	N.P	10, 12, 14	1.52 2.5	0.30 0.35 0.4	NA	2 %3%4%	Oven	24, 48, 72	60, 75, 90	(Luhar et al., 2016)
FA + GGBFS	N.P	12	N.P	N.P	^	^	Ambi.	UT	N.P	(Aslani et al., 2020)
	N.P	12	2.5	0.6	^	^	N.M	NP	N.P	(Pham, 2020)
GGBFS	2.59	N.P	0.39	0.54	^	^	Ambi.	UT	N.P	(Aly et al., 2019)
	3.39	^		0.3	^	^	Heat curing	28-d	45±1	(Rashad and Sadek, 2020)
	1.96	N.P	6.13	0.152	^	^	Ambi.	UT	20±2	(Long et al., 2018)
	2.6	10	0.69	0.6	PA	1 %	Ambi.	UT	23±2	(Rajaei, 2021)
	2.6	10	0.69	0.58	^	^	Ambi.	UT	N.P	(Ameri et al., 2020)
GGBFS + Calciumhydroxide	^	^	^	^	PA defoamer	2.7 % 3.6 % 5 %, 2.9 % 0.1 %	Water	UT	23±3	(Lương et al., 2021)
Metakaolin	N.P	15	2.9	0.84	^	^	Oven	48	65	(Gandoman and Kokabi, 2015)

N.P = Not provided, VMA = viscosity modifying agent, UT = Until testing, NA = naphthalene-based admixture, SP = superplasticizer, PA = polycarboxylate-based admixture.

Moghaddam et al., 2021; Luhar et al., 2019; Pham, 2020). Aside from the sodium hydroxide solution's molarity and SS/SH ratio, values ranging from 0.15 to 0.85 was the AAS to A-S precursor ratio (Wongsa et al., 2018; Long et al., 2018) with an ideal value of 0.40 in rubberized concrete research (Aslani et al., 2020; Azmi et al., 2019).

Natural aggregates

Typically, aggregates are divided into two categories: coarse natural aggregates (CNA) and fine natural aggregates (FNA). CNA has several sources, including, crushed dolomite (Aly et al., 2019), crushed basalt (Luhar et al., 2018), lightweight CAN (Dehdezi et al., 2015), and crushed gravel (Gandoman and Kokabi, 2015; Ali et al., 2020). CNA's largest particle size is 20 mm, and its specific gravity ranged from 2.58 to 2.96 (Luhar et al., 2018; Luhar et al., 2016). Typically, 30–45 % of the overall NA is made up of FNA, and the remaining portion was made up of CNA. This aligns with GPC, where FNA covers 35 to 45 % of the entire NA (Amran et al., 2020). In rubberized geopolymer mortar (RuGM) (Rajendran and Akasi, 2020; Zaetang et al., 2019; Azmi et al., 2016; Zhong et al., 2019; Wongsa et al., 2018; Rajaei, 2021; Chindaprasirt and Ridtirud, 2020); FNA represented the entire amount of aggregates in its entirety. Natural river sand, manufactured sand, and crushed stone sand

Table 3
Fine, coarse, rubber and aggregates and rubber pre-treatment methods.

FNA Type (% Total agg.)	Size (mm)	Specific gravity	CNA Type (% Total agg.)	Size (mm)	Specific gravity	Rubber Type	Size(mm)	Specific gravity	Replacement (%)	Rubber pre-treatment	Ref.
Sand (20–25 %)	NP	NP	CNA (75–80 %)	9.5,16	NP	cr	0.075–4.75	NP	5, 10, 15, 20 by vol. of FNA	-	(Park et al., 2016)
Sand (100 %)	NP	NP	–	–	–	cr	0.073–0.375	NP	5, 10, 15, 20 by vol. of FNA	-	(Azmi et al., 2016)
River sand (100 %)	0.075–4.75	2.63	–	–	–	cr	0–4	1.16	100 % of FNA	-	(Wongsa et al., 2018)
River sand (35 %)	NP	2.61	Crushed basalt (65 %)	1020	2.59	Fibers	W = 2–4 mmL < 22 mm	1.09	10 % by wt. of FNA	-	(Luhar et al., 2018)
River sand (35 %)	NP	2.61	CNA (65 %)	NP	NP	Fibers	W = 2–4 mmL < 22 mm	1.09	10, 20, 30 by wt. of FNA and CNA	-	(Luhar et al., 2019)
Natural sand (35 %)	<0.5	2.65	Crushed dolomite	<12	2.96	cr	Mesh 40(0.42), 1–4	0.45	10, 20, 30 by vol. of FNA and CNA	-	(Aly et al., 2019)
Quartz-sand (40 %)	0.15–4.75	NP	Crushed gravel (60 %)	10	NP	cr	2,4	0.62	10 %, 20 %, 30 % by vol. ofFNA	-	(Ali et al., 2020)
River sand (40 %)	<4.75	NP	Crushed stone	<20	NP	cr	5–10	NP	5 %, 10 %, 15 %, 20 % byvol. of CNA	-	(Yahya et al., 2018)
–	–	–	–	–	–	Rubber powder	0.04	1.0	1 %, 2.5 %, 5 %, 10 %, 15 %by wt. of GGBS	-	(Rashad and Sadek, 2020)
River sand	0.15–4.75	2.63	–	–	–	cr	0.073–4.75	1.16	25 %, 50 %, 75 %, 100 % byvol. of FNA	-	(Zaetang et al., 2019)
River sand (47 %)	NP	2.56	CNA (53 %)	10,20	2.59	Fibers	NP	1.07	10 % by wt. of FNA	-	(Luhar et al., 2016)
River sand	0.125–4.75	–	–	–	–	cr	2–6 (10 %), 1.68 (50 %), 0.595 (40 %)	NP	5 %, 10 %, 15 % of FNA	-	(Zhong et al., 2019)
Natural sand	0.75—4.75	2.26	Crushed gravel	4.75–12.5	2.58	cr	<1	0.38	2 %, 6 %, 10 %, 14 % by wt.of FNA and CNA	-	(Gandoman and Kokabi, 2015)
Silica sand (45 %)	<4	NP	Crushed aggregate (55 %)	7 to 10	NP	cr	2–5, 5–10	1.15	10 %, 20 % of FNA10%, 20 % of CNA	Water soaking	(Aslani et al., 2020)
Crushed aggregates (33 %)	4.75	2.65	Crushed aggregate (67 %)	<20	2.7	cr	FM = 4.2	1.28	5 %, 10 %, 15 % of FNA andCNA	-	(Sreesha et al., 2020)
Dune sand (31 %)	0.24	NP	Crushed aggregate (69 %)	4,7	NP	cr	2–5, 5–7	NP	15 %, 30 % of CNA	NaOH, Water soaking	(Dong et al., 2021)
Silica sand (36 %)	NP	NP	Crushed aggregate (64 %)	<10	NP	cr	1–3, 5–7	0.54	15 %, 30 % by vol. of FNAand CNA	Water soaking	(Pham, 2020)
Sand	0.15–4.75	2.63	–	–	–	cr	0.15–4.75	1.22	20 %, 40 %, 60 % by vol. ofFNA	-	(Long et al., 2018)
–	–	–	–	–	–	Rubber powder	0.4	1.13	5 %, 10 % by wt. of binder	-	(Lương et al., 2021)
Sand	NP	NP	–	–	–	cr	NP	NP	5 %, 10 %, 15 %, 20 % bywt. of FNA	-	(Azmi et al., 2019)
River sand	NP		–	–	–	cr	0.75–4.75	NP	5 % of FNA	NaOH	(Rajendran and Akasi, 2020)
River sand	NP	2.65	–	–	–	Natural rubber latex	NP	NP	1 %, 2 %, 3 %, 5 %, 10 % bywt. of FA	-	(Chindaprasirt and Ridtirud, 2020)
Natural sand	NP	2.5	–	–	–	cr	0–4.75	0.93	20 %, 40 %, 60 % of FNA	Water washing	(Rajaei, 2021)
Copper slag	NP	3.79	–	–	–	cr	0–4.75	0.93	5 %, 10 %, 15 % by vol. ofcopper slag	NaOH	(Ameri et al., 2020)

(*continued on next page*)

Table 3 (*continued*)

FNA Type (% Total agg.)	Size (mm)	Specific gravity	CNA Type (% Total agg.)	Size (mm)	Specific gravity	Rubber Type	Size(mm)	Specific gravity	Replacement (%)	Rubber pre-treatment	Ref.
River sand (40 %)	<1.18	2.62	Stone quarries	<10	2.91	Fibers	W = 0.3 mmL = 20 mm	NP	0.5 %, 1 %, 1.5 %, 2 % byvol. fraction	-	(Arunkumar et al., 2021)
Sand	NP	NP	Gravel	NP	NP	cr	0–4.75	NP	10 % by vol. of FNA	-	(Charkhtab Moghaddam et al., 2021)
River sand	<4.75	2.6	Crushed stone	<20	2.67	Fibers	NP	NP	10 % by wt. of FNA	-	(Luhar and Luhar, 2020)
Fine aggregates (30 %)	<4.75	2.6	Coarse aggregates (70 %)	<14	2.7	cr	0.15–0.60	1.1	10 %, 20 %, 30 % by vol. offNA	NaOH,Water soaking, Cement paste,Ultra-fine slag	(Saloni et al., 2021)

Cr = crumb rubber, W = width, vol. = volume, NP = not provided, L = length, wt. = weight,

are some of the sources of FNA, which has smaller particle sizes that typically range between 0.075 and 4.75 mm (Standard, 2003). Contrarily, the size of CNA particles are greater (>4.75 mm), typical sourced from; dolomite, gravel and crushed stone (Kaplan et al., 2019). By bulk, aggregates make up between 75 and 80 % of concrete (Luhar et al., 2019) and the mechanical and durability qualities of the final concrete are significantly influenced by the appropriate selection and grading of the particles. It is clear that natural river sand, with a specific gravity that ranging between 2.2 and 2.65, was the most common source used for FNA. Silica sand and crushed aggregate were used as additional sources of sand (Aslani et al., 2020; Sreesha et al., 2020), dune sand (Dong et al., 2021) and pure silica sand (Pham, 2020).

Rubber aggregates

In RuGPC, rubber aggregates recycled from used tyres replace a portion of the FNA, CNA, or total NA (Pham, 2020). Natural and polymers, fibres, synthetic rubber, acetone extract, carbon black, and ash are the main components of tyres (Park et al., 2016; Parry, 2004). Rubber hydrocarbon makes up the majority of the essential material (>40 %), followed by carbon black, which accounts for at least 30 %, then acetone extract, and which accounts for at least 8 %. Tyres are processed by being reduced in sizes thereafter they are forwarded to the strip cutter to create rubber strips. After that, a slice cutter is used to trim the strips into smaller, more manageable portions (Thomas and Gupta, 2016). Then, fibre and magnetic separators are used to separate the fibres in the rubber (Yeluri and Yadav, 2020). Mechanical grinding is used to reduce the rubber into three major sizes: ground (0.075–0.475 mm), crumb (0.425–4.75 mm), and shredded/chipped rubber (13–76 mm) after the removal of the textile and steel fibres (Ganjian et al., 2009). Because of their bigger size, shredded rubber aggregates usually take the place of CNA in concrete, whereas CR aggregates usually take the place of FNA. Despite the fact that the binder in RuGPC has been replaced in part with very fine ground rubber (Rashad and Sadek, 2020). The characteristics of ground rubber are not cementitious. Few research used rubber fibres in place of NA, while the majority of studies used CR (Luhar et al., 2018; Luhar et al., 2019; Arunkumar et al., 2021; Luhar and Luhar, 2020; Luhar et al., 2016) and latex made of natural rubber (Chindaprasirt and Ridtirud, 2020). Both natural (made from plants) and manufactured rubber latex have elastic characteristics (Chindaprasirt and Ridtirud, 2020). Although substantially lower than that of NA, the specific gravity of CR aggregates ranges from 0.38 to 1.28. RuGPC saw a 100 % substitution of CR aggregates for NA aggregates (Wongsa et al., 2018) supplying strengths appropriate for RuGPC bricks and blocks (Mohammed et al., 2018). Additional inquiries comprised replacing 60 % of the volume with CR (Long et al., 2018; Rajaei, 2021), nonetheless, most research only considered 30 % replacement. Particle size distribution fine aggregate, type I cement and aluminosilicate precursors are depicted in Fig. 3.

Rubber waste pretreatment

While there is a lot of promise for using waste tyre rubber as a surrogate for fine and coarse aggregates, however its inclusion in GPC negatively affects the mechanical properties of GPC regardless of the alkaline activator solution, curing method or aluminosilicate precursors used (Luhar et al., 2019; Azmi et al., 2016; Dong et al., 2021; Bhavani, 1132; Wang et al., 2022; Youssf et al., 2023). Techniques that can strengthen the geopolymer matrix's bond with the waste rubber aggregates, enhancing the RuGPC mechanical qualities, have been investigated by researchers. Different methods of pre-treatment have been used for rubber aggregates to offset the negative impact of rubber inclusion on GPC characteristics.

In Table 3, pretreatment methods for different RuGPC mixes are listed, with sodium hydroxide pretreatment and water soaking/washing as the main methods. Both methods involve submerging the rubber aggregates in the pretreatment liquid for roughly 1 min before sealing

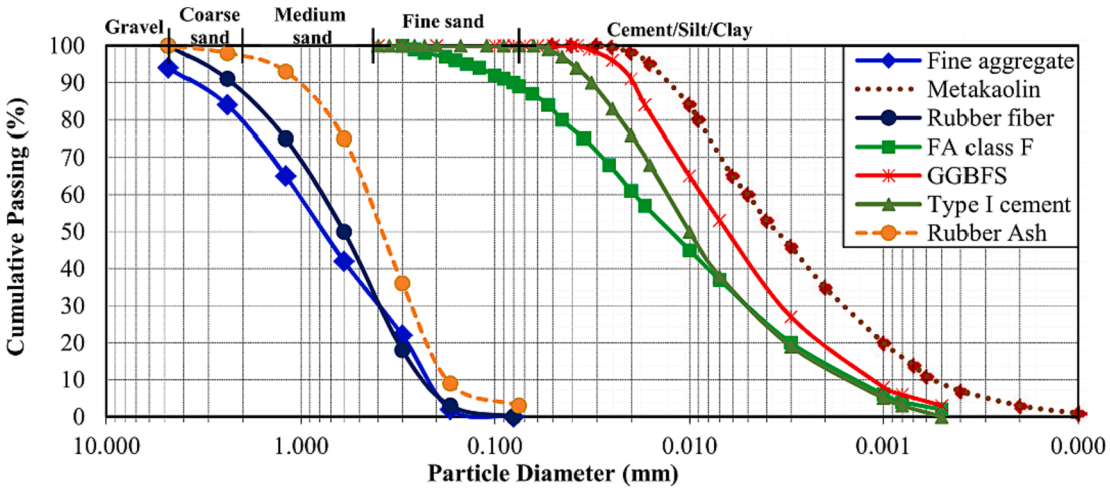

Fig. 3. Particle size distribution fine aggregate, type I cement and aluminosilicate precursors (Luhar et al., 2018; Luhar et al., 2019).

the container and storing it at room temperature for 1 day (Dong et al., 2021). Rubber aggregates are thoroughly cleaned to bring its pH value down to around 7 after draining the solution. In order to obtain saturated surface dry (SSD) conditions, the rubber aggregates are dried. The water is drained off after the rubber aggregates have been soaked for 1-day and allowed to attain saturated surface dry condition before adding it to the mixture (Aslani et al., 2020). The pollutants on the surfaces of the CR aggregates were successfully removed by both pretreatment methods (Pham, 2020) without changing the surface's texture (Dong et al., 2021). However, CR aggregates treated with sodium hydroxide had crystals in the shape of a needles on their surfaces unlike CR aggregates which were soaked in water (Pham, 2020). The zinc stearate layer on the surface of the CR aggregates, which serves as a barrier in adhesion between the geopolymer matrix and rubber aggregates, can be removed when the CR is treated with sodium hydroxide solution (Balaha et al., 2007; Kashani et al., 2017; Guo et al., 2017; Medina et al., 2018). Additionally, submerging the mixture in water can assist in boosting the compressive strength and reduce trapped air (Mohammadi et al., 2014).

Four different CR pretreatment techniques on the properties of RuGPC with fly ash as binder were investigated by Saloni et al. (Saloni et al., 2021). In the pretreatment methods that were investigated, CR aggregates were submerged in water, coated with cement paste or ultra-fine slag, and sodium hydroxide solution. The results showed that all pretreatment approaches had positive effect on the compressive strength (Saloni et al., 2021). The most outstanding compressive strength results were coating with ultra-fine slag and pretreating with sodium hydroxide solution. In contrast to being coated with cement paste, the microstructure of the RuGPC was improved more using ultra-fine slag as fillers and a source of calcium silicate compounds. Modulus of elasticity (MOE), splitting strength, and Flexural strength, of CR aggregates concrete were increased somewhat by pretreatment, notably coating with ultra-fine slag (Saloni et al., 2021). Pretreatment with a sodium hydroxide solution before to immersion in sulfuric and hydrochloric acids produced the highest residual strength when it came to acid resistance, lasting for 90 days (Saloni et al., 2021).

Admixtures

High-range water reducers or superplasticizers (SP) made up the majority of the admixtures employed in RuGPC tests. There are many types of SPs (i.e., distinct chemical bases), including melamine-and modified-polycarboxylate-based, naphthalene-based, and polycarboxylate-based superplasticizers (Palacios et al., 2009; Nematollahi and Sanjayan, 2014). They function by adhering to binder aggregates, preventing reactive sites from being activated, and creating repellency between them. This allows for improved dispersion, hydration, and fluidity (Luukkonen et al., 2019; Łaźniewska-Piekarczyk, 2014; Chandra and Björnström, 2002; Collepardi, 1998).

Because of the high alkalinity of GPC mixes, adding SPs created for OPC concrete that are currently commercially available presents a hurdle. When added to GPC, some SPs behaved poorly (Palacios et al., 2009; Nematollahi and Sanjayan, 2014; Palacios and Puertas, 2005; Criado et al., 2009). Numerous studies examined how SPs affected GPC made with FA (Nematollahi and Sanjayan, 2014; Criado et al., 2009; Laskar and Bhattacharjee, 2013; Rashad, 2014), GGBFS (Palacios and Puertas, 2005; Bakharev et al., 2000), both GGBFS and FA (Jang et al., 2014), and metakaolin (Pacheco-Torgal et al., 2011). It was demonstrated that the activator utilised, the aluminosilicate source material, the amount of water present, and the mixing circumstances all had an impact on how effective SP was. For example, in the investigation by Nematollahi and Sanjayan (Nematollahi and Sanjayan, 2014) a naphthalene-based SP was found to be the most efficient in FA-based GPC when NaOH (8 M) solution was used as the only activator, but when NaOH and Na_2SiO_3 were used to activate the mix, a modified polycarboxylate-based SP had the best performance. Palacios and Puertas (Palacios and Puertas, 2005) also mentioned the possibility of a naphthalene-based SP enhancing the workability, setting time, and compressive strength of GGBFS-based GPC produced using a NaOH solution.

Naphthalene and polycarboxylate-based SPs were primarily utilised in RuGPC mixtures, as shown in Table 2. Second-generation SPs with naphthalene bases repel cementitious aggregates by electrostatic attraction (Burgos-Montes et al., 2012; Gołaszewski and Szwabowski, 2004; Alrefaei et al., 2019), While third generation SPs called polycarboxylate-based SPs use electrostatic repulsion as well as steric repulsion of cementitious binders (Yamada et al., 2000; Puertas et al., 2005). Different RuGPC mixtures received SP dosages ranging from as little as 1 % (Zhong et al., 2019; Rajaei, 2021) up to 5 % of the substance of the binder (Lương et al., 2021). Luhar et al. (Luhar et al., 2016) When examining the impact of various dosages (2–4 %) of naphthalene sulfonate-based SP on the compressive strength of RuGPC, it was discovered that larger dosages had a negative impact. In addition to SPs, other admixtures, like a viscosity-modifying agent (VMA), were also included in RuGPC mixtures (Aslani et al., 2020), a timer setting retarder (Aslani et al., 2020) also a defoamer (0.1 % of binder content) (Lương et al., 2021). While a setting time retarder aids in delaying concrete's setting, a VMA modifies the rheology of the concrete mix to ensure enhanced workability (i.e., the transition from a liquid to a solid state) (Ramachandran and Lowery, 1992; Bong et al., 2019). In GPC, retarders such anhydrous borax, sucrose, and citric acid are frequently utilized

(Liu et al., 2017; Kusbiantoro et al., 2013). In contrast, a defoamer is a chemical addition that lowers the likelihood of foam production in concrete (Lương et al., 2021).

Mix design and proportion of RuGPC

According to reports, RuGPC may be produced using crumb rubber (CR) and source materials including GGBFS, FA, and calcined kaolin, and a suitable mix design is necessary to provide RuGPC the desired compressive strength and other properties. The reason for RuGPC's restricted applicability in structural applications is the lack of an appropriate mix design technique for GPC generally. In any case, some researchers (Pavithra et al., 2016; Ramachandran et al., 2012; Phoo-Ngernkham et al., 2018; Lahoti et al., 2017; Ferdous et al., 2013) have suggested individual mix design procedures for FA, GGBFS-based geopolymer concrete, and Figs. 4 and 22 illustrates the impact of binder type and content on the compressive strength of GPC.

Mixing approaches

In the majority of RuGPC trials, the AAS was prepared a day prior to mixing (Rashad and Sadek, 2020; Lương et al., 2021; Ali et al., 2020). Dry materials such A-S precursors, coarse aggregates, fine aggregates, and rubber aggregates are mixed for 2 to 5 min before being added to the mixture. Additional water and AAS are then added to the dry ingredients after mixing for 2–5 min. The following 1–2 min sees the addition of the mixtures gradually. The next step is to pour concrete into the prepared moulds. To achieve dense samples, samples are frequently casted on a vibrating table in two or three layers. This approach and the mixing process are shown in Fig. 5. The binder and AAS are blended for 3 to 5 min in many investigations on RuGPC before adding natural aggregate followed by rubber aggregates, mixing for another 5 min followed by casting, and compaction (Yahya et al., 2018; Rajaei, 2021).

Curing methods

The curing techniques for RuGPC samples: autoclave/steam, ambient, water, and oven/heat curing are shown in Table 3. Because of the likelihood of free alkalis leaking via the pores of the concrete, causing GP mixture's to be chemically unstable, water curing is less frequently employed with GP mixtures than it is with OPC concrete (Dong et al., 2020; Sharp et al., 2010). In particular for fly ash-based GPC, curing samples at high temperatures enhances strength increase (Hardjito and Rangan, 2005). Samples were subjected to heating at temperatures between 60 and 90 °C in an oven for 1 to 3 days before being removed and left at room temperature until testing (Luhar et al., 2018). For steam curing, on the other hand, samples must be placed at a temperature of 46 °C for seven days in an autoclave (Park et al., 2016).

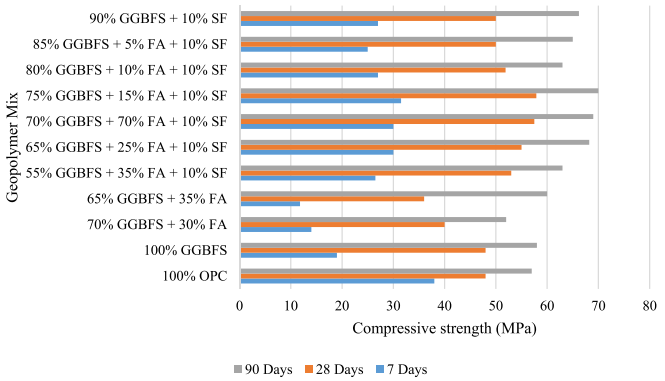

Fig. 4. Compressive strength of geopolymer mixes (Dave et al., 2020).

The samples are then taken out and allowed to cure until the test at room temperature. According to Rajendran and Akasi (Rajendran and Akasi, 2020), curing with steam is more efficient than oven curing by 1.5 times.

In the research by Luhar et al. (Luhar et al., 2016) 48 h of curing was found to be the ideal time duration after researchers examined the effects of the duration of oven curing (24, 48, and 72 hrs) on the compressive strength of RuGPC specimens. Additionally, RuGPC's compressive strength increased with curing temperatures, though only marginally above 75 °C. Ambient curing as an alternative to heat curing is intriguing because it produces concrete with lower shrinking properties, more energy efficiency, and cracks displayed on the surface of the concrete are less compared to heat curing (Zamanabadi et al., 2019; Huseien et al., 2019). Additionally, it was revealed that RuGPC with GGBFS binder does not require thermal curing and may achieve high compressive strength under ambient curing conditions (Wardhono et al., 2017; Bilim et al., 2013).

Physical characteristics of fresh concrete

Workability, flowability

When CR aggregates are used in place of natural aggregate, concrete flow is decreased (Raffoul et al., 2016; Uygunoğlu and Topcu, 2010). For example, the slump of RuGPC was decreased by 16 %, 35 %, and 52 %, in comparison to the control specimen at 20 %, 40 %, and 60 % respectively of CR replacement of fine aggregate (Rajaei, 2021). Similarly, a 17.6 percent slump reduction was achieved when FNA and CNA were substituted with 30 % CR as opposed to the reference concrete (from 175 to 140 mm) (Dong et al., 2021). The decline in workability is attributed to the lower relative density of CR aggregates compared to natural aggregate, which reduces the concrete flowability under its self-weight (Guo et al., 2017). Additionally, CR aggregates that have undergone mechanical processing have rougher surfaces and a greater overall surface area than aggregates made from natural materials, necessitating the use of more water to reduce interparticle friction (AbdelAleem et al., 2018; Siddique and Naik, 2004). As a result of the hydrophobic characteristics of CR, the air that is trapped during mixing, yields an increase in resistance to flow and decreased workability (Rajaei, 2021).

As demonstrated in Fig. 6, in addition to the effect of CR replacement on workability, other factors that affect RuGPC flow include the NaOH molarity, ratio of sodium hydroxide to sodium silicate and AAS to A-S precursor. In comparison to OPC concrete, increasing the alkali activator solution to A-S precursor ratio is comparable to increasing the mix's water content and boosting workability (Sathonsaowaphak et al., 2009). Higher molarity of sodium hydroxide results in a stiffer fresh mixture, which reduces workability (Wongsa et al., 2018). When the ratio of sodium hydroxide to sodium silicate is raised, a similar detrimental effect on workability is seen because the additional sodium hydroxide tends to make the fresh mixture more viscous (Wongsa et al., 2018; Chindaprasirt et al., 2007). Since rougher CR aggregates offer better adhesion qualities and resistance to flow, treating them with a solution of sodium hydroxide reduces the workability of RuGPC (Ameri et al., 2020).

Setting time

The initial and final setting times of GPC increase with the addition of rubber aggregates (Chindaprasirt and Ridtirud, 2020); For instance, the initial and final setting times of GPC increased from 62, and 106 min to 85, and 135 min respectively at 10 % replacement of CR (Chindaprasirt and Ridtirud, 2020). This is partially due to the water that is found in the pores of the CR aggregates, which lead to a little increase in the water content of the mixture as a whole. Similarly, adding 2 % CR to GPC can lead to 36 % and 22 % increase in the initial and final setting durations of RuGPC, as illustrated in Fig. 7 (Arunkumar et al., 2021). In an investigation by Nath and Pabir (Nath and Sarker, 2014) the addition of GGBFS into fly ash GPC shortened the initial and final setting time. Binder with 10, 20, and 30 % of GGBFS attained initial setting time of

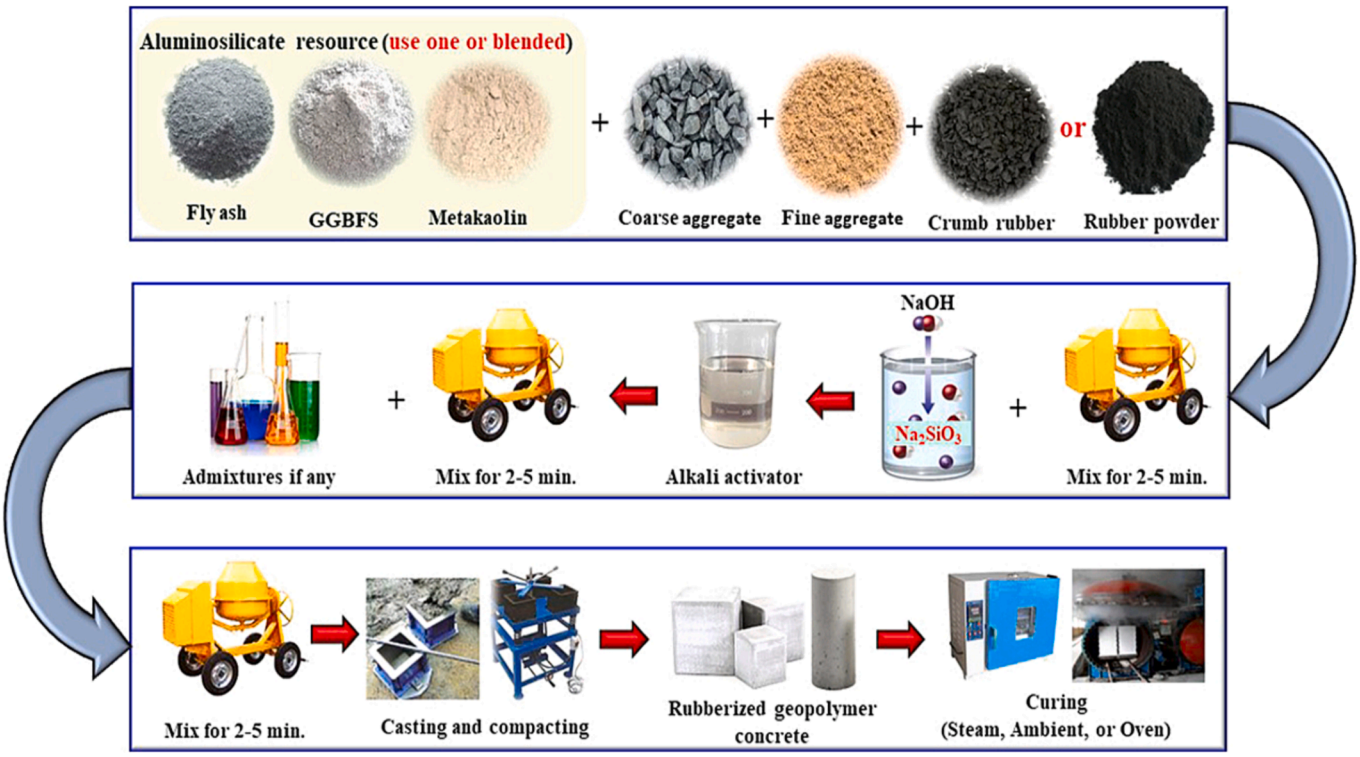

Fig. 5. Commonly used method of mixing RuGPC (Alawi Al-Sodani, 2022).

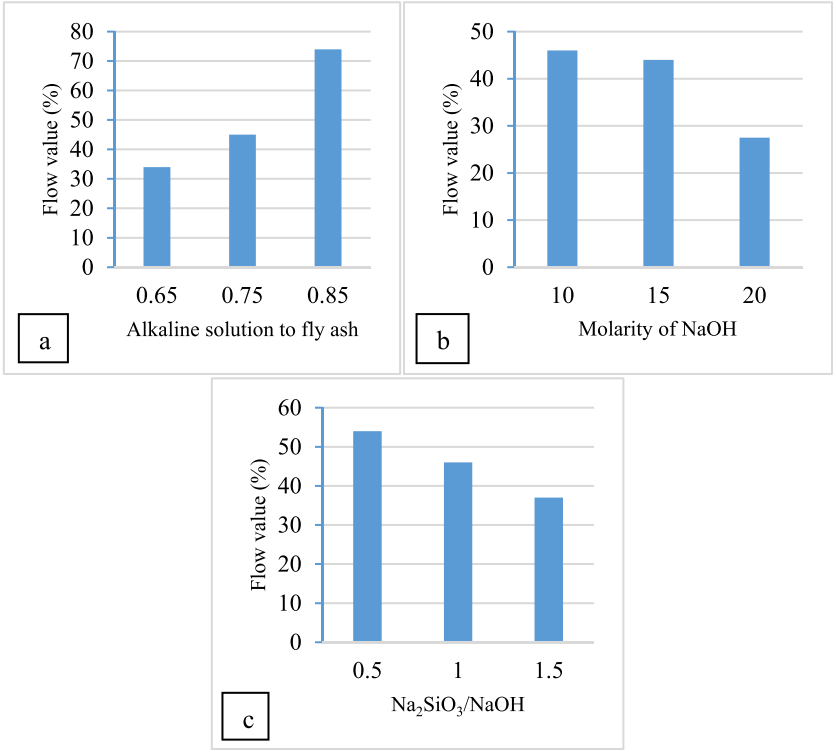

Fig. 6. Relationship of RuGPM flowability to (a) ratio of AAS to fly ash, (b) molarity of NaOH, and (c) Na_2SiO_3/NaOH (Wongsa et al., 2018).

290 min, 94 min, and 41 min respectively unlike fly ash-based GPC that took more than 1 day to show any sign of setting. This is attributed to the fact that GGBFS has a higher content of calcium oxide than fly ash (Kumar et al., 2010).

Water absorption and porosity

Porosity of the CR aggregates, the amount of trapped air in the mixture, the ratio of alkaline liquid to binder, and the specifics of the CR aggregates' interaction with the GP binder are some of the factors that affect the water absorption and porosity of RuGPC samples (Muñoz-

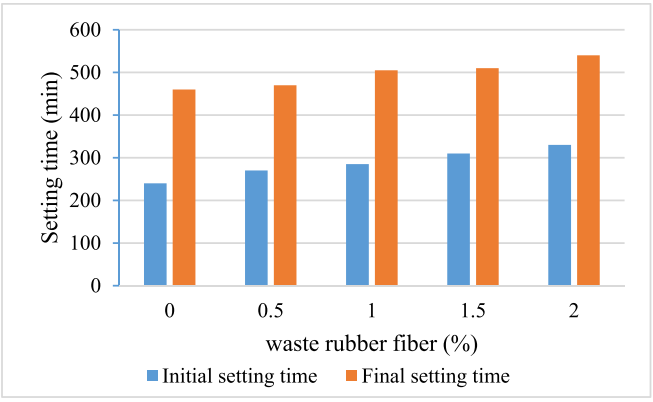

Fig. 7. Time differences between the initial and final settings of a low calcium-based GPC as a result of waste rubber fibre (Arunkumar et al., 2021).

Sánchez et al., 2017). Porosity and water absorption in GPC typically rise when CR aggregates are introduced (Azmi et al., 2019). Wongsa et al. (Wongsa et al., 2018) noticed that the porosity and water absorption of RuGPC increased by 1.5 and 5.7 times respectively at 100 % fine aggregate replacement with CR compared to the control specimen. In like manner, Dehdezi et al. (Dehdezi et al., 2015) discovered that RuGPC with 50 and 20 % fine aggregate replacements had higher porosity of 29.8 % and 27.4 % as compared to the control sample which had 23 %. This occurred due to the high CR content, which increased the overall porosity of the RuGPC by trapping more air, as depicted in Fig. 8.

Furthermore, curing RuGPC at elevated temperatures and a high molarity of sodium hydroxide are capable of reducing the porosity of RuGPC while high AAS to aluminosilicate precursor ratio can cause enhanced porosity in RuGPC (Aslani et al., 2020). In addition, as the ratio of Sodium silicate to sodium hydroxide and curing temperature went up, the RuGPC capacity to absorb water increased (Aslani et al., 2020). Due to improved adhesion between the crumb rubber aggregates and the geopolymer matrix as a result of the treating the rubber aggregates with sodium hydroxide helped to reduce the water absorbing capabilities of the rubber aggregates. Fig. 9 shows the relationship of water absorption of RuGPC and CR substitution.

Density

When the ratio of CR to natural aggregate rose, the density of RuGPC samples dropped (Lương et al., 2021). For example, Yahya, Abdullah et al. (Yahya et al., 2018) reported that when CR of size 5 mm to 10 mm was used to substitute coarse aggregate at 10 % and 20 %, the density of

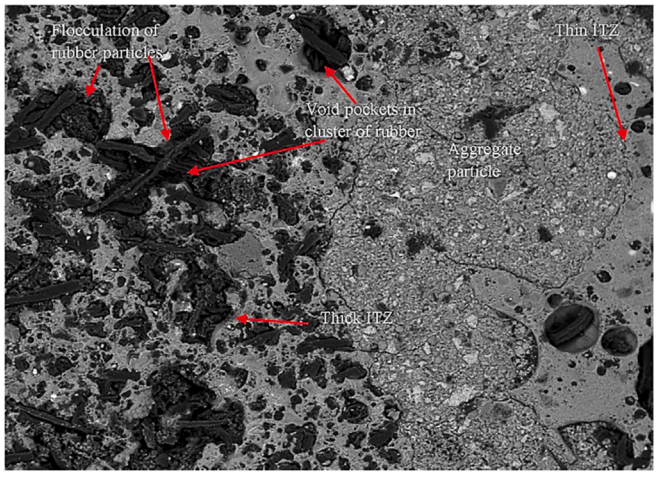

Fig. 8. SEM image of the microstructure of rubberized concrete (Dehdezi et al., 2015).

RuGPC dropped by 4.1 % and 7.2 %, respectively. The density decreased by 15.5 %, from 2340 kg/m^3 to 1980 kg/m^3, when CR was used to replace 30 % of both fine and coarse aggregate (Pham, 2020). In the investigation of rubberized geopolymer mortar with 100 % replacement of fine aggregate with rubber aggregates by Wongsa et al. (Wongsa et al., 2018) the density (between 1067 and 1275 kg/m^3) was seen to drop by 42 % as against the control specimen. Because CR aggregates have a lower relative density than natural aggregate, may be the reason for the density loss brought on by increased CR substitution of natural aggregate, their more capable interior pore size, and because of their serrated surfaces' propensity to trap air in the mixture, as shown in Fig. 10 (Ali et al., 2020).

Lower densities were found in rubberized geopolymer mortar (1075–1950 kg/m^3) compared to rubberized concrete (1299–2150 kg/m^3) replacement at the same CR percentage (25, 50, 75, and 100 %) (Zaetang et al., 2019). Portland cement has a higher specific gravity than GGBFS and fly ash which are geopolymer binders. Additionally, increasing the AAS to aluminosilicate precursor ratio resulted in a modest loss of density in RuGPC (Wongsa et al., 2018). On the other hand, raising the molarity of sodium hydroxide raises the density of RuGPC (Wongsa et al., 2018). Based on earlier research, Fig. 11 shows the density of RuGPC against CR percentage replacement. The graph depicts a reduction in density of RuGPC with corresponding increase in CR percentage replacement. As was already established, this tendency is typically due to the decreased relative density of CR aggregates as compared to natural aggregates, the fact that they can have bigger interior pores, and their propensity to cause air bubbles to form in the mixture because of their serrated surfaces. The density of RuGPC mixes, y, against the 28 days compressive strength, based on many experiments, is shown in Fig. 12. It is evident that a higher CR replacement causes a larger reduction in density and compressive strength, with RuGPM displaying lower densities than RuGPC. RuGPC with 30 % coarse aggregate replacement had the least density of 1752 kg/m^3 (5 MPa) while that of fine aggregate replacement was 1880 kg/m^3 (9.8 MPa). The density can be calculated from the supplied data by applying the following expression:

$$y = 5.1888x + 1883.6\left(R^2 = 0.1344\right) \quad (1)$$

Mechanical properties of rubberized geopolymer concrete

Compressive strength

Regardless of the curing condition, type of binder, or alkaline activator solution employed, increased CR percentage replacement in RuGPC causes a reduction in compressive strength (Aly et al., 2019; Luhar et al., 2019; Azmi et al., 2016; Dong et al., 2021; Bhavani, 1132; Wang et al., 2022; Youssf et al., 2023; Youssf, 2022; Orhan et al., 2023). Azmi et al. (Azmi et al., 2016) discovered that when fine aggregate is substituted in volume by 15 % CR in RuGPC made with fly ash resulted in a reduction of compressive strength by 60 %. Abd-Elaty et al. (Abd-Elaty et al., 2023) also recorded a reduction in 28-day compressive strength of 1 %, 9.2 %, and 12.3 % at 3, 6, and 9 % respectively of CR fine aggregate replacement. As shown in Fig. 13, Zhong et al. (Zhong et al., 2019) noted that the 28-day compressive strength fell by 36.9 % when 15 % CR was used in place of fine aggregate. Wongsa et al. (Wongsa et al., 2018) demonstrated a reduction of 93 % in the 28-day compressive strength which fluctuated between 2 and 3.3 MPa when CR aggregates replaced 100 % of fine and coarse aggregates, however the strength was within the acceptable range for lightweight concrete (2–14 MPa) (Bate, 1979).

Similar to rubberized concrete, RuGPC's compressive strength decreased as CR percentage replacement increased for the following reasons, which can be summed up as follows: (a) A weak interfacial zone develops as a result of the hydrophobic feature of CR's poor binding with the GP matrix; (ii) because the geopolymer mixture has a Modulus of elasticity that is higher than that of CR aggregates, this intensifies the

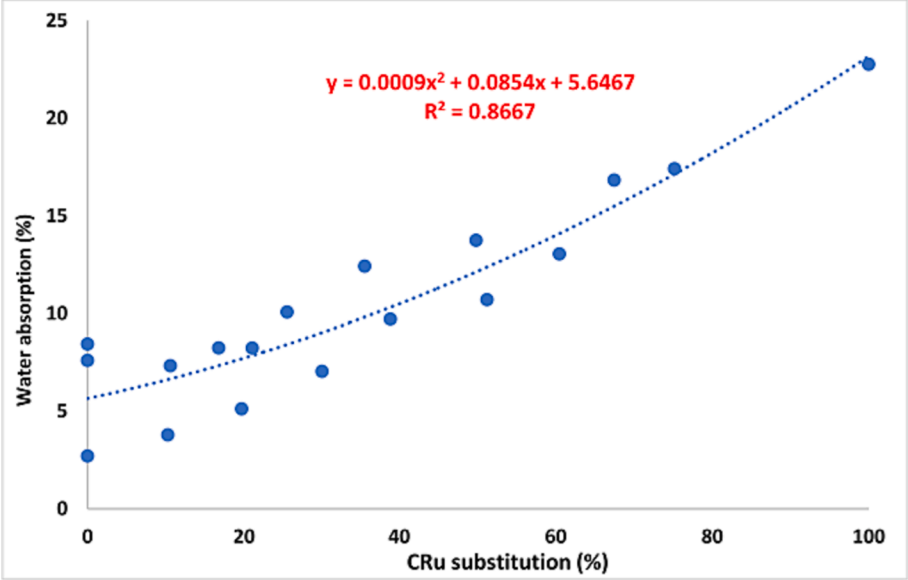

Fig. 9. Relationship between water absorption and CR percentage replacement (Dong et al., 2021; Wongsa et al., 2018; Youssf, 2022; Valente et al., 2022; Lazorenko et al., 2021).

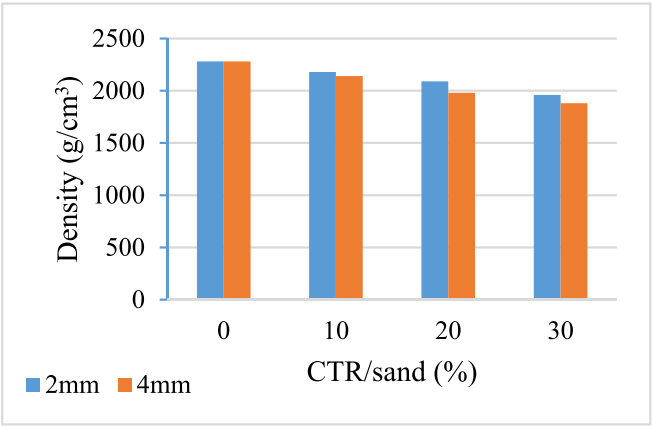

Fig. 10. Various chopped tyre rubber (CTR) with the 28-days density/sand ratios (Ali et al., 2020).

stress within them thus preempting the occurrence of microcracks around them, resulting in a loss in compressive strength; and (iii) CR aggregates' presence in RuGPC, and (iv) RuGPC mix becomes more porous and weaker in compressive strength as a result of the CR aggregates' uneven and rough surface, which causes more air bubbles to become trapped in the material.

The following factors, in addition to the rubber replacement ratio, affect the compressive strength of RuGPC: (a) the binder type, (b) the alkaline activator solution (c) the ratio of alkaline activator solution to binder content, (d) the sizes of the natural aggregates, (e) the aggregates sizes of crumb rubber, and (f) the conditions of curing. Compressive strength is substantially influenced by the amount of calcium oxide in the binder material. In the investigation by, Park et al. (Park et al., 2016) as indicated in Fig. 14 illustrates that when multiple fly ash-based RuGPC mixes were evaluated, the mixture with a greater calcium oxide concentration in the fly ash displayed the maximum compressive strength. Additionally, bigger size aggregates (50–200 m) for the same type of fly ash caused a greater reduction in compressive strength with increased CR addition with respect smaller size aggregates (1–60 m) (Park et al., 2016). Moreover, Dong et al. (Dong et al., 2021) found that the 28-day compressive strength increased by 33 % when amount of GGBFS in the fly ash based geopolymer concrete was changed from 20 to 40 % of the total binder content. This rise was unmistakably associated with GGBFS's greater calcium oxide level.

In the research by Park et al. (Park et al., 2016) the concrete with dosages of 14 molarity sodium hydroxide obtained a higher 7-day compressive strength than the mixture with 8 molarity for the same type of fly ash and CR replacement ratio, as illustrated in Fig. 15. Moreover, Luhar et al. (Luhar et al., 2016) demonstrated that as the molarity of NaOH was increased from 10 to 14 the compressive strength also rose steadily. Wongsa et al. (Wongsa et al., 2018) reported that when the sodium hydroxide solution's molarity was increased from 10 to 15 molarity, they discovered a 9.7 % rise in compressive strength; however, when the molarity was elevated even higher to 20 molarity, they discovered a 13.2 % drop in compressive strength, as seen in Fig. 16. The best molarity of sodium hydroxide for GPC was denoted as 14 (Somna et al., 2011). This demonstrates that molarity in the range of 14 and 15 of sodium hydroxide is the best molarity for enhancing compressive strength.

Furthermore, prior studies have shown that compressive strength is impacted by the ratio of sodium silicate to sodium hydroxide (Park et al., 2016). NaOH and Na_2SiO_3 are the two most popular alkaline liquids used in geo-polymerization (Xu and Van Deventer, 2000); The process of polymerization requires the alkaline liquid. Comparatively, to using simply alkaline hydroxides, polymerization proceeds rapidly when the alkaline liquid also contains soluble silica, The FA and solution react more quickly in an alkaline liquid created by mixing the solutions of NaOH and Na_2SiO_3 (Xu and Van Deventer, 2000). Also, in Park et al. (Park et al., 2016) observation, Fig. 17 illustrates the measured compressive strength improvement of up to 40.7 % when the ratio of sodium silicate to sodium hydroxide was changed from 0.5 to 2. Increasing the amount of sodium hydroxide in the mixture causes more dissolving, which improves the microstructure. However, it was established that sodium silicate to sodium hydroxide ratio that exceeds 2 had a negative impact on compressive strength. According to Luhar et al. (Luhar et al., 2016), compressive strength was enhanced by boosting the ratio of sodium silicate to sodium hydroxide from 1.5 to 2, but was diminished by raising it from 2 to 2.5. The findings show that a ratio of 2 is the ideal ratio for sodium silicate to sodium hydroxide. With respect to the control specimen, the compressive strength of RuGPC with 5, 10, 15, and 20 CR percentage replacement reduced by 7.3 percent, 10.3 percent, 18.5 percent, and 28.8 percent for ratio of sodium silicate to sodium

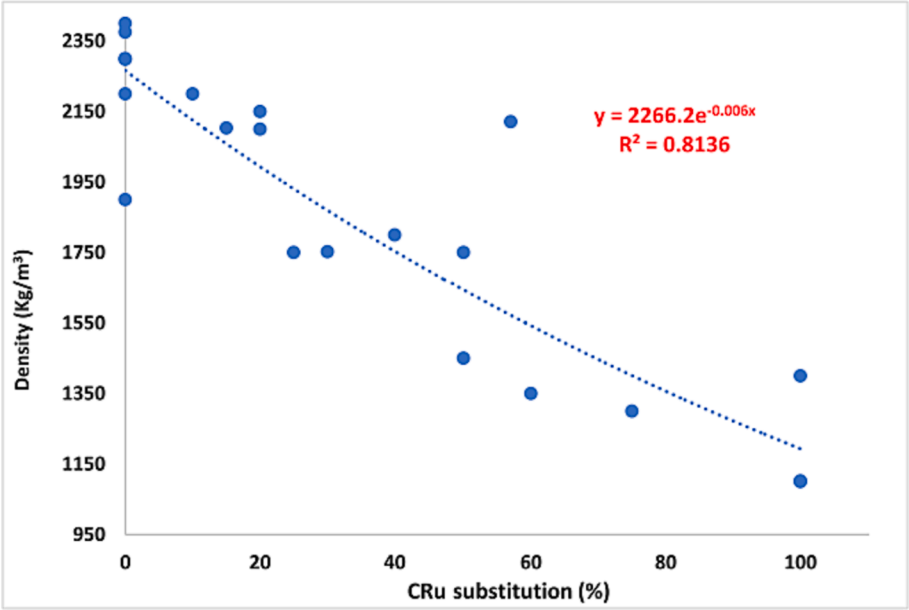

Fig. 11. The density of RuGPC versus CR substitution (Dong et al., 2021; Wongsa et al., 2018; Youssf, 2022; Valente et al., 2022; Pham et al., 2021).

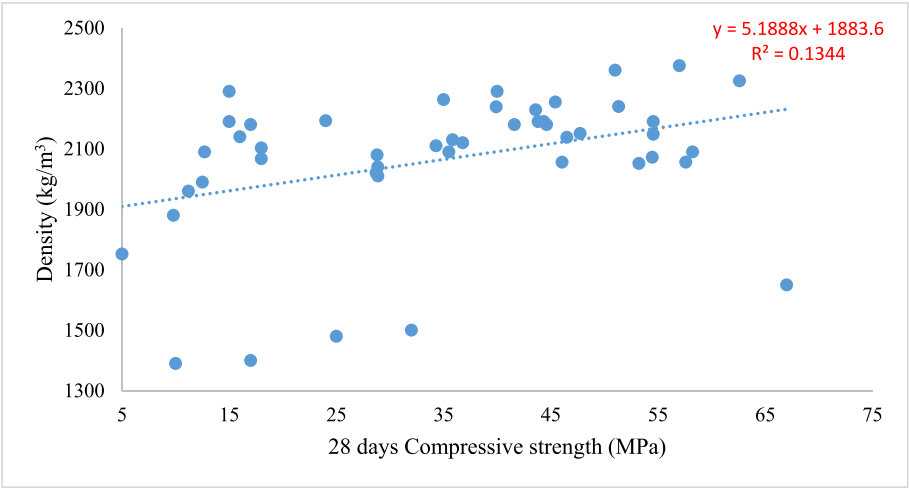

Fig. 12. Relationship between density of RuGPC and 28 days compressive strength (Dong et al., 2021; Yahya et al., 2018; Ali et al., 2020; Azmi et al., 2019; Saloni et al., 2021; Abd-Elaty et al., 2022).

hydroxide of 0.5 and 4.5 percent, 8.7 percent, 13.9 percent, and 24 percent for ratio of sodium silicate to sodium hydroxide of 2, respectively (Park et al., 2016). The compressive strength for sodium silicate to sodium hydroxide ratio of 0.5 is less than 31 MPa even in the absence of CR. Therefore, it is not advised to use RuGPC with a ratio of sodium silicate to sodium hydroxide of 0.5. To obtain a compressive strength loss of under 15 % for a geopolymer concrete made with fly ash a ratio of sodium silicate to sodium hydroxide of 2, CR can be used as a percentage replacement of natural aggregate up to 15 %. Additionally, Wongsa et al. (Wongsa et al., 2018) found that an increase in the ratio of sodium silicate to sodium hydroxide from 0.5 to 1.5, led to 11.5 % increase in the compressive strength of the Rubberized geopolymer mortar at 7- and 28-days curing. Other studies have shown that raising the ratio of sodium silicate to sodium hydroxide from 0.4 to 1.5 can increase compressive strength in a similar manner (Sathonsaowaphak et al., 2009; Chindaprasirt et al., 2007). The 60-day compressive strength of rubberized geopolymer mortar, on the other hand, declined by 11.8 % when the ratio of sodium silicate to sodium hydroxide rose from 0.5 to 1.5. Also, the 180- and 360-day compressive strength of the rubberized geopolymer mortar rose when the ratio of sodium silicate to sodium hydroxide was increased from 1.0 to 1.5 as opposed to decreasing when it was increased from 0.5 to 1.0.

By raising the alkaline activator solution to aluminosilicate precursor ratio from 0.65 to 0.85, compressive strength is reduced (Wongsa et al., 2018). While compressive strength increased with an increase in the AAS to fly ash ratio from 0.3 to 0.35, it decreased with an increase to 0.4 (Luhar and Luhar, 2020). In the research by Aslani et al. (Aslani et al., 2020) 0.4 was chosen as the ideal value after experimental testing to determine the best RuGPC mix design, which involved adjusting the alkaline activator solution to binder content ratio from 0.4 to 0.6. This suggests that for the production of RuGPC with high strength, an alkaline activator solution to binder content ratio of 0.35 to 0.4 is ideal.

Along with the foregoing, it has been shown that RuGPC mixes with smaller coarse aggregate (9.5 mm) has inferior compressive strength than RuGPC larger coarse aggregate (16 mm) (Park et al., 2016), this may be brought on by the larger aggregates' enhanced interlocking properties (Issa et al., 2000). The size of the CR aggregates can also have an impact on the RuGPC's compressive strength. Comparing rubberized

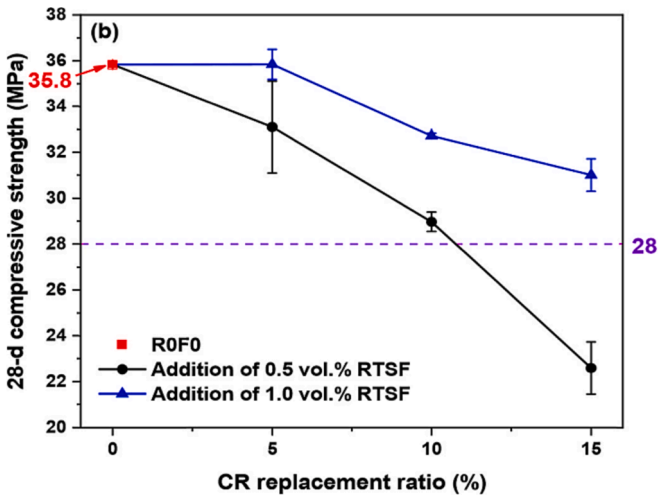

Fig. 13. Compressive strength effects of CR and recycled tyre steel fibre (RTSF) (Zhong et al., 2019).

geopolymer concrete with lesser CR aggregates (2–5 mm) we found that compressive strength was 8.2–9 % higher with respect to those with greater CR aggregates (5–10 mm) (Aslani et al., 2020). RuGPC with the same fine aggregate percentage replacement but different sizes were tested for compressive strength and RuGPC with 2 mm CR aggregates had a compressive strength that was 8.3–15.9 % higher than RuGPC prepared with 4 mm CR aggregates (Ali et al., 2020). The normalised compressive strength versus CR substitution and the correlation between the compressive strength and water absorption of RuGPC are depicted in Figs. 18 and 19, respectively, in prior research.

In order to evaluate the impact of waste rubber size aggregates on the compressive strength, RuGPC was prepared using GGBFS as binder by Abdussalam (Kaplan et al., 2019), fine natural aggregates were replaced at 5, 10, and 15 % by CR aggregates of sizes 0–1, 1–2, 2–4, and 0–4 mm respectively. The findings demonstrated that 5 % RuGPC rubber replacement and rubber size aggregates of 1–2 mm yielded the best compressive strength values of 50.16 at 3 days, 52.87 at 7 days, and 56.18 MPa at 28 days as depicted in Fig. 20. The maximum compressive strength values, meanwhile, were found in RuGPC samples made with rubber that was between 0 and 1 mm in size when the rubber percentage replacement was taken to 10 % and 15 %, respectively. Despite strength reductions of about 15–20 MPa in comparison to RuGPC with 0 % rubber content. It has been noted that for every 5 % of rubber used, the compressive strength of RuGPC reduced by nearly 50 %. In conclusion, the investigator recommends rubber sizes aggregates of 0 to 2 mm, which are in great accord with those found in (Abdelmonim and Bompa, 2021). Other reports claim that coarser CR aggregates or a combination of wide range of sizes yield higher compressive strength than finer CR (Abd-Elaty et al., 2022; Abd-Elaty et al., 2023; Sukontasukkul and Tiamlom, 2012; Guo et al., 2019; Yu and Zhu, 2016), owing to the fact that finer aggregates posses higher surface area of contact thus requiring more geopolymer paste to bond the concrete constituents into a compact

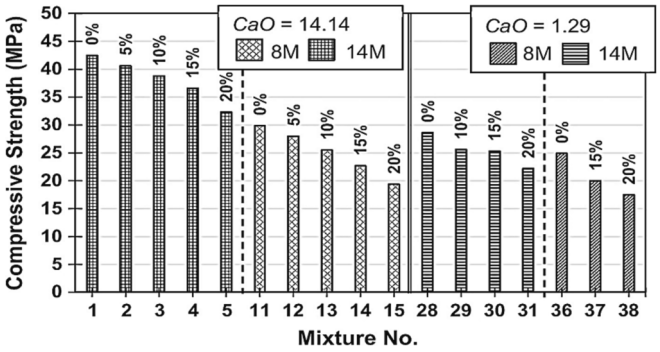

Fig. 15. Compressive strength comparisons based on molarity type (Park et al., 2016).

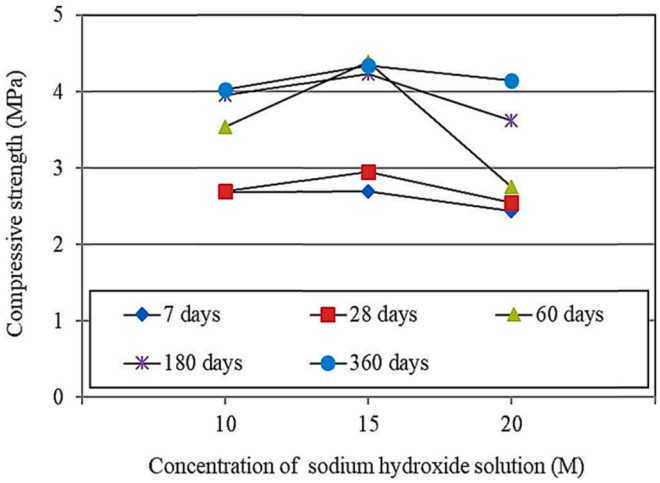

Fig. 16. Compressive strength and sodium hydroxide concentration interaction (Wongsa et al., 2018).

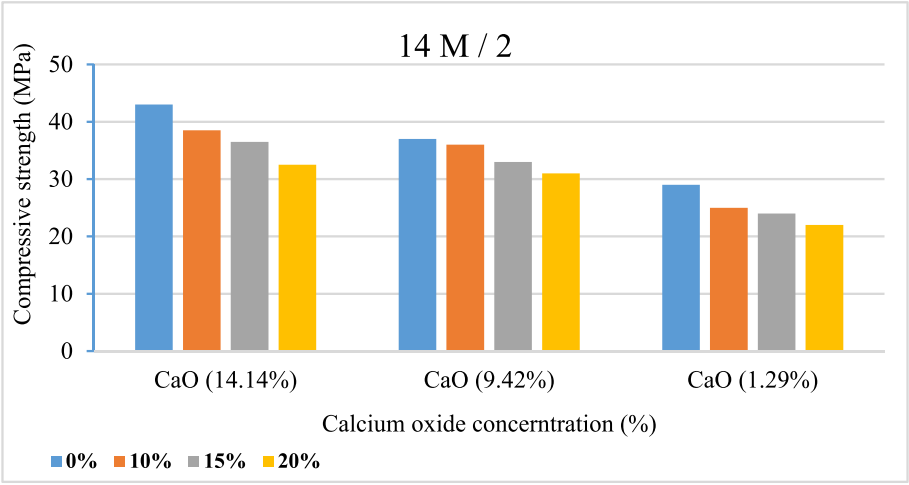

Fig. 14. Compressive strength comparisons based on fly ash type (Park et al., 2016).

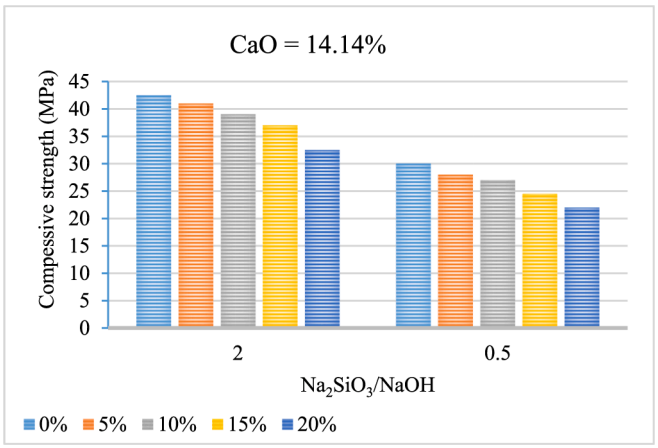

Fig. 17. Compressive strength in relation to the ratio of alkaline solutions is compared (Park et al., 2016).

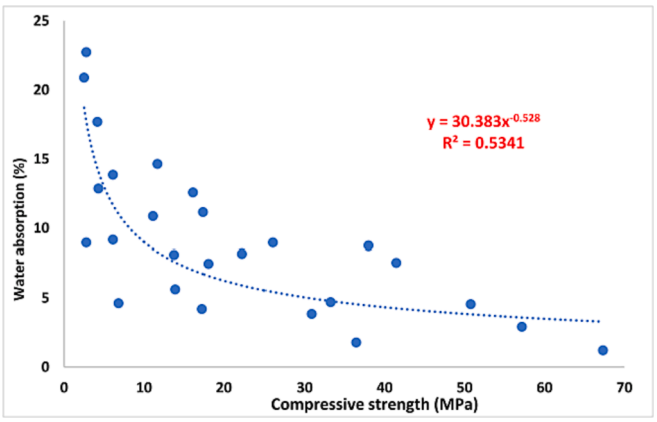

Fig. 19. The correlation between RuGPC's water absorption and compressive strength (Zaetang et al., 2019; Azmi et al., 2016; Dong et al., 2021; Wongsa et al., 2018; Rajaei, 2021).

whole. Aslani et al. (Aslani et al., 2020) observed that, compared to other RuGPC with CR aggregates at 10 % and 20 % replacements which increased the compressive strength by 3.5 % and 13.8 %, the GPC control sample displayed an increase in compressive strength by 28.3 % as the curing age increased from 7 to 28 days. These findings are consistent with all prior research in that an increase in CR percentage replacement causes a drop in the RuGPC compressive strength (Park et al., 2016; Hesami et al., 2016). The volume of CR in RuGPC has a considerably greater impact than CR aggregate size, the compressive strength at 28 days was reduced by 44.7–57.7 % at 10 % CR percentage replacement and 45.7–60 % at 20 % CR percentage replacement, as opposed to RuGPC with CR size of 2–5 mm, RuGPC with CR size of 5–10 mm demonstrated a less than 9 % drop in compressive strength over the course of 28 days.

The compressive strength of RuGPC mixtures significantly decreased in an experiment when CR was used to substitute fine aggregate because the concrete had more weak spots and increased porosity as a result of the failure of FA and CR to bond when exposed to an alkaline solution (AS), causing an increased stress from within the RuGPC perpendicular to the direction of the load applied on the concrete specimen (Charkhtab Moghaddam et al., 2021). RuGPC still outperforms rubberized concrete (RuC) in terms of compressive strength, nevertheless. Luhar et al. (Luhar et al., 2019) noted that RuGPC produced better outcomes than RuC, unlike what was found in (Luhar et al., 2019; Azmi et al., 2016), Baifa Zhang et al. (Zhang et al., 2021) observed a rising trend in the ratio of CR percentage replacement from 0 % to 10 %, which increased the compressive strength of RuGPC prepared with a combination of fly ash and GGBFS. The treatment of CR aggregates with NaOH may be responsible for this improvement in RuGPC's compressive strength. After the treating the CR aggregates prior to mixing, it is possible to increase the CR's roughness and stickiness, and the CR's alkalinity encourages the process of geopolymerization (Youssf et al., 2016). However, as the binder/aggregate ratios were increased and the w/b ratios were decreased, the strength of GPC made with fly ash as binder rose. Similar results were seen in earlier research (Saeli et al., 2019; Haruna et al., 2021). Furthermore, because geopolymer concrete is more durable than only the geopolymer matrix, the binder/aggregates ratio is crucial in the development of GPC's strength. In another investigation, Hamidi et al. (Hamidi et al., 2022) observed higher 28-day compressive strengths of RuGPC with NaOH treated CR coarse aggregate replacement at 5, 10, 15, and 20 % of 21, 41, 26, and 23 MPa respectively compared to the control which had 16 MPa. The 10 % CR aggregate replacement

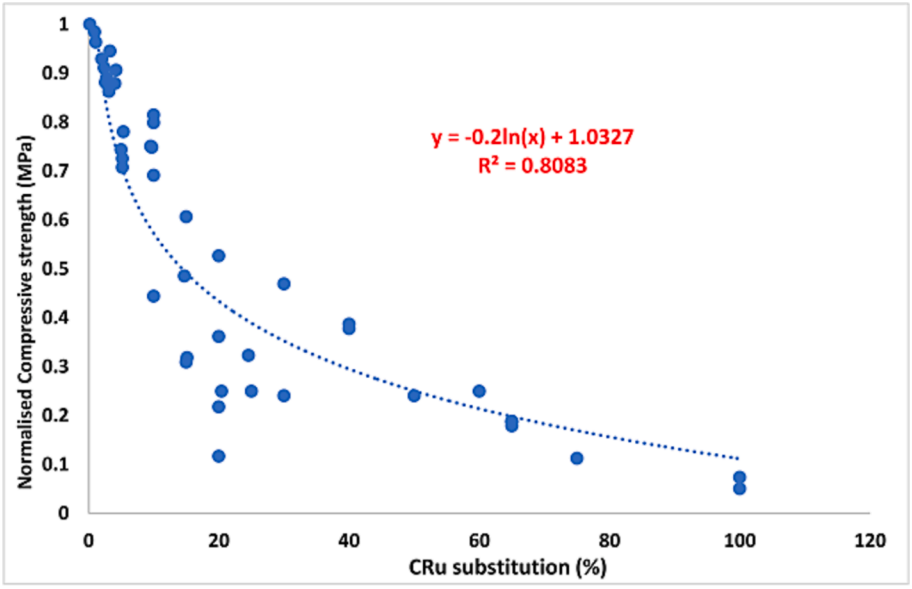

Fig. 18. RuGPC's compressive strength in comparison to CR replacement (Aly et al., 2019; Park et al., 2016; Charkhtab Moghaddam et al., 2021; Luhar et al., 2019; Dong et al., 2021; Wongsa et al., 2018; Saloni et al., 2021; Pham, 2020; Youssf, 2022; Lazorenko et al., 2021; Zhang et al., 2021).

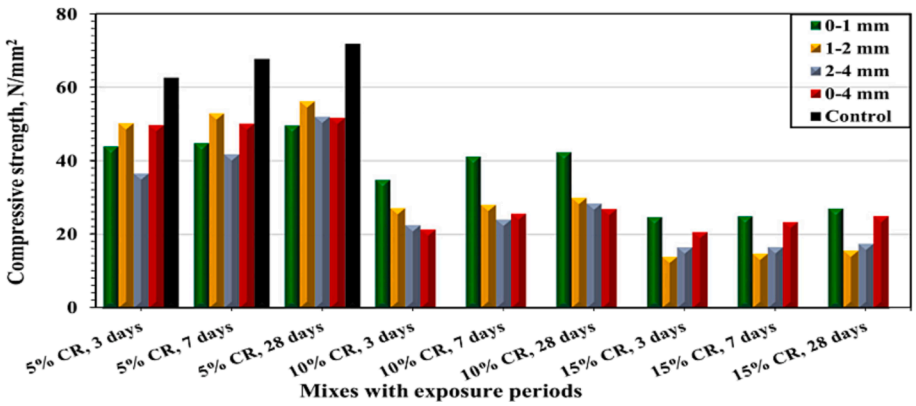

Fig. 20. CR aggregate size and replacement ratio's impact on RuGPC's compressive strength (Sarkaz, 2020).

had the highest result with an increase in compressive strength of 65, 73, and 161 % at 3, 7, and 28 % in comparison to the control specimen. The increased strength recorded at 10 % CR replacement over the control is attributed to the ability of the rubber aggregates to fill the voids with the RuGPC and form a denser microstructure or better adhesion with the geopolymer matrix and binder. However, as the CR content increased the interfacial zone between the CR and the geopolymer matrix became weak propagating cracks when subjected to loading thereby reducing the compressive strength. They concluded that 10 % CR was ideal for structural purposes as it yielded a workable RuGPC.

Bhavani et al. (Bhavani, 1132) introduced zeolite binder and treated rubber aggregates with NaOH to see its effect on the compressive strength of RuGPC. There was about 10–12 % improvement in the compressive strength of RuGPC from 28 to 56 days, recording 63 to 80 MPa at 28 days and 65 to 89.7 MPa at 56 days at 0 % and 20 % replacements respectively as shown in Fig. 21. The reason for the decrease in compressive strength with the introduction of CR is because of lack of proper bond between the CR aggregates and the geopolymer matrix caused by the hydrophobicity of rubber aggregates. In any case, the pretreating the rubber aggregates with 1 M of NaOH was seen to increase the strength at 28 and 56 days. Reason been that the treatment changed the hydrophobic nature of rubber to hydrophilic thus promoting adhesion between the CR and other concrete constituents (Saloni et al., 2021). Increased compressive strength is also attributed to the introduction of zeolite that helped in eradicating the pores in the RuGPC (Bhavani, 1132). It can be concluded that the water absorption capacity of RuGPC with and without treated CR is higher and lower respectively than that of GPC. RuGPC also displayed less resistance to attack by HCL and H_2SO_4.

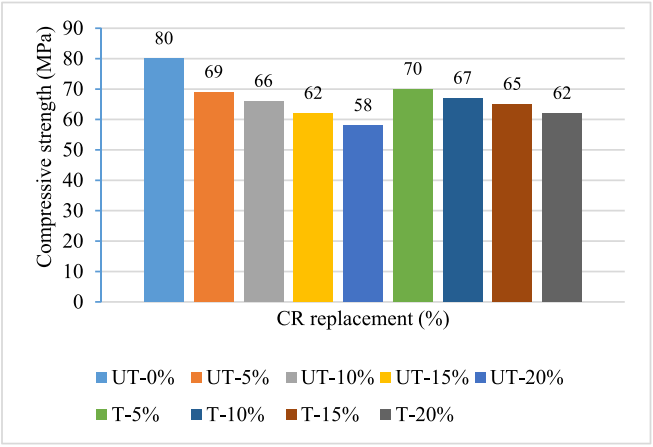

Fig. 21. Effect of GGBS, Zeolite and treatment on FA – Based RuGPC (Bhavani, 1132).

Igbal et al. (Iqbal, 2023) also worked on improving the compressive strength of fly ash based RuGPC with CR as 10, 20, and 30 % fine aggregate replacement by introducing graphene nanoplatelets (GNPs) into the mix. The compressive strength decreased by 15, 29, and 49 % at 10, 20, and 30 % CR replacements respectively owing to the voids formed because of entrapped air due to the hydrophobic nature of rubber aggregates and the poor ITZ that increases cracks in the system when a load is applied. The addition of GNPs by weight of the binder at 0.1 %, 0.2 %, 0.3 %, and 0.4 % raised the compressive strength by 6 %, 12 %, 18 %, and 14 %, respectively, with respect to the control specimen; with 0.3 % producing the best result. The microhardness of 30 % CR specimen increased by 34 % at the addition of 0.3 % GNPs proving that GNPs improves the compactness of the geopolymer paste and the ITZ between the paste and the CR. Fig. 22a, b and c shows the correlation between RuGPC 28-days compressive strength and mix ratios from previous research.

A lot of previous review papers have claimed that the addition of crumb rubber into GPC leads to reduction in compressive strength. However, some recent research has proven it otherwise as this effect can be countered by optimizing the pretreatment of the CR, in contrast to GPC with 0 % CR content, the addition of crumb rubber from 5 % to 10 % at $NaSiO_3$ to NaOH ratio of 2.5 and binder content above 400 kg/m^3 employing a combination of FA and GGBFS as binders was able to boost compressive strength by 5.5 % and 7 %, respectively.

The least compressive strength for RuGPC at 20 % replacement of coarse aggregate by CR was 15 MPa (67 % reduction from the control specimen). Similar results are also achieved when fine aggregate is replaced with CR in a class F FA-based GPC with CaO content of less than 2 % and sodium silicate of less than 1.0. FA class F with CaO of between 5 % and 10 % was applied in most of the research and they yielded amazing 28-days compressive strengths in RuGPC from 5 to 10 % CR replacement either as fine or coarse aggregate.

The introduction of zeolite into GPC with FA and GGBFS enhanced the compressive strength massively giving it the highest compressive strength of 62 MPa at 20 % and 2.5 % CR replacement of fine and coarse aggregate respectively. This qualifies it for application in high strength concrete. Furthermore, graphene nanoplatelets (GNP) introduction into RuGPC also enhanced it compressive strength achieving the highest strength at 0.3 % of the binder. The microhardness of 30 % CR specimen increased by 34 % at the addition of 0.3 % GNPs proving that GNPs improves the compactness of the geopolymer paste and the interfacial transition zone between the paste and the CR.

The results also confirm that treating CR with NaOH can increase its compressive strength than when it is soaked in water or not subjected to any form of treatment regardless of the binder type, molarity or sodium silicate to sodium hydroxide ratio. However, where the molarity of NaOH is high i.e., 16 M and above, treatment by water soaking is enough

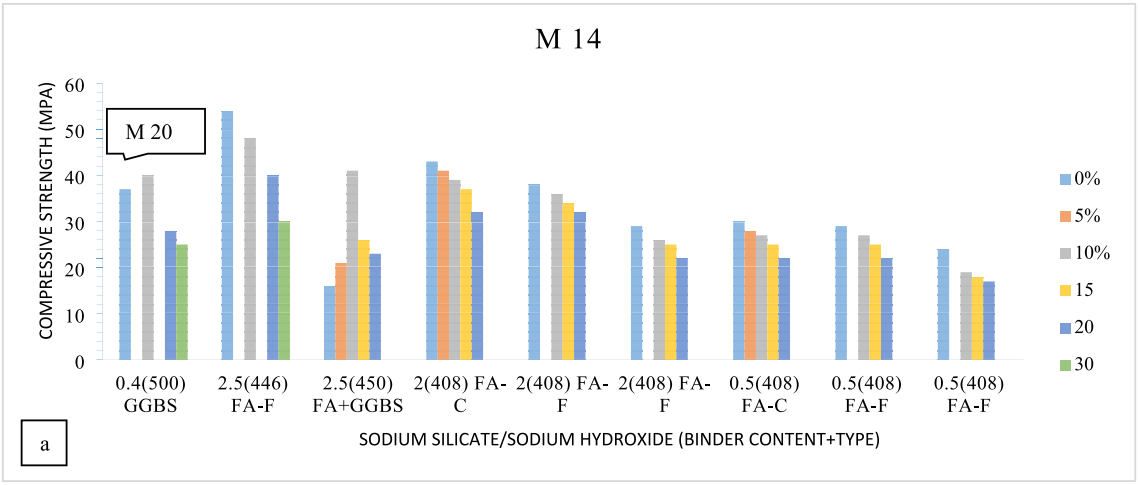

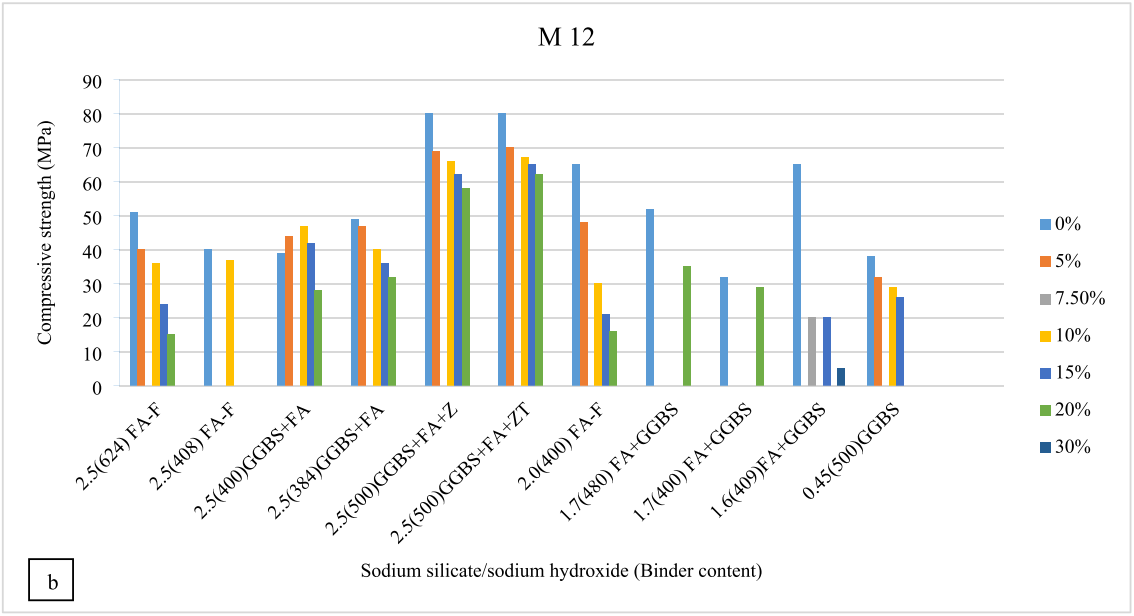

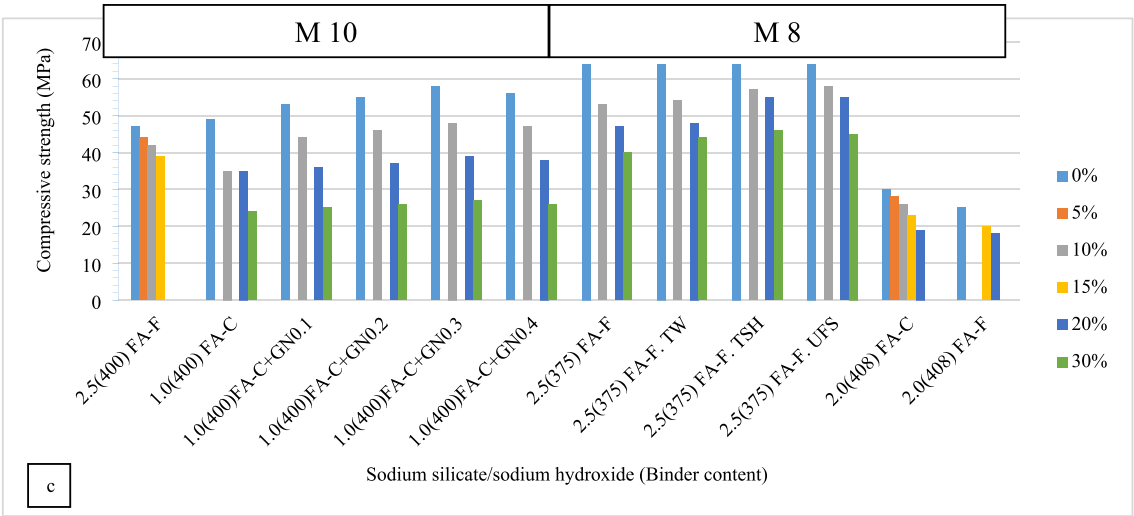

Fig. 22. (a, b and c) The relationship between RuGPC 28-days compressive strength and mix ratios at different NaOH molarity (Aly et al., 2019; Park et al., 2016; Charkhtab Moghaddam et al., 2021; Luhar et al., 2019; Azmi et al., 2016; Dong et al., 2021; Bhavani, 1132; Yahya et al., 2018; Saloni et al., 2021; Wang et al., 2022; Youssf et al., 2023; Youssf, 2022; Valente et al., 2022; Orhan et al., 2023; Zhang et al., 2021; Gill et al., 2023).

as the high concentration of sodium hydroxide in the solution will foster adhesive bond between the geopolymer matrix and the rubber aggregates.

The binder content is directly proportional to the ratio of alkaline activator solution to aluminosilicate precursor which is in the range of 0.35 to 0.5 from previous research. High CaO content in GGBFS and Class C FA shortens the initial setting time drastically thus requiring a higher percentage of retarder, high molarity of NaOH (14 to 20 M) and NaOH content twice the amount or more than that of sodium silicate. This will increase the water content in the geopolymer matrix thus increasing the workability while the high molarity of NaOH and CaO content will handle the bonding force and strength respectively. However, it was observed that GGBS does not attain its maximum compressive strength at 28 days even though its initial setting time may be short. On the other, it is not advisable to use to use sodium silicate to sodium hydroxide of 0.5 on class F Fly ash as it negatively affects the bonding of the concrete constituents, the microstructure and thus the strength.

RuGPC with sodium silicate to sodium hydroxide ratio at 2.5 gave the best results at 28 days compressive strength from 0 % to 30 % CR replacement. At 10 % replacement of CR fine or coarse aggregate replacement 28 days strengths above 40 MPa can be achieved provided the molarity is not below 8 M. However, at molarities of 10 M to 8 M it is advisable to treat the CR with NaOH for a minimum target strength of 25 MPa at 30 % CR fine aggregate replacement, and further introduce either zeolite or 0.3 % graphene nanoplatelets when the target strength is above 40 MPa at 30 % CR fine aggregate replacement.

The combination of GGBFS and class F FA as binders gave the highest strength results as they complement each other in terms of early and late 28-days compressive strength, because fly ash has a low hydration modulus, just a modest quantity of GGBFS helps to increase the early age strength needed for demolding. However, there is no defined percentage ratio for combining both binders in a mix. Since CaO affects the strength and setting time of both binders from Table 1 and applied in previous research, Class F with high CaO content (>5%) had either higher percentage over GGBFS or 50:50 in the combination while Class F with low CaO content (<5%) had lower percentage than GGBFS in the combination.

When crumb rubber was used as coarse aggregate replacement or coarse and fine aggregate replacements, the mix should be designed for high design strength (binder content of 450 to 600 +) due to the percentage reduction in strength (from Table 4) to enable RuGPC at 20 or 30 % CR replacement achieve a strength within the desired limits. This concrete can be applied in areas where impact or energy absorption is important, as RuGPC with CR as coarse aggregate replacement has higher impact resistance and energy absorption capabilities the fine aggregate RuGPC (see section 2.6.2).

It can be concluded that by increasing the amount of aluminosilicate gel, which lowers the amount of void formation, an increase in binder dose from 375 to 500 kg/m^3 results in a denser microstructure and higher compressive strength qualities irrespective of the CR content as a result of huge amount of products available for the geopolymerization reaction. When the binder content exceeds 500 kg/m^3 the percentage increase in compressive strength reduces because of improper compaction resulting to poor workability due to the constant alkaline liquid to binder ratio. This can be taken care of with a naphthalene-based superplasticizer and extra water.

Splitting tensile strength

Aslani et al. (Aslani et al., 2020) found that replacing natural fine aggregate with CR at 10 % and 20 % reduced the 28-day split tensile strength by 18.6 % (1.84 MPa) and 19.5 % (1.82) respectively, with respect to the control specimen. With natural aggregate substituted by 30 % CR, Aly et al. (Aly et al., 2019) reported a 35.5 % decrease in splitting tensile strength, In contrast, Dong et al. (Dong et al., 2021) showed a comparable decline in splitting tensile strength, recording 3.5, 1.2, and 0.7 MPa at 0 %, 15 % and 30 % respectively of CR percentage replacement of coarse aggregate (about 65 % and 80 % reduction in split tensile strength with respect to the control specimen) as can be seen in Fig. 23. The reasons for this decrease are the creation of a weaker interfacial transition zone that surrounds the CR aggregates and less adhesion between the CR aggregates and the surrounding mixture of the geopolymer concrete because of rubber's hydrophobic properties. Fig. 24.

Furthermore, Iqbal et al. (Iqbal, 2023) investigated the split tensile of fly ash-based RuGPC with CR replacing natural fine aggregate by volume from 10 to 30 %. The result showed a steady decrease in the split tensile strength with a percentage increase in CR content. At CR percentage replacement of 30 %, the split tensile strength decreased by 38 % in comparison to the control specimen. Hamidi et al. (Hamidi et al., 2022) worked and enhancing the splitting tensile strength of RuGPC with CR of size 10-mm as replacement of coarse aggregates at 5, 10, 15, and 20 %. The control had early and lateral tensile strengths of 1.15 and 1.16 MPa which were lower than that of RuGPC. The RuGPC with 10 % CR displayed the best tensile strength of 2.353 MPa, as percentage replacement above 10 % decreased the split tensile strength of RuGPC. This may be because the cylinder fails longitudinally when subjected to a tension force, and the increased voids in the mixture result from the increase in CR aggregates (Hamidi et al., 2020; Aslani and Asif, 2019). In another investigation, Aly et al. (Aly et al., 2019) investigated the splitting tensile strength of GGBS-based-RuGPC with CR at 10, 20, and 30 % of fine, and coarse aggregate replacements. The 28-day split tensile strength at 10, 20, and 30 % CR replacement was reduced by 34.60, 23, and 35.5 % respectively in comparison to the control specimen. Normally the tensile strength of concrete is about 10 % lower than that of compressive strength and its strain limits. In every scenario, concrete tensile strength is a key factor in the design of airfields and artificial slabs, just like in situations where resistance to shear and crack are paramount. These shortfalls are heightened by the introduction of CR aggregate to GPC. If the tensile strength is generally trending downward, the same factors that affect compressive strength may be at blame. However, there are lots of parameters that influence the connection between split tensile strength and compressive strength, namely, the curing regime, shape and type of aggregate, and particle size distribution (sieve analysis) (Youssf and Elgawady, 2012). Abd-Elaty et al. (Abd-Elaty et al., 2022) worked on rubberized geopolymer mortar (RuGPM) replacing fine aggregate with CR of sizes 0–1 mm, 1–3 mm, 4 mm at 10, 20, and 30 %. Irrespective of the CR aggregate size the 28-day split tensile strength dropped by an average of 12.3 % at 10 % CR aggregate replacement, besides the reduction in split tensile strength is largely affected by the percentage replacement of CR more than its size. However, finer CR aggregates are seen to have more impact on the split tensile strength than coarse aggregates. The RuGPM flexural strength of 20 % CR for type RA and RD dropped by 38 % and 19 % respectively. The result correlates with those of previous research (Aly et al., 2019).

The decrease in strength is associated with the hydrophobic property of rubber aggregates, hence an increase in CR content reduces the adhesive force at the ITZ between the geopolymer matrix and the CR aggregates thus allowing for the occurrence of cracks and progression of cracks at weak interfacial transition zone due to rupture of bonding force between the CR aggregates and paste under tension. Air bubbles are also trapped within the concrete by rubber aggregates that generate voids (Hamidi et al., 2022), which makes the GPC paste weaker in strength and thus the entire concrete. This is the reason why RuGPC with more than 10 % CR has higher zones of localized failure (Hamidi et al., 2020), 5 % CR geopolymer concrete had a 28-day tensile strength 37.5 % lower than that of the 10 % CR replacement (Hamidi et al., 2022) which could be as a result of limited CR aggregates in the mix to occupy the pores within the paste that reduces the compactness of the concretes' microstructure.

However, when Bhavani et al. (Bhavani, 1132) introduced zeolite binder and treated rubber aggregates with NaOH to see its effect on the

Table 4
Summary of the 28 – days approximate strengths and mix ratios of RuGPC.

Aluminosilicateprecursor (AP)	CR Aggregate rep (%)		AAS/AP orBc	NaOH (M)	AAS Ratio	CR Rep. (%)							Ref
	FA	CR				0	5	7.5	10	15	20	30	
28-days compressive strength (MPa)													
GGBFS	10, 20, 30	10, 20, 30	500	20	0.4	37			40		28	25	(Aly et al., 2019)
GGBFS **(KOH)**	5, 10, 15		500	12	0.45	38	32		29	26			(Orhan et al., 2023)
GGBFS		5, 10, 15	500	12	–	40	38		36	35			(Yolcu et al., 2022)
GGBFS		5, 10, 15	400	12	–	37	36		35	34			(Yolcu et al., 2022)
GGBFS		5, 10, 15	300	12	–	20	18		16	14			(Yolcu et al., 2022)
Class C-FA [CaO: 14.14 %]Disc	5, 10, 15, 20		408	14	2.0	43	41		39	37	32		(Park et al., 2016)
	5, 10, 15, 20		408	14	0.5	30	28		27	25	22		(Park et al., 2016)
	5, 10, 15, 20		408	8	2.0	30	28		26	23	19		(Park et al., 2016)
Class C-FA	10, 20, 30		400	10	1.0	49			42		35	24	(Iqbal, 2023)
Class CFA,**0.1 %GNP**	10, 20, 30		400	10	1.0	53			44		36	25	(Iqbal, 2023)
Class CFA,**0.2 %GNP**	10, 20, 30		400	10	1.0	55			46		37	26	(Iqbal, 2023)
Class CFA,**0.3 %GNP**	10, 20, 30		400	10	1.0	58			48		39	27	(Iqbal, 2023)
Class CFA,**0.4 %GNP**	10, 20, 30		400	10	1.0	56			47		38	26	(Iqbal, 2023)
Class F-FA (mortar)	10, 20, 30		625	16	2.5	51			42		36	29	(Abd-Elaty et al., 2022)
Class F-FA (mortar)	10, 20, 30		625	16	2.5	51			45		34	28	(Abd-Elaty et al., 2022)
Class F-FA (mortar)	10, 20, 30		625	16	2.5	51			44		36	29	(Abd-Elaty et al., 2022)
Class F-FA (mortar)	10, 20, 30		625	16	2.5	51			43		37	29	(Abd-Elaty et al., 2022)
Class F-FA		5, 10, 15, 20	624	12	2.5	51	40		36	24	15		(Yahya et al., 2018)
Class F-FA (mortar)	10, 20, 30		500	14	2.5				25		22	19	(Giri, 2023)
Class F-FA (mortar)	10, 20, 30		500	12	2.5				18		17	13	(Giri, 2023)
Class F-FA (mortar)	10, 20, 30		500	10	2.5				13		12	11	(Giri, 2023)
Class F-FA	10, 20, 30		446.43	14	2.5	54			48		40	30	(Luhar et al., 2019)
Class F-FA [CaO: 9.42 %]	10, 15, 20		408	14	2.0	38			36	34	32		(Park et al., 2016)
	10, 15, 20		408	14	0.5	29			27	25	22		(Park et al., 2016)
Class F-FA [CaO: 1.29 %]Disc	10, 15, 20		408	14	2.0	29			26	25	22		(Park et al., 2016)
	10, 15, 20		408	14	0.5	24			19	18	17		(Park et al., 2016)
	15, 20		408	8	2.0	25				20	18		(Park et al., 2016)
Class F-FA	10		408	12	2.5	40			37				(Charkhtab Moghaddam et al., 2021)
Class F-FA	5, 10, 15, 20		400	12	2.0	65	48		30	21	16		(Azmi et al., 2016)
Class F-FA	5, 10, 15		400	10	2.5	47	44		42	39			(Gill et al., 2023)
Class F-FA	10, 20, 30		375	8	2.5	63			53		47	40	(Saloni et al., 2021)
Class F-FA. **TW**	10, 20, 30		375	8	2.5	63			54		48	44	(Saloni et al., 2021)
Class F-FA. **TSH**	10, 20, 30		375	8	2.5	63			57		55	46	(Saloni et al., 2021)
Class F-FA. **UFS**	10, 20, 30		375	8	2.5	63			58		55	45	(Saloni et al., 2021)
(Class F FA 35 %, Zeolite 5 %), GGBS (40:60): **TSH**	5, 10, 15, 20	2.5	500	12	2.5	80	70		67	65	62		(Bhavani, 1132)

(*continued on next page*)

Table 4 (*continued*)

Aluminosilicateprecursor (AP)	CR Aggregate rep (%)		AAS/AP orBc	NaOH (M)	AAS Ratio	CR Rep. (%)							Ref
	FA	CR				0	5	7.5	10	15	20	30	
(Class F FA 35 %, Zeolite 5 %), GGBS (40:60)	5, 10, 15, 20	2.5	500	12	2.5	80	69		66	62	58		(Bhavani, 1132)
FA, GGBS (50:50). Disc	20		480	12	1.7	52					35		(Youssf, 2022)
FA,GGBS (78:22). **TW**		5, 10, 15, 20	450	14	2.5	16	21		41	26	23		(Hamidi et al., 2022)
FA, GGBS (80:20).	15, 30		409	12	1.6	65				20		5	(Dong et al., 2021)
FA, GGBS (80:20)	7.5	7.5	409	12	1.6	65		20					(Dong et al., 2021)
Class F FA, GGBS (50:50)	20, 40, 60		400	12	1.7	32					29		(Youssf et al., 2023)
Class F FA, GGBS (50:50)	5, 10, 15, 20		400	12	2.5	39	44		47	42	38		(Zhang et al., 2021)
FA, GGBS (50:50)	5, 10, 15, 20		384	12	2.5	49	47		40	36	32		(Wang et al., 2022)
28-days split tensile strength (MPa)													
GGBFS	10, 20, 30	10, 20, 30	500	20	0.4	3.6			3.4		2.8	2.3	(Aly et al., 2019)
GGBFS		5, 10, 15	500	12	–	3.5	3.6		3.9	4.0			(Yolcu et al., 2022)
GGBFS		5, 10, 15	400	12	–	3.3	3.4		3.5	3.6			(Yolcu et al., 2022)
GGBFS		5, 10, 15	300	12	–	2.1	2.4		2.5	2.7			(Yolcu et al., 2022)
Class C-FA	10, 20, 30		400	10	1.0	4.4			3.9		3.3	2.6	(Iqbal, 2023)
Class CFA,**0.1 %GNP**	10, 20, 30		400	10	1.0	4.8			4.2		3.5	2.8	(Iqbal, 2023)
Class CFA,**0.2 %GNP**	10, 20, 30		400	10	1.0	5.1			4.5		3.7	2.8	(Iqbal, 2023)
Class CFA,**0.3 %GNP**	10, 20, 30		400	10	1.0	5.5			4.8		3.9	3.0	(Iqbal, 2023)
Class CFA,**0.4 %GNP**	10, 20, 30		400	10	1.0	5.3			4.6		3.8	2.9	(Iqbal, 2023)
Class F-FA (mortar)	10, 20, 30		625	16	2.5	4.1			3.6		2.5	2.48	(Abd-Elaty et al., 2022)
Class F-FA (mortar)	10, 20, 30		625	16	2.5	4.1			3.8		2.8	2.3	(Abd-Elaty et al., 2022)
Class F-FA (mortar)	10, 20, 30		625	16	2.5	4.1			3.6		2.9	2.2	(Abd-Elaty et al., 2022)
Class F-FA (mortar)	10, 20, 30		625	16	2.5	4.1			3.6		3.4	2.9	(Abd-Elaty et al., 2022)
Class F-FA	10, 20, 30		446.43	14	2.5	5.0			5.1		5.2	5.3	(Luhar et al., 2019)
Class F-FA	10, 20, 30		375	8	2.5	4.7			4.2		3.9	3.6	(Saloni et al., 2021)
Class F-FA. **TW**	10, 20, 30		375	8	2.5	4.7			4.3		4.0	3.8	(Saloni et al., 2021)
Class F-FA. **TSH**	10, 20, 30		375	8	2.5	4.7			4.5		4.3	3.9	(Saloni et al., 2021)
(Class F FA 35 %, Zeolite 5 %), GGBS (40:60): **TNaOH**	5, 10, 15, 20	2.5	500	12	2.5	5.6	5.1		5.3	5.3	4.2		(Bhavani, 1132)
(Class F FA 35 %, Zeolite 5 %), GGBS (40:60)	5, 10, 15, 20	2.5	500	12	2.5	5.6	5.2		4.9	4.2	4.0		(Bhavani, 1132)
Class F FA, GGBS (50:50)	5, 10, 15, 20		400	–	2.5	3.2	4.0		4.3	3.8	3.5		(Zhang et al., 2021)
FA, GGBS (50:50)	5, 10, 15, 20		384	12	2.5	4.9	4.5		3.5	3.1	2.7		(Wang et al., 2022)
28-days flexural strength (MPa)													
GGBFS		5, 10, 15	500	12	–	7.3	7.4		7.5	7.8			(Yolcu et al., 2022)
GGBFS		5, 10, 15	400	12	–	6.5	7.2		7.3	7.5			(Yolcu et al., 2022)
GGBFS		5, 10, 15	300	12	–	2.4	3.2		3.2	3.8			(Yolcu et al., 2022)
Class C-FA	10, 20, 30		400	10	1.0	6.4			5.5		4.7	3.4	(Iqbal, 2023)
Class CFA,**0.1 %GNP**	10, 20, 30		400	10	1.0	7.1			6.1		5.0	3.7	(Iqbal, 2023)
Class CFA,**0.2 %GNP**	10, 20, 30		400	10	1.0	7.5			6.3		5.2	3.8	(Iqbal, 2023)
Class CFA,**0.3 %GNP**	10, 20, 30		400	10	1.0	8.2			6.7		5.4	4.0	(Iqbal, 2023)
Class CFA,**0.4 %GNP**	10, 20, 30		400	10	1.0	5.5			5.8		5.5	5.4	(Iqbal, 2023)

(*continued on next page*)

Table 4 (*continued*)

Aluminosilicateprecursor (AP)	CR Aggregate rep (%)		AAS/AP orBc	NaOH (M)	AAS Ratio	CR Rep. (%)							Ref
	FA	CR				0	5	7.5	10	15	20	30	
Class F-FA (mortar)	10, 20, 30		625	16	2.5	6.8			5.7		5.2	4.9	(Abd-Elaty et al., 2022)
Class F-FA (mortar)	10, 20, 30		625	16	2.5	6.8			5.1		4.5	3.8	(Abd-Elaty et al., 2022)
Class F-FA (mortar)	10, 20, 30		625	16	2.5	6.8			5.57		4.97	3.9	(Abd-Elaty et al., 2022)
Class F-FA (mortar)	10, 20, 30		625	16	2.5	6.8			5.6		5.2	4.7	(Abd-Elaty et al., 2022)
Class F-FA	10, 20, 30		500	14	2.5				3.1		2.8	2.5	(Giri, 2023)
Class F-FA	10, 20, 30		500	12	2.5				2.7		2.3	2.3	(Giri, 2023)
Class F-FA	10, 20, 30		500	10	2.5				2.4		1.9	1.7	(Giri, 2023)
Class F-FA	10, 20, 30		446.43	14	2.5	6.4			6.5		6.7	6.8	(Luhar et al., 2019)
Class F-FA	5, 10, 15		400	10	2.5	5.3	5.1		4.9	4.5			(Gill et al., 2023)
Class F-FA	10, 20, 30		375	8	2.5	5.5			5.1		4.7	4.4	(Saloni et al., 2021)
Class F-FA. **TW**	10, 20, 30		375	8	2.5	5.5			5.2		4.8	4.6	(Saloni et al., 2021)
Class F-FA. **TSH**	10, 20, 30		375	8	2.5	5.5			5.3		5.2	4.8	(Saloni et al., 2021)
FA,GGBS (78:22). **TW**		5, 10, 15, 20	450	14	2.5	2.1	2.0		4.8	3.4	3.5		(Hamidi et al., 2022)
FA, GGBS (50:50)	5, 10, 15, 20		384	12	2.5	5.3	4.4		3.5	2.9	2.5		(Wang et al., 2022)

CR = crumb rubber, AAS = Alkaline activator solution (NaOH, KOH, Na_2SiO_3), B_c = Binder content, TSH: Treated with NaOH, TW: Soaked in water, GNP: Graphene nanoplatelets.

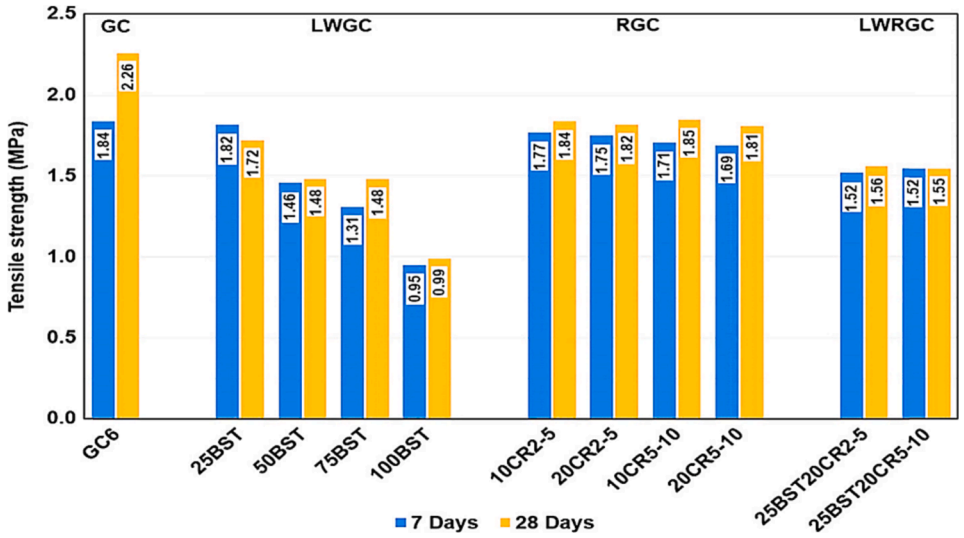

Fig. 23. The 7 and 28 days tensile strength of geopolymer concrete (GC), lightweight geopolymer concrete (LWGC), rubberized geopolymer concrete (RGC), and lightweight rubberized geopolymer concrete (LWRGC) mixes (Aslani et al., 2020).

split tensile strength of RuGPC, different trends were observed. RuGPC was made with CR replacing fine aggregate at 5, 10, 15, 20 % while coarse aggregates were replaced by rubber at 2.5 %. The factors that caused reduction in compressive strength are the same that negatively affected the splitting tensile strength. The introduction of treated CR, and zeolite somewhat increase the splitting tensile strength up to G7 after which the effect of the zeolite was subdued by increased CR percentage. The control specimen had a tensile strength of 5.57 MPa while that of treated RuGPC was 5.25 at 10 and 15 % CR replacement, untreated RuGPC had the least result of 4 MPa at 20 % replacement. Once again, it proves the improvement in the surface of rubber aggregate (hydrophobic to hydrophilic) brought about by NaOH pretreatment, that increases the adhesion between CR aggregate and other concrete constituents (Huan-xiu et al., 2007), and the presence of zeolite that helped to reduce the porosity of RuGPC thus increasing its strength properties (Bhavani, 1132).

Iqbal et al. (Iqbal, 2023) investigated the effect of graphene nanoplatelets (GNPs) on the split tensile strength of fly ash-based RuGPC with CR replacing natural fine aggregate by volume from 10 to 30 % and the inclusion of GNPs at 0.1 to 0.4 % by weight of the geopolymer binder. The result showed that the incorporation of GNPs improved the split tensile strength of RuGPC up to 0.3 %, after that it began to decline. The

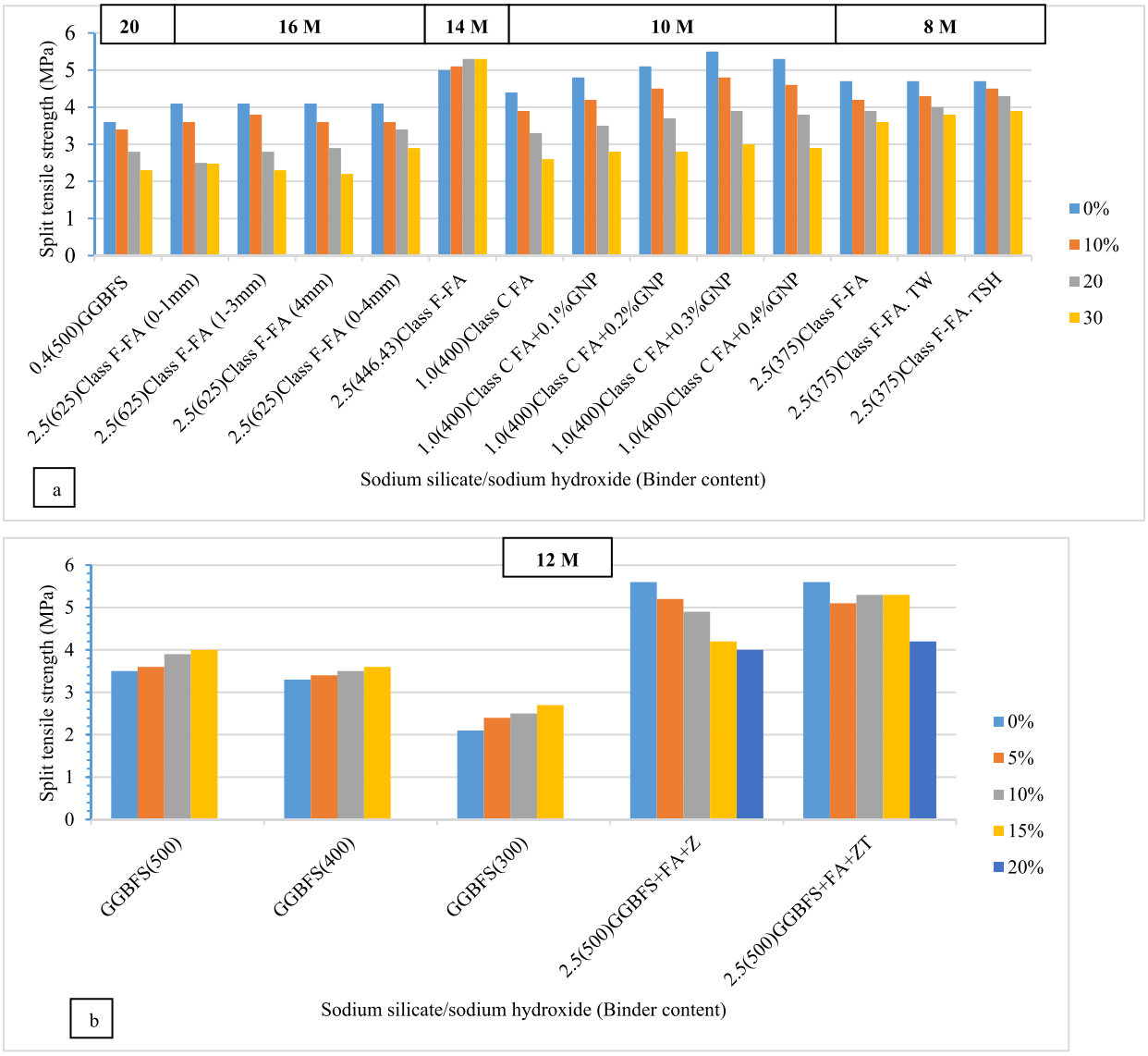

Fig. 24. (a, b) The relationship between RuGPC 28-days splitting stensile strength and mix ratios at different NaOH molarity (Aly et al., 2019; Luhar et al., 2019; Bhavani, 1132; Saloni et al., 2021; Wang et al., 2022; Abd-Elaty et al., 2022; Zhang et al., 2021; Iqbal, 2023; Giri, 2023).

addition of 0.3 % GNPs increased the split tensile strength of RuGPC with 10 % CR by 13 % over the GPC control specimen without GNPs. The increased strength is attributed to the ability of GNPs to bridge and divert the cracks in the RuGPC specimen (Ranjbar et al., 2015). In addition, an improvement was observed in the geopolymer paste microhardness by the GNPs, which proves an increase in the compactness of the geopolymer matrix and the interfacial zone due to the presence of GNPs that yielded an increased strength.

Luhar et al. (Luhar et al., 2019) compared the split tensile strength of RuGPC and OPC concrete. Both concrete displayed split tensile strength between 5.34 and 5.49 MPa at 365 days, with RuGPC having higher strength than that of OPC concrete reason being that the geopolymer matrix bonded better with aggregates than the cement paste (Rangan, 2008; Sofi et al., 2007). The GPC control specimen had the least split tensile strength at 28 days while RuGPC with 30 % CR fine aggregate replacement had the highest split tensile strength at 365 days. They reported that an increase in the percentage replacement of CR aggregate led to an increase in the split tensile strength of RuGPC from 0 % to 30 %, as was also observed by (Fernandez-Jimenez et al., 2006). During the split test, it was observed that no aggregate fell off in the RuGPC specimen unlike that of the OPC specimen and this is attributed to the strong geopolymeric bond that exists between aggregates and the geopolymer matrix, as a result of the chemical bond between the aggregates and the alkaline liquid (Andrews-Phaedonos, 2008).

Flexural strength

Similar to compressive strength, RuGPC's flexural strength declined correspondingly as the percentage of CR aggregate replacement increased (Long et al., 2018). With an application of 10 % and 20 % CR as a surrogate of natural coarse and fine aggregate in RuGPC, Aly et al. (Aly et al., 2019) reported that flexural strength dropped by up to 20 % and 30 % respectively. A loss in flexural strength of up to 74 % was reported by Rajaei et al. (Rajaei, 2021) when CR was used as a fine aggregate surrogate at 60 %, as seen in Fig. 25.

In another experiment, Zaetang et al. (Zaetang et al., 2019) reported reductions of 61.4 % to 77.3 % in flexural strength at 50 % and 100 % respectively of CR aggregate percentage replacement of coarse, and fine aggregates in comparison to the control specimen. Furthermore, Iqbal et al. (Iqbal, 2023) investigated the flexural strengths of fly ash-based RuGPC with CR replacing natural fine aggregate by volume from 10 to 30 %. The result showed a steady decrease in the flexural strength with a percentage increase in CR content. At CR percentage replacement of 30

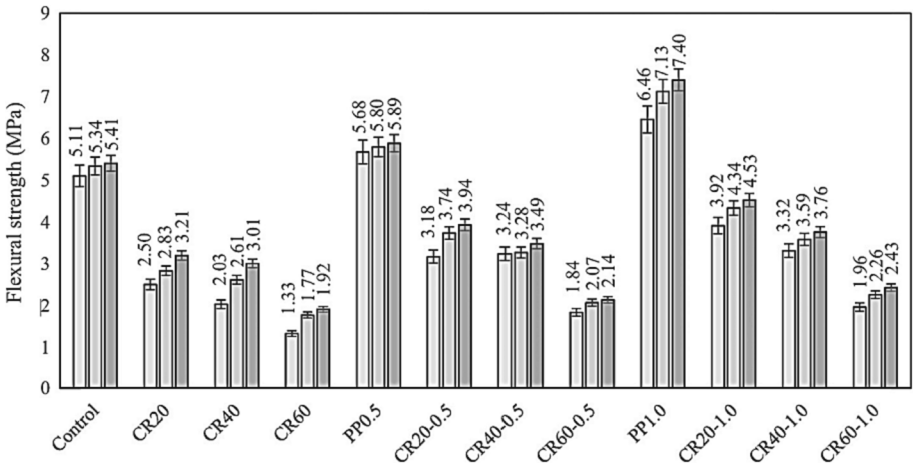

Fig. 25. Flexural strength of GPC at various ages (Rajaei, 2021).

% the flexural strength decreased by 43 %. Aly et al. (Aly et al., 2019) investigate the flexural strength of GGBS-based-RuGPC with CR at 10, 20, and 30 % of fine, and coarse aggregate replacements. The introduction of CR at 20, and 30 % reduced the flexural strength by 30 % at a flexural force of 1.75 KN, however at 10 % the flexural strength reduction was 20 % at a force value of 2.00 KN with respect to the control specimen. A similar trend in reduction of strength was recorded by Gill et al. (Gill et al., 2023) where fine aggregate CR replacement at 5, 10, and 15 % caused the flexural strength to reduce by 3.52 %, 8.23 %, and 14.92 % respectively. Low CR aggregate adhesion to the geopolymer paste is mostly to blame for the decline in flexural strength.

Abd-Elaty et al. (Abd-Elaty et al., 2022) worked on rubberized geopolymer mortar replacing fine aggregate with CR of sizes 0–1 mm, 1–3 mm, 4 mm at 10, 20, and 30 %. Irrespective of the CR sizes used the flexural strength decreased with an increase in CR aggregate replacement. The flexural strength dropped by 17 % and 44 % at 10 and 30 % CR aggregate percentage replacement respectively. Aslani et al. (Aslani et al., 2020) in his report approved the CR aggregate size on the flexural strength of RuGPC with GGBFS as binder. The least flexural strength was recorded by RuGPC of sizes 1–2 mm at 20 % CR replacement while 5 % CR replacement with rubber sizes of 0–1 mm yielded the highest flexural strength. About 80 to 90 % of the flexural strengths were observed after 3-days curing. Sarkaz (Sarkaz, 2020) observed that GPC specimen had flexural strength 6 % higher than those of RuGPC. However, it was noticed that RuGPC with 20 % CR and sizes 2–5 mm had flexural strengths 29 % lower than that of the control specimen. The fact that the prism is not reinforced is the cause for this reduction, as the capacity of the beam in flexure was controlled by the tensile strength. In this case the flexural strength appears to be proportional to the tensile of compressive strength of the specimen. In contrast to the findings for compressive strength, CR content has a significantly smaller impact on flexural strength than CR size. The 28-day flexural strength of RuGPC with 10 % and 20 % CR was reduced by 0–5.6 and 2.2–29 %, respectively. While RuGPC with CR sizes of 2–5 and 5–10 mm shown increases in flexural strength of 6 % and 38 %, respectively, after 28 days.

Hamidi et al. (Hamidi et al., 2022) report contradicted the reduction in flexural strength with CR percentage increase. They worked on enhancing the flexural strength of RuGPC with CR of size 10-mm as replacement of coarse aggregates at 5, 10, 15, and 20 %. The RuGPC mixes outperformed that of the control specimen in terms of early-age flexural strength, and this difference was most noticeable for the mixes containing 10 %, 15 %, and 20 % CR aggregates, similar to report by (Abd-Elaty et al., 2023). The 10 % CR produced the highest 28-day flexural strength with an increase of 114 % over that of the control specimen. Gupta et al. (Gupta et al., 2014) and Bisht and Ramana (Bisht and Ramana, 2017) also reported a decline in the flexural strength of GPC with a corresponding increase in the percentage replacement of CR. The irregularity in the shape of the CR aggregates prevented the formation of adequate bonds between the rubber aggregates and the geopolymer matrix, thereby reducing the compactness of the microstructure that led to the reduction in RuGPC flexural strength. Other reasons could be the lack of proper bonding between the geopolymer matrix and CR aggregate coupled with the discrepancies in stiffness between CR and nominal aggregates.

Iqbal et al. (Iqbal, 2023) investigated the effect of graphene nanoplatelets (GNPs) on the flexural strength of fly ash-based RuGPC with CR replacing natural fine aggregate by volume from 10 to 30 % and the inclusion of GNPs at 0.1 to 0.4 % by weight of the geopolymer binder. The result showed that the incorporation of GNPs improved the flexural strength of RuGPC up to 0.3 %, after that it began to decline. The flexural strengths of RuGPC increased by 5, 8, 15, and 11 % at 0.1, 0.2, 0.3, and 0.4 % of GNPs, with the 0.3 % GNPs displaying the highest strength. The increased strength is attributed to the ability of GNPs to bridge and divert the cracks in the RuGPC specimen (Ranjbar et al., 2015). In addition, an improvement was observed in the geopolymer paste microhardness by the GNPs, which proves an increase in the compactness of the geopolymer matrix and the interfacial zone due to the presence of GNPs that yielded an increased strength.

Luhar et al. (Luhar et al., 2019) compared the flexural strength of RuGPC and OPC concrete and observed that the strength increased with age. The flexural strength of OPC concrete was in the range of 5.35 to 6.86 MPa, while that of RuGPC was between 6.45 and 9.97 MPa proving that OPC has flexural strength lower than that of RuGPC. Similar results were noted in some past research (Guelmine et al., 2016; Lee and Van Deventer, 2004). The characteristics of OPC concrete are inferior to those of geopolymer concrete under tension (split tensile and flexural strengths) due to the enhanced bond between the aggregates and the geopolymer matrix. They reported an increase in the flexural strength of OPC and RuGPC as the percentage replacement of CR increased. This is attributed to the presence of CR aggregates that close the crack gap initiated by the applied load. Previous research also augments this report (Ganesan et al., 2013; Segre and Joekes, 2000). Table 4 summarizes the 28 days approximate strengths results and mix ratios of RuGPC.

Most of the previous research reported reduction in the compressive strength of RuGPC with percentage increase in CR from 30 % and above. Increment was recorded from 5 % to 20 % in some cases, and 10 % replacement recording the highest increase of 161 % with workability suitable for structural design purpose. In the same vein, much research reported decrease in splitting tensile and flexural strengths, with increases recorded at 10 %, 15 % and 30 % in some cases favoring its application in the design of airfield slabs and concrete pavement. The

weak bond between the rubber aggregates and other geopolymer concrete constituents is the reason for the reduction in mechanical properties. Treating CR aggregates improves the interfacial bond, and further introduction of zeolite or graphene nanoplatelets improves the compression and bending qualities of CR with the binder. This is the major reason for why the mechanical properties increased in some reports and decreased in other reports. Reports also suggest the addition of micro silica and steel fiber improves the mechanical properties of RuGPC. Many other factors that affect the mechanical properties of RuGPC are the binder content, the molarity of sodium hydroxide, size of CR aggregates and particle size distribution, and alkaline activator solution. For precast structural elements, the superplasticizer and extra water are key factors that affects the strength characteristics of the elements as it prolongs the initial setting time, enables flowability and efficient compaction during casting. It is worth noting that the mechanical properties of RuGPC have shown the potentials to outperform NC, RuC and even GPC if research is conducted on the improving the interfacial bond between crumb rubber and the geopolymer matrix.

Elasticity modulus of RuGPC

As additional CR was used as a surrogate for natural aggregate, the elasticity modulus of RuGPC samples fell (Luhar et al., 2019). For RuGPC produced with CR as 15 % and 30 % coarse aggregate replacement, the 28-day elasticity modulus reduced by 39 % and 74 % at 15 and 30 % replacement respectively giving values of 18.2 and 7.8 GPa in comparison to the control sample which had a value of 30 GPa (Dong et al., 2021). Rajaei et al. (Rajaei, 2021) reported similar results, noting reductions in the elasticity modulus of RuGPC with CR as fine aggregate surrogate at 20.9 %, 40.9 %, and 60.0 % by approximately 29 %, 66.9 %, and 81.9 % respectively. According to Luhar et al. (Luhar et al., 2019), 30 % incorporation of CR aggregates into RuGPC as fine aggregate replacement by weight, as illustrated in Fig. 26, yielded a 36.3 % reduction in the elasticity modulus of RuGPC. Due to the deformability and softness of the CR aggregates, there is a drop in the elasticity modulus of RuGPC as CR percentage replacement rises. Concrete that is more elastic and has a lower elasticity modulus can be made by using CR in place of natural aggregate (Carroll and Helminger, 2016).

Abd-Elaty at al. (Abd-Elaty et al., 2022) worked on rubberized geopolymer mortar (RuGPM) replacing fine aggregate with CR of sizes 0–1 mm, 1–3 mm, 4 mm at 10, 20, and 30 %. They observed that using finer CR aggregates resulted in a higher reduction in the elasticity modulus of RuGPM. The elasticity modulus was reduced by 23.3 % and 35 % at 20 and 30 % respectively of CR replacement. Iqbal et al. (Iqbal, 2023) also reported a reduction in the elasticity modulus of RuGPC with 0 % and 30 % CR giving values of 24.63 GPa and 14.53 GPa respectively. This is attributed to the fact that rubber aggregate has stiffness and elasticity modulus lower than that of natural aggregates (Albidah et al., 2022; Qaidi et al., 2021). Previous research also mentioned that the increased CR percentage replacement reduces the homogeneity of RuGPC (Luhar et al., 2019), which decreases both the elasticity modulus and strength of RuGPC. In addition, because CR is softer than natural aggregate and has a higher tendency to deform this negatively affects the modulus of elasticity of RuGPC (Qaidi, 2022). Iqbal et al. (Iqbal, 2023) investigated the effect of graphene nanoplatelets (GNPs) on the elasticity modulus of fly ash-based RuGPC with CR replacing natural fine aggregate by volume from 10 to 30 % and the inclusion of GNPs at 0.1 to 0.4 % by weight of the geopolymer binder. They observed improvements in the elasticity modulus of RuGPC when GNPs were added to the mix. The elasticity modulus of RuGPC at 10, 20, and 30 % CR improved by 20, 21, and 20 % respectively at 0.3 % addition of GNPs and was the highest result. This increase in elasticity modulus is attributed to the nanoplatelets' high modulus properties (Sanchez and Sobolev, 2010), which increases their load-carrying capacity and eventually their elasticity modulus and strength characteristics.

Luhar et al. (Luhar et al., 2019) compared the elasticity modulus of fine aggregate RuGPC and OPC concrete. GPC and OPC concrete had elasticity modulus in the range of 20 to 31.5 GPa and 18 to 27.5 GPa respectively. The addition of rubber up to 30 % into the mix reduced the elasticity modulus of the concrete by 34.54 and 36.34 % for OPC and RuGPC respectively. The elasticity modulus of GPC concrete is dependent on the microstructure of the geopolymeric matrix regardless of the source. This causes a reduction in the elasticity modulus of GPC and OPC as the percentage replacement of CR increases. The result proves that the control specimen has more rigidity than RuGPC specimens, which is why the elasticity modulus of RuGPC reduced with increased rubber content, as was also observed in previous investigations (Fernandez-Jimenez et al., 2006).

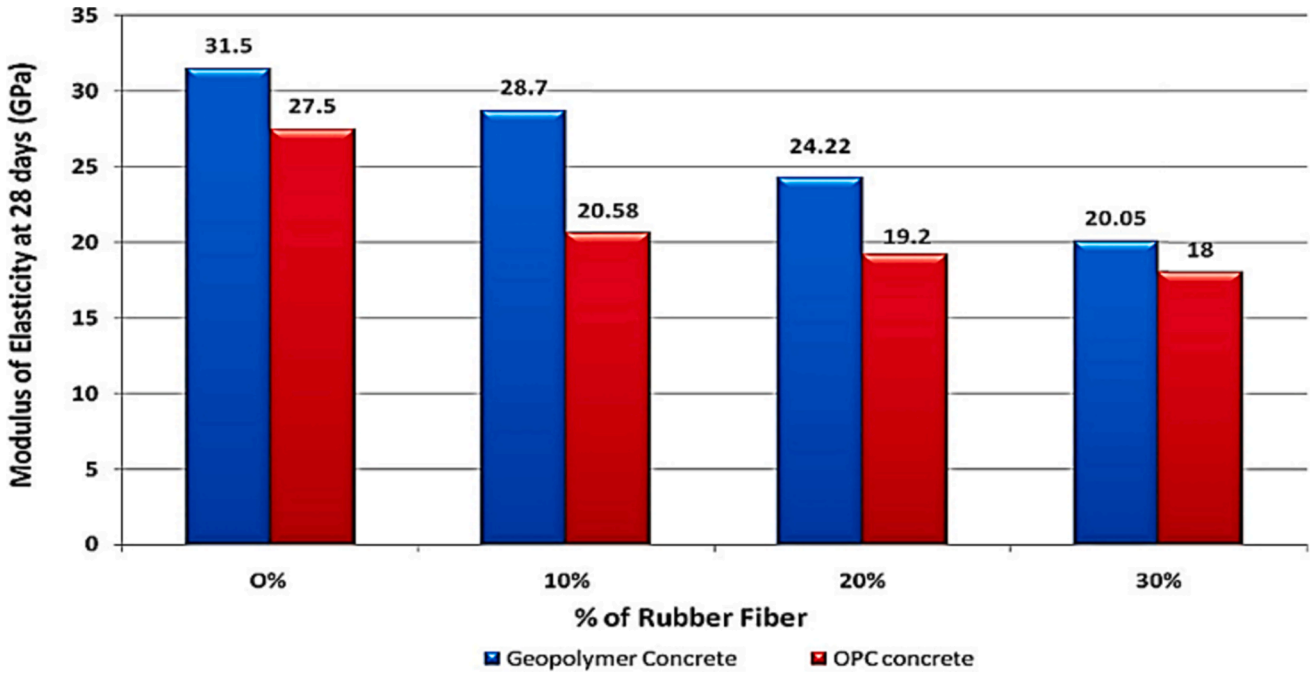

Fig. 26. Elasticity Modulus of GPC with different CR % and OPC (Luhar et al., 2019).

Stress–strain relationship

Analysis of the sample's stress–strain relationship is necessary to determine how well CR aggregates affect the curvature of deflection and their flexural behavior when subjected to compressive force. According to the results of the 28-day test, the stress–strain relationship for GPC control specimen, GPC with rubber aggregates, and Lightweight GPC all cured at ambient temperature is shown in Fig. 27 from the study of Hamidi et al. (Hamidi et al., 2022). From Fig. 27 the control geopolymer concrete (CGC) specimen got to a 1.136 micro-strain at a region of hardening deflection at a peak stress of 16.55 MPa. This indicates that the control specimen resisted plastic deformation micro-strain of 0.836 before getting to the yield point. Percentage replacement of CR in the geopolymer concrete at RGC5, RGC10, RGC15, and RGC20 (i.e., 5, 10, 15, and 20 %) was made to deform at peak stresses of 19.5, 40.9, 27.45, and 22.8 MPa by micro-stain of 1.45, 2.17, 0.92, and 1.14 respectively, before it got to the yield point. Hence all RuGPC specimens had elongated hardening deflection and bigger peak stress than the control specimen, recording the highest result at 10 % CR replacement. This implies that RuGPC has the capability to resist higher forces of compression and still maintain its structural integrity before getting the yield point.

The spiralding arm of the stress–strain relationship consists of two separate zones, the preliminary ascending linear area and the zone of non-linear strain-hardening when the normal stress–strain relationship for conventional concrete under compression was taken into account, according to the authors. Until the weight reaches the cracking limit of the binder, the concrete will behave elastically in compression without cracks within the cement paste. The strength of the sample increases with the slope of the linear section, suggesting that the concrete will deflect less before developing cracks. The concrete experiences permanent plastic deformation in the non-linear strain-hardening zone due to the interaction between the paste and the aggregates that causes the formation of a number of microcracks inside the cement matrix, until it hits the yield point, which is the highest amount of compression stress that concrete can tolerate, (Nath and Sarker, 2017; Aslani et al., 2020). The first section of the curve which is elastic covers around 40 % of the highest load (Bashar et al., 2016), the percentage of the stress equal to 40 % of the related strain and strength at yield can be used to compute the elasticity modulus of the concrete specimen (Aslani and Jowkarmeimandi, 2012). The ductile region is contained in the sloped branch of the curve in the stress–strain relationship, where a lot of little fissures appear in the concrete, and the ductility characteristics of the concrete are defined by these small, localized fissures (Aslani et al., 2020; Bashar et al., 2016). It is interesting to note that strain hardening region and peak stress increased by 49.6 % and 109.8 % at 5 % and 10 % CR aggregate replacements. However, they reduced by 57.8 % and 32.9 % at 15 % CR aggregate replacement and 47.5 % and 44.23 % at 20 % CR aggregate replacement, with respect to RuGPC with 10 % CR aggregate replacement. Compared to conventional concrete, the GPC stress–strain profile is similar. Zhong et al. (Zhong et al., 2019) studied the deflection characteristics of RuPGC reinforced with steel fibers, and 100 % CR as fine aggregate replacement which can be seen in Fig. 28. They found that increasing the steel fibre dose lengthened the deflection-hardening phase while decreasing the elastic efficacy of the RuGPC reinforced with steel fiber.

In a prior study, Hamidi et al. (Hamidi et al., 2022) summarised their findings by stating that curvature of the stress–strain relationship of RuGPC also showed that 10 % CR aggregates might be the ideal concentration of rubber aggregate inside GPC matrix to be certain of the desired load-bearing capacity and stop cracks from developing. This is because of the RuGPC's more compressed microstructure, which contains 10 % CR aggregates, the augmentation of the alkaline gel solution, and the area where the paste and rubber aggregates interacted throughout their 28-day curing phase. The filling strength of the CR aggregates reduces when the percentage replacement of CR surpasses 10 %, acting as within the GPC matrix. When the concentration of the binder is low, the formation of microstructure that is thick by the CR aggregates is less likely at below 10 %, which affects the homogeneity of the paste.

Iqbal et al. (Iqbal, 2023) investigated the effect of graphene nanoplatelets (GNPs) on the stress–strain behavior of fly ash-based RuGPC with CR replacing natural fine aggregate by volume from 10 to 30 % and the inclusion of GNPs at 0.1 to 0.4 % by weight of fly ash. They reported a decrease in the capacity of RuGPC to resist applied force as the percentage replacement of CR increased, which could be because rubber aggregates have lower stiffness than natural aggregates. In any case, a lower brittleness and an improvement were noticed in the deformation capacity of RuGPC with CR below 20 % by Wang et al. (Wang et al., 2022). RuGPC possesses high ductility and lower brittleness making it very suitable for several applications where durability and flexibility characteristics are paramount (Ye et al., 2021). RuGPC with 10 % CR displayed bigger strain values than GPC without rubber aggregates, and this was attributed to the higher deformability of qualities of rubber aggregates over natural fine aggregate (Wang et al., 2022). The investigation reported improvement in the stress–strain behavior of GPC (control specimen) by 9, 18, 26, and 25 %, and RuGPC of 20 % CR by 4, 8, 16, and 6 % with the introduction of GNPs at 0.1, 0.2, 0.3, and 0.4 % respectively, as it also had positive impacts on the mechanical properties of GPC. The strain capacity of the concrete is enhanced due to the ability

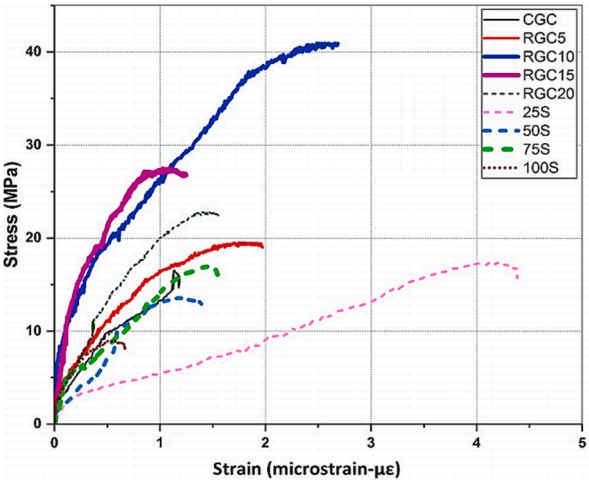

Fig. 27. Stress–strain curves for RuGPC and Lightweight GPC under compression (Hamidi et al., 2022).

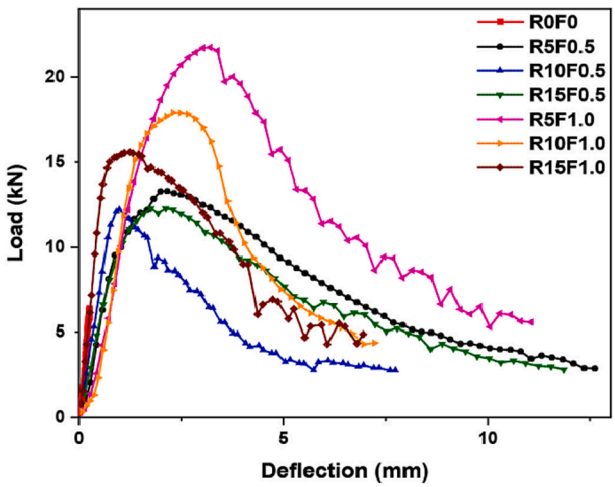

Fig. 28. Load-deflection curve under four-point bending (Zhong et al., 2019).

of GNPs to bridge the micro-cracks and lessen their progression (Han et al., 2015). Amongst all mixes, 0.3 % GNPs had the highest resistance value to uniaxial stress under compression. Abd-Elaty at al. (Abd-Elaty et al., 2022) worked on rubberized geopolymer mortar (RuGPM) replacing fine aggregate with CR of sizes 0–1 mm, 1–3 mm, 4 mm at 10, 20, and 30 %. The overall toughness of the mortar was increased by 4.6 %, 27.5 %, and 3.3 % at 20 % CR replacement, implying that CR has less effect on the toughness of RuGPM as a result of a reduction in flexural strength compared to that of the control specimen.

Dynamic properties of rubberized geopolymer concrete

Strain rate effects

As seen in Fig. 29, Split Hopkinson pressure bar experiments were performed on a RuGPC cylinder disc specimen with a diameter of 100 mm and a height of 50 mm. The strain rates tested were 50, 70, 90, and 1301/s (Pham, 2020). Concrete specimens open to levels of strain that are bearable are frequently subjected to the split Hopkinson pressure bar test to determine their dynamic properties and increase in dynamic factor (Grote et al., 2001; Zhang et al., 2009). According to the findings, under conditions of extreme strain, specimens of RuGPC were not damaged, however, the samples without CR completely crumbled. The incorporation of CR aggregates as partial surrogate of natural aggregate similarly modifies the curvature of the stress–strain relationship of the samples, after the highest applied load, the slope curvature of stress–-strain relationship of RuGPC specimens are horizontal, indicating that the increasing the percentage replacement of CR aggregates in RuGPC increase the ductility of the concrete (Pham, 2020). There is evidence

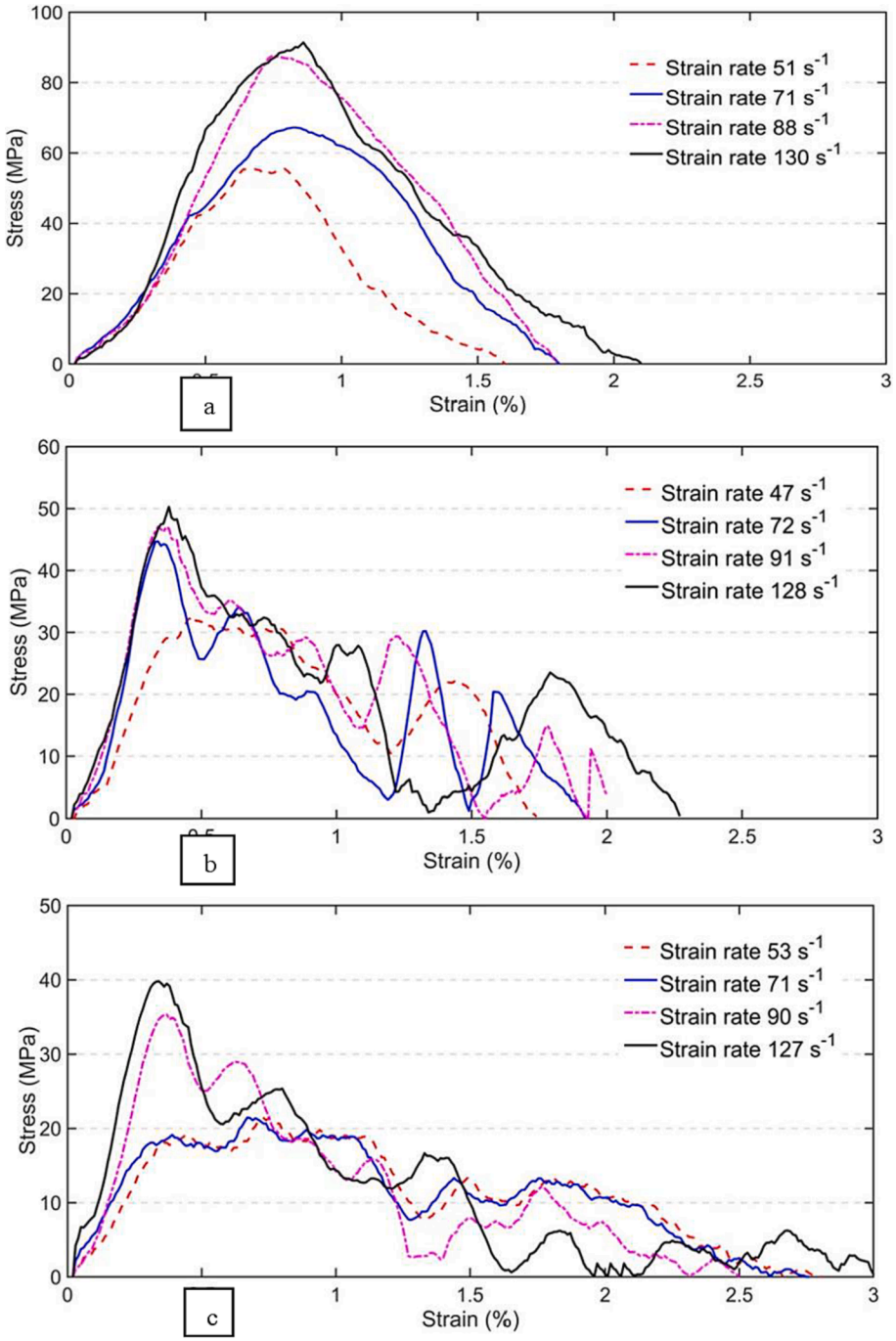

Fig. 29. Stress–strain diagrams of (a) 0%, (b) 15%, and (30%) RuGPC at different strain rates (Pham, 2020).

that as the percentage of CR replacement in RuGPC increases, the corresponding dynamic compressive strength declines (Pham, 2020). With a CR percentage replacement of 0 %, the control specimen showed, displayed higher dynamic strength compressively with respect to RuGPC samples with CR as surrogate of fine and coarse aggregates at 15 % and 30 %. As opposed to that, in RuGPC specimens with CR replacement of high percentage, the dynamic increase factor was larger. For instance, the factor of dynamic increase ranged from 1.37 to 3.4 for RuGPC with 30 % CR replacement with strain rates between 50 and 1301/s (Pham, 2020). In contrast, the RuGPC with 0 % CR aggregates at the same strain rates displayed a dynamic increase factor ranging from 1.04 to 1.87 (Pham, 2020). The enhanced deformability of CR and their capacity to prevent fracture development account for this rise in the dynamic increase factor (Aly et al., 2019).

Impact resistance properties

Aly et al. (Aly et al., 2019) in accordance with AC-544 (A.C. 544, 2018) performed a drop weight test on RuGPC cylindrical disc specimens of size 150 mm diameter by 65 mm height. The test entailed lowering a 4.5 kg steel ball from a fixed height of 450 mm and determining how many impacts were needed to start and complete cracks of the concrete discs. The findings demonstrated that as the CR ratio was raised, initial and final cracks were generated by additional impacts, it implied that the substance's ability to withstand impacts improved as well.

Using the Erdem et al. (Erdem et al., 2011) approach, Dehdezi et al. (Dehdezi et al., 2015) conducted a drop weight test on RuGPC test specimens, which saw the falling of a 5 kg steel cylinder ball from a height of 1 m. For RuGPC mixtures with CR aggregates as partial replacement of natural fine aggregates at 0 %, 20 %, and 50 %, the 3, 5, and 7 strikes respectively initiated the first cracks while the final 4, 17, and 38 strikes were the final strikes, with each of the RuGPC specimens displaying impact energies at the failure of 250 kN mm, 900 kN mm, and 1900 kN mm. The impact resistance of RuGPC is improved by increasing the percentage replacement of rubber aggregates as depicted in Fig. 30 because CR aggregates have lower stiffness and higher capacity to be deformed, which improves the energy absorption and flexibility of RuGPC (Aly et al., 2019). Geopolymer paste and conventional aggregate do not display the same characteristics, when RuGPC is exposed to impact load test, rubber aggregates can help stop the formation of cracks and increase the impact resistance of RuGPC (Erdem et al., 2011). RuGPC discs specimens also failed more ductilely, as evidenced by the appearance of many cracks, while the control specimens typically broke in half after failing with a single, large crack.

From Fig. 31, it can be noticed that the impact resistance of treated RuGPC and untreated RuGPC increased with percentage increase in CR.

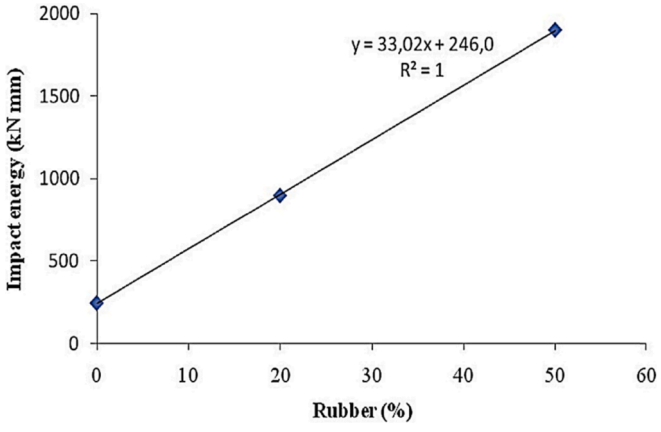

Fig. 30. Relationship between impact energy of concrete and rubber content (Erdem et al., 2011).

Introducing CR into GPC reduces the stiffness and brittleness thereby increasing the flexibility of RuGPC and energy absorption above that of GPC, the results tally with the experiment results in Fig. 32. RuGPC with treated CR had the maximum impact resistance with 68 blows unlike the control specimen that could resist only 12 blows (G1 – G4: Untreated CR, G5 – G7: Treated CR specimen at 5, 10, 15 and 20 %). This is the strongest characteristic of RuGPC and its advantage over GPC, hence should be a key factor with respect to its structural application.

Aly et al. (Aly et al., 2019) investigate the impact resistance of GGBS-based-RuGPC with CR at 10, 20, and 30 % of fine, and coarse aggregate replacements. They reported that the increase in CR percentage replacement increased the number of blows that caused the initial and final cracks on the concrete, and the space between the two cracks. An increase in CR up to 30 % increased the initial and final cracks by up to 3.0 and 2.5 times. Iqbal et al. (Iqbal, 2023) investigated the impact resistance of fly ash-based RuGPC with CR replacing natural fine aggregate by volume from 10 to 30 % and the inclusion of GNPs at 0.1 to 0.4 % by weight of the geopolymer binder. The research reported an increase in the impact energy absorption with the percentage increase in CR, recording 9.15, 12.36, and 16.27 kJ at 10, 20, and 30 % respectively of CR replacement while that of the control specimen was 6.20 kJ. The result tallys with the reported by Aly et al. (Aly et al., 2019). This result proves that the brittleness and ductility of GPC reduce and increase respectively with an increase in CR percentage. This is attributed to the low stiffness characteristics of the CR aggregates which increases the overall flexibility of RuGPC composite and its energy absorption qualities over that of the control specimen without rubber. Iqbal et al. (Iqbal, 2023) investigated the effect of graphene nanoplatelets (GNPs) on the impact resistance of fly ash-based RuGPC with CR replacing natural fine aggregate by volume from 10 to 30 % and the inclusion of GNPs at 0.1 to 0.4 % by weight of the geopolymer binder. The results showed that the inclusion of GNPs improved the impact resistance of RuGPC. The initial impact energy of GPC increased by 10, 18, 21, and 8 % while the final impact energy increased by 8, 17, 25, and 20 % at 0.1, 0.2, 0.3, and 0.4 % GNPs respectively, and these results are much lower than GPC specimens with rubber aggregates. The inclusion of GNPs improves the strength in addition to the impact resistance properties of RuGPC.

Conclusions

The following summarizes the review's conclusions:

- Higher CR percentage replacement of natural aggregate increases the drying shrinkage characteristics of RuGPC. On the contrary, increase

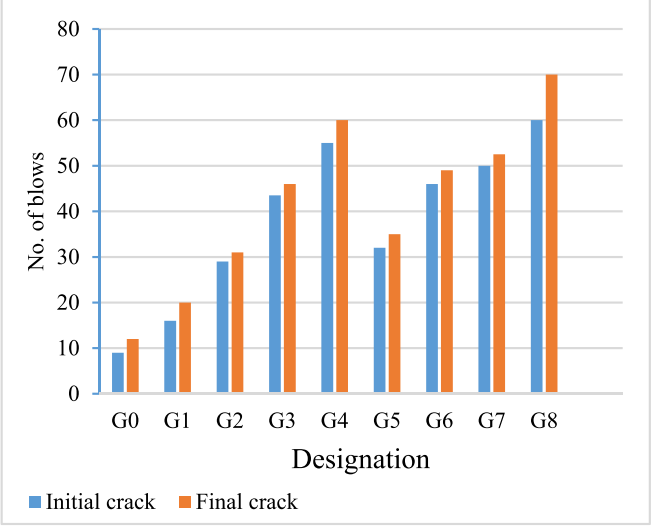

Fig. 31. Impact resistance test (Bhavani, 1132).

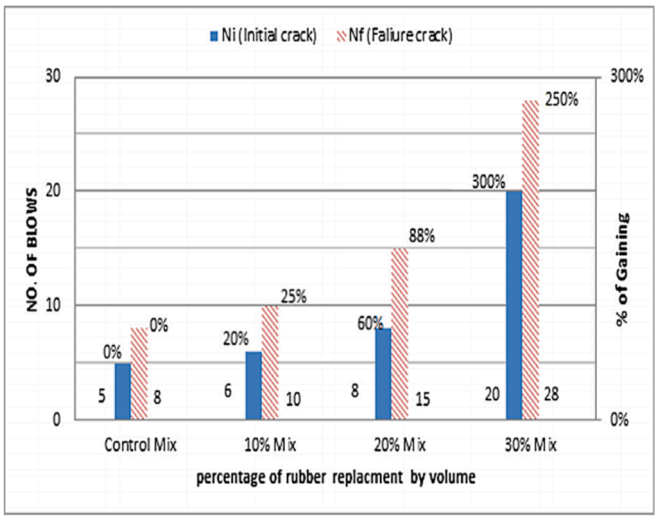

Fig. 32. Impact resistance test (Aly et al., 2019).

percentage replacement of CR in RuGPC reduces the thermal conductivity characteristics of the RuGPC specimen, dropping by 82 % at 100 % CR percentage replacement.

- The addition of CR did not cause reduction in the flowability of GPC at a small percentage, however, at 15 % and 20 % CR replacement minor segregation may set in.
- RuGPC with natural aggregate replacement by CR at 50 % and 100 % yielded dry density results that reduced by 33.5 % and 42 % respectively, with respect to the control specimen.
- RuGPC with CR replacing the total natural aggregates can have a water absorption value up to 2.5 times that of the control specimen.
- Coating with ultra-fine slag and pretreating with sodium hydroxide solution had the most outstanding result on mechanical properties of RuGPC.
- The addition of admixtures zeolite and graphene nanoplatelets (GNPs) had best effect on the mechanical properties of RuGPC.
- Steam curing for RuGPC is 1.5 times less effective than the curing of RuGPC specimen in oven. Duration of up to 48 h of heating at 75 ^{0}C are the ideal curing conditions for the oven.
- The sodium silicate to sodium hydroxide ratio of 2.5 gave the highest compressive strength in RuGPC, while the ideal molarity of NaOH is in the range of 8 to 14. Ratio of between 0.35 and 0.6 is the suggested ratio between the alkaline activator solution and geopolymer binder (binder content of 375 to 625 kg/m^3).
- The combination of class F FA and GGBFS as aluminosilicate precursor gave the best mechanical strength results. GGBFS and Class C FA have a shorter initial setting time because of the high percentage of calcium oxide. Naphthalene based superplasticizer and extra water must be added to the mix to increase the workability, and their percentage is dependent on the desired workability.
- Alkaline activator solution ratio of 0.4 to 0.5 can be used on GGBFS based RuGPC but not advisable in low Class F FA based RuGPC.
- Smaller aggregate sizes (0 – 1 mm) can be used for RuGPC at 5 % replacement. However, wider range of aggregate sizes is recommended from 10 % to 20 % (0 – 3 mm) and up to 4 mm above 20 %.
- Compressive strength decreased from 30 % to 100 % in most research, but increased from 5 % to 20 % in some cases, and 10 % replacement recording the highest increase of 161 % with workability suitable for structural design purpose.
- Tensile strength decreased by 34.6 %, 23 %, and 35.5 % when the CR content increased from 0 % to 10 %, 20 %, and 30 %, respectively and increased up to 30 % CR replacement in some research.
- Most of the results on flexural strength decreased with the addition of CR, but few reports recorded increase from 5 % to 30 % replacements for both cases.
- Replacing fine and coarse aggregates with CR at 30 % each reduced the elasticity modulus by more than 35 % and 70 % respectively.
- RuGPC specimens show a larger dynamic increase factor than GPC specimens and remain intact at high strain levels in comparison to specimens without rubber. Upon impact, RuGPC disc samples showed beneficial ductile failure mechanisms.
- Addition of 10 % CR aggregates is the ideal concentration of rubber aggregate inside GPC matrix to be certain of the desired load-bearing capacity and stop cracks from developing.
- The impact resistance of GPC increased with the increase in CR content in the mix containing both treated and untreated CR, with CR coarse aggregates showing higher impact resistance than fine aggregates.

Recommendations

1. From the reviewed literature graphene nanoplatelets had a tremendous effect on the properties of RuGPC. More research should be done on the admixture with 100 % CR replacement, and rubber aggregates of different sizes to harness its full capacity.
2. Graphene nanoplatelets should be used in RuGPC with different binder type other than class C fly ash to see its effect.
3. Zeolite should also be used as an admixture in RuGPC with different binder type other than class F fly ash to see its effect.
4. There are currently no investigations on structural components made of RuGPC materials that have been loaded in different ways. To fully understand and quantify the performance of the structural components of the RuGPC, more research is needed.
5. The characteristics of GGBFS-based rubberized geopolymer concrete as of right now have not been studied in detail.
6. Up until recently, there has been very little research done on the behavior of rubberized one-part GPC. There is a need for fundamental research into the materials constituents and their structural performance.
7. Two-part GPC has been the focus of the majority of previous research on RuGPC materials. Another choice is one-part GPC, which combines the dry geopolymer binder and alkaline-activator solution before adding water.
8. To reduce bond difficulties, it is important to increase the adhesion of CR aggregates with the geopolymer paste, which is another unknown field of study on RuGPC.
9. Regarding durability, no studies have been conducted to determine how RuGPC will perform under heavy loads for an extended period of time, and the majority of available information on the corrosion of reinforcement, resistance to sulphate attack, shrinkage, efflorescence, sorptivity, and resistance to freeze–thaw is frequently insufficient.
10. It is crucial to assess the whole spectrum of stress–strain responses and develop fundamental models for design objectives in order to make RuGPC adaptable and practical in a variety of settings.

CRediT authorship contribution statement

Noor Abbas Al-Ghazali: Funding acquisition. **Raizal S.M. Rashid:** Supervision. **Nabilah A. Bakar:** Supervision.

Declaration of competing interest

The authors declare that they have no known competing financial interests or personal relationships that could have appeared to influence the work reported in this paper.

Data availability

Data will be made available on request.

Acknowledgements

The authors would like to express their gratitude to the Ministry of Education, Malaysia, for providing financial support for this study under the Fundamental Research Grant Scheme (FRGS/1/2020/TKO/UPM/02/32) with Vot no: 5540372 for the study titled "An investigation of characterization and parametric effect of kenaf bast fibre in the properties of geopolymer enhanced concrete."

References

A.C. 544, 2018. Guide to Design with Fiber-Reinforced Concrete. American Concrete Institute".

AbdelAleem, B.H., Ismail, M.K., Hassan, A.A.A., 2018. The combined effect of crumb rubber and synthetic fibers on impact resistance of self-consolidating concrete. Constr Build Mater 162, 816–829.

Abd-Elaty, M.A.A., Farouk Ghazy, M., Hussein Khalifa, O., 2022. Mechanical and thermal properties of fibrous rubberized geopolymer mortar. Constr Build Mater 354. https://doi.org/10.1016/j.conbuildmat.2022.129192.

Abd-Elaty, M.A.A., Ghazy, M.F., Khalifa, O.H., 2023. Mechanical and Impact Properties of Fibrous Rubberized Geopolymer Concrete. Mansoura Engineering Journal 48 (4). https://doi.org/10.58491/2735-4202.3054.

Abdelmonim, A., Bompa, D.V., 2021. Mechanical and fresh properties of multi-binder geopolymer mortars incorporating recycled rubber particles. Infrastructures (basel) 6 (10). https://doi.org/10.3390/infrastructures6100146.

Adesina, A., 2021. Performance and sustainability overview of sodium carbonate activated slag materials cured at ambient temperature. Resources, Environment and Sustainability 3, 100016. https://doi.org/10.1016/J.RESENV.2021.100016.

Akbarnezhad, A., Huan, M., Mesgari, S., Castel, A., 2015. Recycling of geopolymer concrete. Constr Build Mater 101, 152–158. https://doi.org/10.1016/J.CONBUILDMAT.2015.10.037.

M. M. Al, B. Abdullah, H. Mohammed, H. Kamarudin, S. Profile, and K. Nizar, "Review on fly ash-based geopolymer concrete without Portland Cement," 2011. [Online]. Available: www.academicjournals.org/JETR.

Alaloul, W.S., et al., 2020. Mechanical and deformation properties of rubberized engineered cementitious composite (ECC). Case Stud. Constr. Mater. 13, e00385.

Alawi Al-Sodani, K.A., 2022. "Mix design, mechanical properties and durability of the rubberized geopolymer concrete: A review", Case Studies. Constr. Mater. 17 https://doi.org/10.1016/j.cscm.2022.e01480.

Albidah, A., Alsaif, A., Abadel, A., Abbas, H., Al-Salloum, Y., 2022. Role of recycled vehicle tires quantity and size on the properties of metakaolin-based geopolymer rubberized concrete. J. Mater. Res. Technol. 18, 2593–2607.

Alhozaimy, A.M., 2008. "Chemical Composition of Cements Produced in Saudi Arabia and. Its Influence on Concrete Strength".

Ali, A.S., Hasan, T.M., 2019. "Properties of different types of concrete containing waste tires rubber- A review", in IOP Conference Series: Materials Science and Engineering. Institute of Physics Publishing. https://doi.org/10.1088/1757-899X/584/1/012051.

Ali, I.M., Naje, A.S., Nasr, M.S., 2020. Eco-friendly chopped tire rubber as reinforcements in fly ash based geopolymer concrete. Glob. Nest J. 22, 342–347.

Alrefaei, Y., Wang, Y.-S., Dai, J.-G., 2019. The effectiveness of different superplasticizers in ambient cured one-part alkali activated pastes. Cem Concr Compos 97, 166–174.

K. A. A. Al-Sodani, A. Batin, H. Al Batin, S. Arabia, "Effect of Exposure Temperatures on Chloride Penetration Resistance of Concrete 2 Incorporating Polypropylene Fibers, Silica Fume and Metakaolin." [Online]. Available: https://ssrn.com/abstract=4098359.

Aly, A.M., El-Feky, M.S., Kohail, M., Nasr, E.S.A.R., 2019. Performance of geopolymer concrete containing recycled rubber. Constr Build Mater 207, 136–144. https://doi.org/10.1016/j.conbuildmat.2019.02.121.

Ameri, F., Shoaei, P., Musaeei, H.R., Zareei, S.A., Cheah, C.B., 2020. Partial replacement of copper slag with treated crumb rubber aggregates in alkali-activated slag mortar. Constr Build Mater 256, 119468.

M. Amin, B.A. Tayeh, and I. Saad Agwa, "Investigating the mechanical and microstructure properties of fibre-reinforced lightweight concrete under elevated temperatures," *Case Studies in Construction Materials*, vol. 13, p. e00459, 2020, doi: 10.1016/J.CSCM.2020.E00459.

Amran, Y.H.M., Soto, M.G., Alyousef, R., El-Zeadani, M., Alabduljabbar, H., Aune, V., 2020. Performance investigation of high-proportion Saudi-fly-ash-based concrete. Results in Engineering 6, 100118.

Amran, Y.H.M., Alyousef, R., Alabduljabbar, H., El-Zeadani, M., 2020. Clean production and properties of geopolymer concrete; A review. J Clean Prod 251, 119679.

F. Andrews-Phaedonos, "Test methods for the assessment of durability of concrete," in *ARRB conference, 23rd*, 2008.

Arunkumar, K., Muthukannan, M., Ganesh, A.C., 2021. Mitigation of waste rubber tire and waste wood ash by the production of rubberized low calcium waste wood ash based geopolymer concrete and influence of waste rubber fibre in setting properties and mechanical behavior. Environ Res 194, 110661.

Aslani, F., Asif, Z., 2019. Properties of ambient-cured normal and heavyweight geopolymer concrete exposed to high temperatures. Materials 12 (5), 740.

Aslani, F., Deghani, A., Asif, Z., 2020. Development of lightweight rubberized geopolymer concrete by using polystyrene and recycled crumb-rubber aggregates. J. Mater. Civ. Eng. 32 (2), 04019345.

Aslani, F., Hamidi, F., Valizadeh, A., Dang, A.-T.-N., 2020. High-performance fibre-reinforced heavyweight self-compacting concrete: Analysis of fresh and mechanical properties. Constr Build Mater 232, 117230.

Aslani, F., Jowkarmeimandi, R., 2012. Stress–strain model for concrete under cyclic loading. Mag. Concr. Res. 64 (8), 673–685.

ASTM, 2012. ASTM C 618-Standard specification for coal fly ash and raw or calcined natural pozzolan for use in concrete. ASTM West Conshohocken.

Azevedo, A., et al., 2021. Circular economy and durability in geopolymers ceramics pieces obtained from glass polishing waste. Int J Appl Ceram Technol 18. https://doi.org/10.1111/IJAC.13780.

Azevedo, F., Pacheco-Torgal, F., Jesus, C., Barroso De Aguiar, J.L., Camões, A.F., 2012. Properties and durability of HPC with tyre rubber wastes. Constr Build Mater 34, 186–191. https://doi.org/10.1016/J.CONBUILDMAT.2012.02.062.

Azmi, A.A., Al Bakri, A.M.M., Ghazali, C.M.R., Sandu, A.V., Kamarudin, H., Sumarto, D. A., 2016. A review on fly ash based geopolymer rubberized concrete. Key Eng Mater 700, 183–196.

Azmi, A.A., Abdullah, M.M.A.B., Ghazali, C.M.R., Sandu, A.V., Hussin, K., 2016. "Effect of crumb rubber on compressive strength of fly ash based geopolymer concrete", in MATEC web of conferences. EDP Sciences 01063.

Azmi, A.A., Abdullah, M.M.A.B., Ghazali, C.M.R., Ahmad, R., Musa, L., Rou, L.S., 2019. The effect of different crumb rubber loading on the properties of fly ash-based geopolymer concrete. In: IOP Conference Series: Materials Science and Engineering. IOP Publishing, p. 012079.

B.S. EN, 2012. 450-1, Fly Ash for Concrete—Definition, Specifications and Conformity Criteria. British Standards Institution.

Bakharev, T., Sanjayan, J.G., Cheng, Y.-B., 2000. Effect of admixtures on properties of alkali-activated slag concrete. Cem Concr Res 30 (9), 1367–1374.

M. M. Balaha, A. A. M. Badawy, M. Hashish, "Effect of using ground waste tire rubber as fine aggregate on the behaviour of concrete mixes," 2007.

Bashar, I.I., Alengaram, U.J., Jumaat, M.Z., Islam, A., Santhi, H., Sharmin, A., 2016. Engineering properties and fracture behaviour of high volume palm oil fuel ash based fibre reinforced geopolymer concrete. Constr Build Mater 111, 286–297.

Bate, S.C.C., 1979. Guide for structural lightweight aggregate concrete: report of ACI committee 213. Int. J. Cem. Compos. Light. Concr. 1 (1), 5–6.

Bhatt, A., Priyadarshini, S., Mohanakrishnan, A.A., Abri, A., Sattler, M., Techapaphawit, S., 2019. Physical, chemical, and geotechnical properties of coal fly ash: A global review. Case Stud. Constr. Mater. 11, e00263.

S. Bhavani, G. Nagesh kumar, M. S. Reddy, E. Sanjeeva Rayudu, "Experimental Study on Geopolymer Rubberized concrete using natural Zeolite," *IOP Conf Ser Mater Sci Eng*, vol. 1132, no. 1, p. 012038, 2021, doi: 10.1088/1757-899x/1132/1/012038.

Bilim, C., Karahan, O., Atiş, C.D., Ilkentapar, S., 2013. Influence of admixtures on the properties of alkali-activated slag mortars subjected to different curing conditions. Mater Des 44, 540–547.

Bisht, K., Ramana, P.V., 2017. Evaluation of mechanical and durability properties of crumb rubber concrete. Constr Build Mater 155, 811–817.

Bong, S.H., Nematollahi, B., Nazari, A., Xia, M., Sanjayan, J., 2019. Efficiency of different superplasticizers and retarders on properties of 'one-Part'Fly ash-slag blended geopolymers with different activators. Materials 12 (20), 3410.

Bright Singh, S., Murugan, M., 2022. Effect of metakaolin on the properties of pervious concrete. Constr Build Mater 346. https://doi.org/10.1016/j.conbuildmat.2022.128476.

Burgos-Montes, O., Palacios, M., Rivilla, P., Puertas, F., 2012. Compatibility between superplasticizer admixtures and cements with mineral additions. Constr Build Mater 31, 300–309.

Carroll, J.C., Helminger, N., 2016. Fresh and hardened properties of fiber-reinforced rubber concrete. J. Mater. Civ. Eng. 28 (7), 04016027.

Chandra, S., Björnström, J., 2002. Influence of superplasticizer type and dosage on the slump loss of Portland cement mortars—Part II. Cem Concr Res 32 (10), 1613–1619.

S. Charkhtab Moghaddam, R. Madandoust, M. Jamshidi, and I.M. Nikbin, "Mechanical properties of fly ash-based geopolymer concrete with crumb rubber and steel fiber under ambient and sulfuric acid conditions," *Constr Build Mater*, vol. 281, p. 122571, 2021, doi: 10.1016/J.CONBUILDMAT.2021.122571.

Chindaprasirt, P., Chareerat, T., Sirivivatnanon, V., 2007. Workability and strength of coarse high calcium fly ash geopolymer. Cem Concr Compos 29 (3), 224–229. https://doi.org/10.1016/j.cemconcomp.2006.11.002.

Chindaprasirt, P., Ridtirud, C., 2020. High calcium fly ash geopolymer containing natural rubber latex as additive. GEOMATE Journal 18 (69), 124–129.

Collepardi, M., 1998. Admixtures used to enhance placing characteristics of concrete. Cem Concr Compos 20 (2–3), 103–112.

Criado, M., Palomo, A., Fernández-Jiménez, A., Banfill, P.F.G., 2009. Alkali activated fly ash: effect of admixtures on paste rheology. Rheol Acta 48, 447–455.

da Cruz, T.A.M., Henrique Geraldo, R., Damasceno Costa, A.R., Rándello Dantas Maciel, K., Pereira Gonçalves, J., Camarini, G., 2022. Microstructural and mineralogical compositions of metakaolin-lime-recycled gypsum plaster ternary systems. Journal of Building Engineering 47. https://doi.org/10.1016/j.jobe.2021.103770.

Dai, X., Aydin, S., Yardimci, M.Y., De Schutter, G., 2022. Rheology and structural build-up of sodium silicate- and sodium hydroxide-activated GGBFS mixtures. Cem Concr Compos 131. https://doi.org/10.1016/j.cemconcomp.2022.104570.

N. Dave, V. Sahu, A. Misra, "Development of geopolymer cement concrete for highway infrastructure applications," *Journal of Engineering, Design and Technology*, vol. ahead-of-print, 2020, doi: 10.1108/JEDT-10-2019-0263.
Davidovits, J., 1988. Geopolymer chemistry and properties. In: In Proceedings of the 1st International Conference on Geopolymer, pp. 25–48.
J. Davidovits, "Geopolymers of the first generation: siliface-process, geopolymer," 1988. [Online]. Available: https://www.researchgate.net/publication/304822628.
J. Davidovits, "Chemistry of Geopolymeric systems, terminology in: proceedings of 99 international conference. eds," *Joseph Davidovits, R. Davidovits & C. James, France*, 1999.
de Azevedo, A.R.G., Marvila, M.T., Rocha, H.A., Cruz, L.R., Vieira, C.M.F., 2020. Use of glass polishing waste in the development of ecological ceramic roof tiles by the geopolymerization process. Int J Appl Ceram Technol 17 (6), 2649–2658. https://doi.org/10.1111/ijac.13585.
de Vargas, A.S., Dal Molin, D.C.C., Masuero, Â.B., Vilela, A.C.F., Castro-Gomes, J., de Gutierrez, R.M., 2014. Strength development of alkali-activated fly ash produced with combined NaOH and Ca (OH) 2 activators. Cem Concr Compos 53, 341–349.
Deb, P.S., Sarker, P.K., Barbhuiya, S., 2016. Sorptivity and acid resistance of ambient-cured geopolymer mortars containing nano-silica. Cem Concr Compos 72, 235–245. https://doi.org/10.1016/J.CEMCONCOMP.2016.06.017.
Dehdezi, P.K., Erdem, S., Blankson, M.A., 2015. Physico-mechanical, microstructural and dynamic properties of newly developed artificial fly ash based lightweight aggregate – Rubber concrete composite. Compos B Eng 79, 451–455. https://doi.org/10.1016/J.COMPOSITESB.2015.05.005.
Dong, M., et al., 2019. Circular steel tubes filled with rubberised concrete under combined loading. J Constr Steel Res 162, 105613. https://doi.org/10.1016/J.JCSR.2019.05.003.
Dong, M., Elchalakani, M., Karrech, A., Hassanein, M.F., Xie, T., Yang, B., 2019. Behaviour and design of rubberised concrete filled steel tubes under combined loading conditions. Thin-Walled Struct. 139, 24–38. https://doi.org/10.1016/J.TWS.2019.02.031.
Dong, M., Elchalakani, M., Karrech, A., 2020. Development of high strength one-part geopolymer mortar using sodium metasilicate. Constr Build Mater 236, 117611.
Dong, M., Feng, W., Elchalakani, M., Li, G.K., Karrech, A., Sheikh, M.N., 2020. Material and glass-fibre-reinforced polymer bond properties of geopolymer concrete. Mag. Concr. Res. 72 (10), 509–525. https://doi.org/10.1680/jmacr.18.00273.
Dong, M., Elchalakani, M., Karrech, A., Yang, B., 2021. Strength and durability of geopolymer concrete with high volume rubber replacement. Constr Build Mater 274, 121783.
Duxson, P., Provis, J.L., Lukey, G.C., van Deventer, J.S.J., 2007. The role of inorganic polymer technology in the development of 'green concrete'. Cem Concr Res 37 (12), 1590–1597. https://doi.org/10.1016/J.CEMCONRES.2007.08.018.
Edeskär, T., 2004. Technical and environmental properties of tyre shreds focusing on ground engineering applications. Luleå Tekniska Universitet.
Elchalakani, M., Hassanein, M.F., Karrech, A., Fawzia, S., Yang, B., Patel, V.I., 2018. Experimental tests and design of rubberised concrete-filled double skin circular tubular short columns. Structures 15, 196–210. https://doi.org/10.1016/J.ISTRUC.2018.07.004.
Elyamany, H.E., Abd Elmoaty, M., Elshaboury, A.M., 2018. Setting time and 7-day strength of geopolymer mortar with various binders. Constr Build Mater 187, 974–983.
Erdem, S., Dawson, A.R., Thom, N.H., 2011. Microstructure-linked strength properties and impact response of conventional and recycled concrete reinforced with steel and synthetic macro fibres. Constr Build Mater 25 (10), 4025–4036.
Esparham, A., Vatin, N.I., Kharun, M., Hematibahar, M., 2023. A study of modern eco-friendly composite (geopolymer) based on blast furnace slag compared to conventional concrete using the life cycle assessment approach. Infrastructures (basel) 8 (3), 58.
Fang, G., Ho, W.K., Tu, W., Zhang, M., 2018. Workability and mechanical properties of alkali-activated fly ash-slag concrete cured at ambient temperature. Constr Build Mater 172, 476–487.
M. W. Ferdous, O. Kayali, A. Khennane, "A Detailed Procedure Of Mix Design For Fly Ash Based Geopolymer Concrete," 2013.
Fernandez-Jimenez, A.M., Palomo, A., Lopez-Hombrados, C., 2006. Engineering properties of alkali-activated fly ash concrete. ACI Mater J 103 (2), 106.
Gandoman, M., Kokabi, M., 2015. Sound barrier properties of sustainable waste rubber/geopolymer concretes. Iran. Polym. J. 24, 105–112.
Ganesan, N., Raj, J.B., Shashikala, A.P., 2013. Flexural fatigue behavior of self compacting rubberized concrete. Constr Build Mater 44, 7–14.
Ganjian, E., Khorami, M., Maghsoudi, A.A., 2009. Scrap-tyre-rubber replacement for aggregate and filler in concrete. Constr Build Mater 23 (5), 1828–1836.
Giang, D.T.H., Pheng, L.S., 2011. Role of construction in economic development: Review of key concepts in the past 40 years. Habitat Int 35 (1), 118–125.
Gill, P., Jangra, P., Roychand, R., Saberian, M., Li, J., 2023. Effects of various additives on the crumb rubber integrated geopolymer concrete. Cleaner Materials 8. https://doi.org/10.1016/j.clema.2023.100181.
Giri, Y.G.A.P., et al., 2023. Mechanical and Microstructural Properties of Rubberized Geopolymer Concrete: Modeling and Optimization. Buildings 13 (8), 2021.
Gołaszewski, J., Szwabowski, J., 2004. Influence of superplasticizers on rheological behaviour of fresh cement mortars. Cem Concr Res 34 (2), 235–248.
Grote, D.L., Park, S.W., Zhou, M., 2001. Dynamic behavior of concrete at high strain rates and pressures: I. experimental characterization. Int J Impact Eng 25 (9), 869–886.
Guelmine, L., Hadjab, H., Benazzouk, A., 2016. Effect of elevated temperatures on physical and mechanical properties of recycled rubber mortar. Constr Build Mater 126, 77–85. https://doi.org/10.1016/J.CONBUILDMAT.2016.09.018.
Guo, S., Dai, Q., Si, R., Sun, X., Lu, C., 2017. Evaluation of properties and performance of rubber-modified concrete for recycling of waste scrap tire. J Clean Prod 148, 681–689.
Guo, J., Huang, M., Huang, S., Wang, S., 2019. An experimental study on mechanical and thermal insulation properties of rubberized concrete including its microstructure. Appl. Sci. 9 (14), 2943.
Gupta, T., Chaudhary, S., Sharma, R.K., 2014. Assessment of mechanical and durability properties of concrete containing waste rubber tire as fine aggregate. Constr Build Mater 73, 562–574. https://doi.org/10.1016/J.CONBUILDMAT.2014.09.102.
I. Hakem Aziz *et al.*, "Manufacturing of Fire Resistance Geopolymer: A Review", doi: 10.1051/01023.
Hamada, H.M., Al-attar, A.A., Yahaya, F.M., Muthusamy, K., Tayeh, B.A., Humada, A.M., 2020. Effect of high-volume ultrafine palm oil fuel ash on the engineering and transport properties of concrete. Case Stud. Constr. Mater. 12, e00318.
Hamidi, F., Aslani, F., Valizadeh, A., 2020. Compressive and tensile strength fracture models for heavyweight geopolymer concrete. Eng Fract Mech 231, 107023.
Hamidi, R.M., Man, Z., Azizli, K.A., 2016. Concentration of NaOH and the effect on the properties of fly ash based geopolymer. Procedia Eng 148, 189–193.
Hamidi, F., Valizadeh, A., Aslani, F., 2022. The effect of scoria, perlite and crumb rubber aggregates on the fresh and mechanical properties of geopolymer concrete. Structures 38, 895–909. https://doi.org/10.1016/j.istruc.2022.02.031.
Han, B., Sun, S., Ding, S., Zhang, L., Yu, X., Ou, J., 2015. Review of nanocarbon-engineered multifunctional cementitious composites. Compos Part A Appl Sci Manuf 70, 69–81.
D. Hardjito, B.V. Rangan, "Development and properties of low-calcium fly ash-based geopolymer concrete," 2005.
Haruna, S., Mohammed, B.S., Wahab, M.M.A., Al-Fakih, A., 2021. Effect of aggregate-binder proportion and curing technique on the strength and water absorption of fly ash-based one-part geopolymer mortars. IOP Conf Ser Mater Sci Eng 1101 (1), 012022. https://doi.org/10.1088/1757-899x/1101/1/012022.
Hasanbeigi, A., Price, L., Lin, E., 2012. Emerging energy-efficiency and CO2 emission-reduction technologies for cement and concrete production: A technical review. Renew. Sustain. Energy Rev. 16 (8), 6220–6238. https://doi.org/10.1016/J.RSER.2012.07.019.
Hernández-Olivares, F., Barluenga, G., 2004. Fire performance of recycled rubber-filled high-strength concrete. Cem Concr Res 34 (1), 109–117. https://doi.org/10.1016/S0008-8846(03)00253-9.
Hesami, S., Hikouei, I., Emadi, S., 2016. Mechanical behavior of self-compacting concrete pavements incorporating recycled tire rubber crumb and reinforced with polypropylene fiber. J Clean Prod 133. https://doi.org/10.1016/j.jclepro.2016.04.079.
Huan-xiu, X., Ning-jian, A., Hai-sheng, T., 2007. "Effect of polyorganosilaxane on solvent resistance of NR surface", China. Elastomerics 6 (002).
Huseien, G.F., Sam, A.R.M., Shah, K.W., Mirza, J., Tahir, M.M., 2019. Evaluation of alkali-activated mortars containing high volume waste ceramic powder and fly ash replacing GBFS. Constr Build Mater 210, 78–92.
Iqbal, H.W., et al., 2023. Effect of graphene nanoplatelets on engineering properties of fly ash-based geopolymer concrete containing crumb rubber and its optimization using response surface methodology. Journal of Building Engineering 75. https://doi.org/10.1016/j.jobe.2023.107024.
Issa, S.A., Islam, M., Issa, M.A., Yousif, A.A., 2000. Specimen and aggregate size effect on concrete compressive strength. Cement, Concrete, and Aggregates 22 (2), 103–115.
Jang, J.G., Lee, N.K., Lee, H.-K., 2014. Fresh and hardened properties of alkali-activated fly ash/slag pastes with superplasticizers. Constr Build Mater 50, 169–176.
Kaja, A.M., Lazaro, A., Yu, Q.L., 2018. Effects of Portland cement on activation mechanism of class F fly ash geopolymer cured under ambient conditions. Constr Build Mater 189, 1113–1123. https://doi.org/10.1016/j.conbuildmat.2018.09.065.
Kangar, P.M., 2011. Microstructure of different NaOH molarity of fly ash-based green polymeric cement. Journal of Engineering and Technology Research 3 (2), 44–49.
G. Kaplan, A. M. H. Sarkaz, S. Memiş, H. Yaprak, "Oral Presentation Effect of Waste Tire Rubber and Fly Ash on Lightweight Geopolymer Concrete Production," 2019. [Online]. Available: https://www.researchgate.net/publication/336903515.
Kartika Ilma Pratiwi, "Durability of Fly Ash Based Geopolymer Concrete against Chloride and Sulphuric Acid Attack 1 Kartika Ilma Pratiwi, currently pursuing Master Degree Program in Civil Engineering." [Online]. Available: www.ijisrt.com, 2023.
Kashani, A., Ngo, T.D., Mendis, P., Black, J.R., Hajimohammadi, A., 2017. A sustainable application of recycled tyre crumbs as insulator in lightweight cellular concrete. J Clean Prod 149, 925–935.
Klima, K.M., Schollbach, K., Brouwers, H.J.H., Yu, Q., 2022. Enhancing the thermal performance of Class F fly ash-based geopolymer by sodalite. Constr Build Mater 314. https://doi.org/10.1016/j.conbuildmat.2021.125574.
P. Krivenko, "Why alkaline activation - 60 years of the theory and practice of alkali-activated materials," *Journal of Ceramic Science and Technology*, vol. 8, no. 3. Goller Verlag, pp. 323–333, 2017. doi: 10.4416/JCST2017-00042.
Kumar, S., Kumar, R., Mehrotra, S.P., 2010. Influence of granulated blast furnace slag on the reaction, structure and properties of fly ash based geopolymer. J Mater Sci 45, 607–615.
Kusbiantoro, A., Ibrahim, M.S., Muthusamy, K., Alias, A., 2013. Development of sucrose and citric acid as the natural based admixture for fly ash based geopolymer. Procedia Environ Sci 17, 596–602.
Lahoti, M., Narang, P., Tan, K.H., Yang, E.H., 2017. Mix design factors and strength prediction of metakaolin-based geopolymer. Ceram Int 43 (14), 11433–11441. https://doi.org/10.1016/j.ceramint.2017.06.006.
Laskar, A.I., Bhattacharjee, R., 2013. Effect of Plasticizer and Superplasticizer on Rheology of Fly-Ash-Based Geopolymer Concrete. ACI Mater J 110 (5).

Łaźniewska-Piekarczyk, B., 2014. The methodology for assessing the impact of new generation superplasticizers on air content in self-compacting concrete. Constr Build Mater 53, 488–502.
Lazorenko, G., Kasprzhitskii, A., Mischinenko, V., 2021. Rubberized geopolymer composites: Effect of filler surface treatment. J Environ Chem Eng 9 (4), 105601.
Lee, N.K., Lee, H.-K., 2013. Setting and mechanical properties of alkali-activated fly ash/slag concrete manufactured at room temperature. Constr Build Mater 47, 1201–1209.
Lee, W.K.W., Van Deventer, J.S.J., 2004. The interface between natural siliceous aggregates and geopolymers. Cem Concr Res 34 (2), 195–206.
Li, Z., Ding, Z., Zhang, Y., 2004. "Development of sustainable cementitious materials", in Proceedings of international workshop on sustainable development and concrete technology. China, Beijing, pp. 55–76.
Liu, M.Y.J., Alengaram, U.J., Santhanam, M., Jumaat, M.Z., Mo, K.H., 2016. Microstructural investigations of palm oil fuel ash and fly ash based binders in lightweight aggregate foamed geopolymer concrete. Constr Build Mater 120, 112–122.
Liu, H., Sanjayan, J.G., Bu, Y., 2017. The application of sodium hydroxide and anhydrous borax as composite activator of class F fly ash for extending setting time. Fuel 206, 534–540.
Long, W.J., Li, H.D., Wei, J.J., Xing, F., Han, N., 2018. Sustainable use of recycled crumb rubbers in eco-friendly alkali activated slag mortar: Dynamic mechanical properties. J Clean Prod 204, 1004–1015. https://doi.org/10.1016/J.JCLEPRO.2018.08.306.
Luhar, S., Chaudhary, S., Dave, U., 2016. Effect of different parameters on the compressive strength of rubberized geopolymer concrete. Multi-Disciplinary Sustainable Engineering: Current and Future Trends 77–86.
Luhar, S., Luhar, I., 2020. Rubberized geopolymer concrete: application of taguchi method for various factors. Int. J. Recent Technol. Eng 8, 1167–1174.
Luhar, S., Chaudhary, S., Luhar, I., 2018. Thermal resistance of fly ash based rubberized geopolymer concrete. Journal of Building Engineering 19, 420–428. https://doi.org/10.1016/J.JOBE.2018.05.025.
Luhar, S., Chaudhary, S., Luhar, I., 2019. Development of rubberized geopolymer concrete: Strength and durability studies. Constr Build Mater 204, 740–753. https://doi.org/10.1016/j.conbuildmat.2019.01.185.
Luo, Y., Klima, K.M., Brouwers, H.J.H., Yu, Q., 2022. Effects of ladle slag on Class F fly ash geopolymer: Reaction mechanism and high temperature behavior. Cem Concr Compos 129. https://doi.org/10.1016/j.cemconcomp.2022.104468.
Lương, Q.-H., Nguyễn, H.H., Choi, J.-I., Kim, H.-K., Lee, B.Y., 2021. Effects of crumb rubber particles on mechanical properties and sustainability of ultra-high-ductile slag-based composites. Constr Build Mater 272, 121959.
Luukkonen, T., Abdollahnejad, Z., Yliniemi, J., Kinnunen, P., Illikainen, M., 2018. One-part alkali-activated materials: A review. Cem Concr Res 103, 21–34.
Luukkonen, T., Abdollahnejad, Z., Ohenoja, K., Kinnunen, P., Illikainen, M., 2019. Suitability of commercial superplasticizers for one-part alkali-activated blast-furnace slag mortar. J Sustain Cem Based Mater 8 (4), 244–257.
Mačiulaitis, R., Vaičiene, M., Žurauskiene, R., 2009. The effect of concrete composition and aggregates properties on performance of concrete. J. Civ. Eng. Manag. 15 (3), 317–324.
Medina, N.F., Garcia, R., Hajirasouliha, I., Pilakoutas, K., Guadagnini, M., Raffoul, S., 2018. Composites with recycled rubber aggregates: Properties and opportunities in construction. Constr Build Mater 188, 884–897.
Mithun, B.M., Narasimhan, M.C., 2016. Performance of alkali activated slag concrete mixes incorporating copper slag as fine aggregate. J Clean Prod 112, 837–844.
Mohammadi, I., Khabbaz, H., Vessalas, K., 2014. In-depth assessment of Crumb Rubber Concrete (CRC) prepared by water-soaking treatment method for rigid pavements. Constr Build Mater 71, 456–471.
Mohammed, B.S., Liew, M.S., Alaloul, W.S., Al-Fakih, A., Ibrahim, W., Adamu, M., 2018. Development of rubberized geopolymer interlocking bricks. Case Stud. Constr. Mater. 8, 401–408.
Mucsi, G., Szenczi, Á., Nagy, S., 2018. Fiber reinforced geopolymer from synergetic utilization of fly ash and waste tire. J Clean Prod 178, 429–440.
Muñoz-Sánchez, B., Arévalo-Caballero, M.J., Pacheco-Menor, M.C., 2017. Influence of acetic acid and calcium hydroxide treatments of rubber waste on the properties of rubberized mortars. Mater Struct 50, 1–16.
Nath, P., Sarker, P.K., 2014. Effect of GGBFS on setting, workability and early strength properties of fly ash geopolymer concrete cured in ambient condition. Constr Build Mater 66, 163–171.
Nath, P., Sarker, P.K., 2017. Fracture properties of GGBFS-blended fly ash geopolymer concrete cured in ambient temperature. Mater Struct 50, 1–12.
Nematollahi, B., Sanjayan, J., 2014. Effect of different superplasticizers and activator combinations on workability and strength of fly ash based geopolymer. Mater Des 57, 667–672.
Nuaklong, P., Jongvivatsakul, P., Pothisiri, T., Sata, V., Chindaprasirt, P., 2020. Influence of rice husk ash on mechanical properties and fire resistance of recycled aggregate high-calcium fly ash geopolymer concrete. J Clean Prod 252, 119797.
Ober, J.A., Survey, U.S.G., 2018. "Mineral commodity summaries 2018", Reston. VA. https://doi.org/10.3133/70194932.
Orhan, T.Y., Karakoç, M.B., Özcan, A., 2023. Durability characteristics of slag based geopolymer concrete modified with crumb rubber. Constr Build Mater 404, 132851. https://doi.org/10.1016/j.conbuildmat.2023.132851.
Özbay, E., Erdemir, M., Durmuş, H.İ., 2016. Utilization and efficiency of ground granulated blast furnace slag on concrete properties–A review. Constr Build Mater 105, 423–434.
Pacheco-Torgal, F., Moura, D., Ding, Y., Jalali, S., 2011. Composition, strength and workability of alkali-activated metakaolin based mortars. Constr Build Mater 25 (9), 3732–3745.
Palacios, M., Puertas, F., 2005. Effect of superplasticizer and shrinkage-reducing admixtures on alkali-activated slag pastes and mortars. Cem Concr Res 35 (7), 1358–1367.
Palacios, M., Houst, Y.F., Bowen, P., Puertas, F., 2009. Adsorption of superplasticizer admixtures on alkali-activated slag pastes. Cem Concr Res 39 (8), 670–677.
Park, Y., Abolmaali, A., Kim, Y.H., Ghahremannejad, M., 2016. Compressive strength of fly ash-based geopolymer concrete with crumb rubber partially replacing sand. Constr Build Mater 118, 43–51.
T. Parry, "Briefing: Development of asphalt and concrete products incorporating alternative aggregates," in *Proceedings of the Institution of Civil Engineers-Engineering Sustainability*, Thomas Telford Ltd, 2004, pp. 111–112.
Pavithra, P., Srinivasula Reddy, M., Dinakar, P., Hanumantha Rao, B., Satpathy, B.K., Mohanty, A.N., 2016. A mix design procedure for geopolymer concrete with fly ash. J Clean Prod 133, 117–125. https://doi.org/10.1016/j.jclepro.2016.05.041.
Pham, T.M., et al., 2020. Dynamic compressive properties of lightweight rubberized geopolymer concrete. Constr Build Mater 265, 120753. https://doi.org/10.1016/J.CONBUILDMAT.2020.120753.
Pham, T.M., Lim, Y.Y., Pradhan, S.S., Kumar, J., 2021. Performance of rice husk Ash-Based sustainable geopolymer concrete with Ultra-Fine slag and Corn cob ash. Constr Build Mater 279, 122526.
Phoo-Ngernkham, T., Phiangphimai, C., Damrongwiriyanupap, N., Hanjitsuwan, S., Thumrongvut, J., Chindaprasirt, P., 2018. A Mix Design Procedure for Alkali-Activated High-Calcium Fly Ash Concrete Cured at Ambient Temperature. Adv. Mater. Sci. Eng. 2018 https://doi.org/10.1155/2018/2460403.
Puertas, F., Santos, H., Palacios, M., Martínez-Ramírez, S., 2005. Polycarboxylate superplasticiser admixtures: effect on hydration, microstructure and rheological behaviour in cement pastes. Adv. Cem. Res. 17 (2), 77–89.
Qaidi, S.M.A., et al., 2022. Rubberized geopolymer composites: A comprehensive review. Ceram Int 48 (17), 24234–24259.
Qaidi, S.M.A., Dinkha, Y.Z., Haido, J.H., Ali, M.H., Tayeh, B.A., 2021. Engineering properties of sustainable green concrete incorporating eco-friendly aggregate of crumb rubber: A review. J Clean Prod 324, 129251.
Qiu, J., Ruan, S., Unluer, C., Yang, E.H., 2019. Autogenous healing of fiber-reinforced reactive magnesia-based tensile strain-hardening composites. Cem Concr Res 115, 401–413. https://doi.org/10.1016/J.CEMCONRES.2018.09.016.
Z. Qu, Z. Liu, R. Si, Y. Zhang, "Effect of Various Fly Ash and Ground Granulated Blast Furnace Slag Content on Concrete Properties: Experiments and Modelling," *Materials*, vol. 15, no. 9, 2022, doi: 10.3390/ma15093016.
Qu, F., Li, W., Tang, Z., Wang, K., 2021. Property degradation of seawater sea sand cementitious mortar with GGBFS and glass fiber subjected to elevated temperatures. J. Mater. Res. Technol. 13, 366–384. https://doi.org/10.1016/j.jmrt.2021.04.068.
Raffoul, S., Garcia, R., Pilakoutas, K., Guadagnini, M., Medina, N.F., 2016. Optimisation of rubberised concrete with high rubber content: An experimental investigation. Constr Build Mater 124, 391–404. https://doi.org/10.1016/J.CONBUILDMAT.2016.07.054.
Rajaei, S., et al., 2021. RETRACTED: Rubberized alkali-activated slag mortar reinforced with polypropylene fibres for application in lightweight thermal insulating materials. Elsevier.
Rajendran, M., Akasi, M., 2020. Performance of crumb rubber and nano fly ash based ferro-geopolymer panels under impact load. KSCE J. Civ. Eng. 24, 1810–1820.
A. Ramachandran, R. Anuradha, V. Sreevidya, R. Venkatasubramani, B. V Rangan, "Modified guidelines for geopolymer concrete mix design using Indian standard First articelBase Isolation Techniquea View project Investigations On The Flexural Behaviour Of Ferro Geopolymer Composite Slabs View Project Modified Guidelines For Geopolymer Concrete Mix Design Using Indian Standard," 2012. [Online]. Available: https://www.researchgate.net/publication/286998254.
Ramachandran, V.S., Lowery, M.S., 1992. Conduction calorimetric investigation of the effect of retarders on the hydration of Portland cement. Thermochim Acta 195, 373–387.
Rangan, B.V., 2008. Mix design and production of flyash based geopolymer concrete. The Indian Concrete Journal 82 (5), 7–15.
Rangan, B.V., 2009. "Engineering properties of geopolymer concrete", in Geopolymers. Elsevier 211–226.
B. V Rangan, D. Hardjito, and S. E. Wallah, "Studies on Fly Ash-based Geopolymer Concrete," 2017. [Online]. Available: https://www.researchgate.net/publication/43649864.
Ranjbar, N., Mehrali, M., Mehrali, M., Alengaram, U.J., Jumaat, M.Z., 2015. Graphene nanoplatelet-fly ash based geopolymer composites. Cem Concr Res 76, 222–231.
Rashad, A.M., 2014. A comprehensive overview about the influence of different admixtures and additives on the properties of alkali-activated fly ash. Mater Des 53, 1005–1025.
Rashad, A.M., 2016. A comprehensive overview about recycling rubber as fine aggregate replacement in traditional cementitious materials. Int. J. Sustain. Built Environ. 5 (1), 46–82. https://doi.org/10.1016/J.IJSBE.2015.11.003.
Rashad, A.M., Sadek, D.M., 2020. Behavior of alkali-activated slag pastes blended with waste rubber powder under the effect of freeze/thaw cycles and severe sulfate attack. Constr Build Mater 265, 120716.
G. Recycling, "Recycled construction waste in Europe," *URL: https://global-recycling. info/archive s/2964 (date of access: 05.04. 2020)*, 2019.
R. Rosenberger, "Behaviour of Reinforced Crumb Rubber Ordinary Portland Cement and Geopolymer Concrete Beams," *The UNSW Canberra at ADFA Journal of Undergraduate Engineering Research*, vol. 11, no. 2, 2018.
Saeli, M., Senff, L., Tobaldi, D., Seabra, M., Labrincha, J.A., 2019. Novel biomass fly ash-based geopolymeric mortars using lime slaker grits as aggregate for applications in construction: Influence of granulometry and binder/aggregate ratio. Constr Build Mater 227, 116643. https://doi.org/10.1016/j.conbuildmat.2019.08.024.

Sajedi, F., Razak, H.A., 2011. Comparison of different methods for activation of ordinary Portland cement-slag mortars. Constr Build Mater 25 (1), 30–38.
Saloni, P., Pham, T.M., Lim, Y.Y., Malekzadeh, M., 2021. Effect of pre-treatment methods of crumb rubber on strength, permeability and acid attack resistance of rubberised geopolymer concrete. Journal of Building Engineering 41. https://doi.org/10.1016/j.jobe.2021.102448.
Sanchez, F., Sobolev, K., 2010. Nanotechnology in concrete–a review. Constr Build Mater 24 (11), 2060–2071.
Saraya, M.-E.-S.-I., 2014. Study physico-chemical properties of blended cements containing fixed amount of silica fume, blast furnace slag, basalt and limestone, a comparative study. Constr Build Mater 72, 104–112.
Sarkaz, A.M.H., 2020. " Investigation of the Mechanical Properties of Waste Tire Added Geopolymer Concrete [dissertation]", Institute of sciences. Kastamonu University, T. R.
Sathonsaowaphak, A., Chindaprasirt, P., Pimraksa, K., 2009. Workability and strength of lignite bottom ash geopolymer mortar. J Hazard Mater 168 (1), 44–50. https://doi.org/10.1016/j.jhazmat.2009.01.120.
Schneider, M., Romer, M., Tschudin, M., Bolio, H., 2011. Sustainable cement production—present and future. Cem Concr Res 41 (7), 642–650. https://doi.org/10.1016/J.CEMCONRES.2011.03.019.
Segre, N., Joekes, I., 2000. Use of tire rubber particles as addition to cement paste. Cem Concr Res 30 (9), 1421–1425. https://doi.org/10.1016/S0008-8846(00)00373-2.
Shang, J., Dai, J.-G., Zhao, T.-J., Guo, S.-Y., Zhang, P., Mu, B., 2018. Alternation of traditional cement mortars using fly ash-based geopolymer mortars modified by slag. J Clean Prod 203, 746–756.
Sharp, J.H., Gartner, E.M., Macphee, D.E., 2010. Novel cement systems (sustainability). Session 2 of the fred glasser cement science symposium. Adv. Cem. Res. 22 (4), 195–202.
Shi, C., Qian, J., 2000. High performance cementing materials from industrial slags—a review. Resour Conserv Recycl 29 (3), 195–207.
Siddique, R., Naik, T.R., 2004. Properties of concrete containing scrap-tire rubber–an overview. Waste Manag. 24 (6), 563–569.
Singh, B., Ishwarya, G., Gupta, M., Bhattacharyya, S.K., 2015. Geopolymer concrete: A review of some recent developments. Constr Build Mater 85, 78–90.
Sofi, M., Van Deventer, J.S.J., Mendis, P.A., Lukey, G.C., 2007. Engineering properties of inorganic polymer concretes (IPCs). Cem Concr Res 37 (2), 251–257.
Somna, K., Jaturapitakkul, C., Kajitvichyanukul, P., Chindaprasirt, P., 2011. NaOH-activated ground fly ash geopolymer cured at ambient temperature. Fuel 90 (6), 2118–2124.
Sreesha, S., Esakkiraj, P., Sreevidya, V., 2020. Development of Self Curing Geopolymer Concrete Incorporating Expanded Polystyrene, Recycled Coarse Aggregate and Rubber Crumbs. International Journal of Recent Technology and Engineering (IJRTE) 9 (2), 292–296. https://doi.org/10.35940/ijrte.B3489.079220.
Standard, A., 2003. "C33, 'Standard Specification for Concrete Aggregates', ASTM. International vol. i, no". C.
Suh, J.-I., Yum, W., Sim, S., Park, H.-G., Oh, J.E., 2020. Effect of magnesium formate as compared with magnesium oxide on the strength enhancement and microstructures of CaO-activated Class F fly ash system. Constr Build Mater 253, 119140. https://doi.org/10.1016/j.conbuildmat.2020.119140.
Sukontasukkul, P., Tiamlom, K., 2012. Expansion under water and drying shrinkage of rubberized concrete mixed with crumb rubber with different size. Constr Build Mater 29, 520–526.
Tayeh, B.A., Saffar, D.M.A., Alyousef, R., 2020. The Utilization of Recycled Aggregate in High Performance Concrete: A Review. J. Mater. Res. Technol. 9 (4), 8469–8481. https://doi.org/10.1016/J.JMRT.2020.05.126.
Tayeh, B.A., Zeyad, A.M., Agwa, I.S., Amin, M., 2021. Effect of elevated temperatures on mechanical properties of lightweight geopolymer concrete. Case Stud. Constr. Mater. 15, e00673.
Teh, S.H., Wiedmann, T., Castel, A., de Burgh, J., 2017. Hybrid life cycle assessment of greenhouse gas emissions from cement, concrete and geopolymer concrete in Australia. J Clean Prod 152, 312–320. https://doi.org/10.1016/J.JCLEPRO.2017.03.122.
Thomas, B.S., Gupta, R.C., 2016. A comprehensive review on the applications of waste tire rubber in cement concrete. Renew. Sustain. Energy Rev. 54, 1323–1333. https://doi.org/10.1016/J.RSER.2015.10.092.
Tu, W., Zhu, Y., Fang, G., Wang, X., Zhang, M., 2019. Internal curing of alkali-activated fly ash-slag pastes using superabsorbent polymer. Cem Concr Res 116, 179–190.
Tudjono, S., Purwanto, X.X.X., Apsari, K.T., 2014. Study the effect of adding nano fly ash and nano lime to compressive strength of mortar. Procedia Eng 95, 426–432.
Turgut, P., Yesilata, B., 2008. Physico-mechanical and thermal performances of newly developed rubber-added bricks. Energy Build 40 (5), 679–688. https://doi.org/10.1016/J.ENBUILD.2007.05.002.
United Nations Department of Economic and Social Affairs, "68% of the world population projected to live in urban areas by 2050, says UN," 2023.
Uygunoğlu, T., Topcu, I.B., 2010. The role of scrap rubber particles on the drying shrinkage and mechanical properties of self-consolidating mortars. Constr Build Mater 24 (7), 1141–1150.
Valente, M., Sambucci, M., Chougan, M., Ghaffar, S.H., 2022. Reducing the emission of climate-altering substances in cementitious materials: A comparison between alkali-activated materials and Portland cement-based composites incorporating recycled tire rubber. J Clean Prod 333, 130013.
A. Vredestein, "ETRMA members Tyre Corporate National Associations Affi liated members." [Online]. Available: , 2023.
Wang, H., Wu, Y., Cheng, B., 2022. Mechanical properties of alkali-activated concrete containing crumb rubber particles. Case Stud. Constr. Mater. 16 https://doi.org/10.1016/j.cscm.2021.e00803.
Wardhono, A., Gunasekara, C., Law, D.W., Setunge, S., 2017. Comparison of long term performance between alkali activated slag and fly ash geopolymer concretes. Constr Build Mater 143, 272–279.
Wongpa, J., Kiattikomol, K., Jaturapitakkul, C., Chindaprasirt, P., 2010. Compressive strength, modulus of elasticity, and water permeability of inorganic polymer concrete. Mater Des 31 (10), 4748–4754. https://doi.org/10.1016/J.MATDES.2010.05.012.
Wongsa, A., Sata, V., Nematollahi, B., Sanjayan, J., Chindaprasirt, P., 2018. Mechanical and thermal properties of lightweight geopolymer mortar incorporating crumb rubber. J Clean Prod 195, 1069–1080.
Xu, H., Van Deventer, J.S.J., 2000. "The geopolymerisation of alumino-silicate minerals". www.elsevier.nlrlocaterijminpro, [Online]. Available.
Z. Yahya, M. M. A. B. Abdullah, S. N. H. Ramli, M. G. Minciuna, R. Abd Razak, "Durability of Fly Ash Based Geopolymer Concrete Infilled with Rubber Crumb in Seawater Exposure," in *IOP Conference Series: Materials Science and Engineering*, Institute of Physics Publishing, 2018. doi: 10.1088/1757-899X/374/1/012069.
Yamada, K., Takahashi, T., Hanehara, S., Matsuhisa, M., 2000. Effects of the chemical structure on the properties of polycarboxylate-type superplasticizer. Cem Concr Res 30 (2), 197–207.
Ye, J., Cui, C., Yu, J., Yu, K., Xiao, J., 2021. Fresh and anisotropic-mechanical properties of 3D printable ultra-high ductile concrete with crumb rubber. Compos B Eng 211, 108639.
Yeddula, B.S.R., Karthiyaini, S., 2020. Experimental investigations and prediction of thermal behaviour of ferrosialate-based geopolymer mortars. Arab J Sci Eng 45 (5), 3937–3958.
S. C. Yeluri and N. Yadav, "Mechanical properties of rubber aggregates based geopolymer concrete-A review," in *IOP Conference Series: Materials Science and Engineering*, IOP Publishing, 2020, p. 012014.
Yeluri, S.C., Yadav, N., 2020. "Mechanical properties of rubber aggregates based geopolymer concrete - A review", in IOP Conference Series: Materials Science and Engineering. IOP Publishing Ltd. https://doi.org/10.1088/1757-899X/989/1/012014.
Yolcu, A., Karakoç, M.B., Ekinci, E., Özcan, A., Sağır, M.A., 2022. Effect of binder dosage and the use of waste rubber fiber on the mechanical and durability performance of geopolymer concrete. Journal of Building Engineering 61. https://doi.org/10.1016/j.jobe.2022.105162.
Youssf, O., et al., 2022. Mechanical performance and durability of geopolymer lightweight rubber concrete. Journal of Building Engineering 45. https://doi.org/10.1016/j.jobe.2021.103608.
O. Youssf, M.A. Elgawady, "An overview of sustainable concrete made with scrap rubber," 2012.
Youssf, O., Mills, J.E., Hassanli, R., 2016. Assessment of the mechanical performance of crumb rubber concrete. Constr Build Mater 125, 175–183. https://doi.org/10.1016/j.conbuildmat.2016.08.040.
Youssf, O., Mills, J.E., Elchalakani, M., Alanazi, F., Yosri, A.M., 2023. Geopolymer Concrete with Lightweight Fine Aggregate: Material Performance and Structural Application. Polymers (basel) 15 (1). https://doi.org/10.3390/polym15010171.
Yu, Y., Zhu, H., 2016. Influence of rubber size on properties of crumb rubber mortars. Materials 9 (7), 527.
Zaetang, Y., Wongsa, A., Chindaprasirt, P., Sata, V., 2019. Utilization of crumb rubber as aggregate in high calcium fly ash geopolymer mortars. GEOMATE Journal 17 (64), 158–165.
Zamanabadi, S.N., Zareei, S.A., Shoaei, P., Ameri, F., 2019. Ambient-cured alkali-activated slag paste incorporating micro-silica as repair material: Effects of alkali activator solution on physical and mechanical properties. Constr Build Mater 229, 116911.
Zhang, B., Feng, Y., Xie, J., Lai, D., Yu, T., Huang, D., 2021. Rubberized geopolymer concrete: Dependence of mechanical properties and freeze-thaw resistance on replacement ratio of crumb rubber. Constr Build Mater 310. https://doi.org/10.1016/j.conbuildmat.2021.125248.
Zhang, M., Wu, H.J., Li, Q.M., Huang, F.L., 2009. Further investigation on the dynamic compressive strength enhancement of concrete-like materials based on split Hopkinson pressure bar tests. Part I: Experiments. Int J Impact Eng 36 (12), 1327–1334.
Zhong, H., Poon, E.W., Chen, K., Zhang, M., 2019. Engineering properties of crumb rubber alkali-activated mortar reinforced with recycled steel fibres. J Clean Prod 238, 117950.
Živica, V., Palou, M., Kuzielová, E., Žemlička, M., 2016. Super High Strength Metabentonite Based Geopolymer. Procedia Eng 151, 133–140. https://doi.org/10.1016/J.PROENG.2016.07.354.